

Numerical calculation of automorphic functions for finite index subgroups of triangle groups

Dissertation
zur
Erlangung des Doktorgrades (Dr. rer. nat.)
der
Mathematisch-Naturwissenschaftlichen Fakultät
der
Rheinischen Friedrich-Wilhelms-Universität Bonn

von
Stefan Krämer
aus
Lahnstein

Bonn, 2015

Dieser Forschungsbericht wurde als Dissertation von der
Mathematisch-Naturwissenschaftlichen Fakultät der Universität Bonn angenommen
und ist auf dem Hochschulschriftenserver der ULB Bonn
http://hss.ulb.uni-bonn.de/diss_online elektronisch publiziert.

1. Gutachter: Prof. Dr. Hartmut Monien
2. Gutachter: Prof. Dr. Bas Edixhoven

Tag der Promotion: 03. Juli 2015
Erscheinungsjahr: 2015

Contents

| | |
|--------------------------------------------------------------------------------|-----------|
| 1. Introduction | 1 |
| Outline of this work | 1 |
| Notations and terminology | 3 |
| 2. Hyperbolic geometry and Fuchsian groups | 5 |
| Introduction to hyperbolic geometry | 5 |
| Fuchsian groups | 11 |
| Fundamental domains and Riemann surfaces | 13 |
| Coverings | 17 |
| 3. Automorphic forms and functions | 21 |
| Automorphic forms | 22 |
| The rational covering R_Γ | 27 |
| 4. Triangle groups | 29 |
| Introduction to triangle groups | 29 |
| Geometric realizations of the triangle groups $\Delta(a, b, \infty)$ | 31 |
| Subgroups and permutations | 38 |
| 5. Dessins d'enfants | 43 |
| Belyĭ functions | 43 |
| Dessins d'enfants | 44 |
| Subgroups of triangle groups | 46 |
| Computation of Belyĭ functions | 47 |
| 6. Generalized Farey symbols | 51 |
| Special polygons | 52 |
| Generalized Farey symbols | 56 |
| Algorithms for generalized Farey symbols | 61 |
| An example of a $(2, 4)$ -Farey symbol – discussed in detail | 68 |
| 7. The Schwarzian derivative | 73 |
| Introduction to the Schwarzian derivative | 73 |
| Conformal mappings | 75 |
| The calculation of the hauptmodul for triangle groups | 79 |
| The Picard-Fuchs equation | 81 |

| | |
|--------------------------------------------------------------|------------|
| 8. Numerics | 85 |
| Series expansions | 85 |
| The FEM-method for the calculation of a hauptmodul | 88 |
| 9. Results | 97 |
| Non-congruence subgroups of the modular group | 97 |
| Sporadic groups | 101 |
| 10. Perspectives | 105 |
| Possible improvements | 105 |
| Further perspectives | 106 |
| A. Selected Mathematica programs | 109 |
| B. FreeFem++ | 113 |
| C. The software system Sage | 119 |
| Bibliography | 137 |
| List of Figures | 139 |
| List of Symbols | 141 |
| Index | 145 |

Chapter 1.

Introduction

If you don't know where you are going, you might wind up
someplace else.

(Yogi Berra)

In this thesis, we present a new method to calculate automorphic functions for finite index subgroups of triangle groups. Since automorphic functions are holomorphic, it is well known that the real and the imaginary part are both harmonic. The central idea of my advisor Monien was to look at the two parts separately. We solve the Laplace equation to find the real and imaginary part of an automorphic function. This solution can be calculated using numerical methods.

Algorithm. For a finite index subgroup of a triangle group, find a fundamental domain in the upper half plane. Solve the Laplace equation on this fundamental domain with two different boundary conditions: Periodic boundary condition on the identified boundaries and Dirichlet boundary conditions to obtain the correct asymptotic behavior. The Dirichlet boundary condition is different depending on whether we are calculating the real or the imaginary part.

To each finite index subgroup of a triangle group we can associate a Belyĭ function and a dessin d'enfant. The zeros of this Belyĭ function are the values of the automorphic function we calculated at elliptic points. Hence, we can find an approximation for the coefficients of the Belyĭ function. The precision of this approximation is increased by the use of Newton's method. Once we have an approximation with high accuracy, we find the correct algebraic number using the LLL algorithm. From the exact Belyĭ function we can reconstruct the exact automorphic function.

In order to handle finite index subgroups of triangle groups, we introduce the notion of generalized Farey symbols. These symbols are a generalization of the classical Farey symbols for the modular group. They are used to do efficient calculations with subgroups of Hecke groups. Especially the generalized Farey symbols provide a method to find a connected fundamental domain.

Outline of this work

In chapter 2 we give a quick overview of hyperbolic geometry and Fuchsian groups. The model of hyperbolic geometry we are working with is the Poincaré half plane model. We

state the main theorems of hyperbolic geometry which we need later. We define Fuchsian groups and construct the corresponding Riemann surfaces. For a finite index subgroup of a Fuchsian group we obtain a branched covering of Riemann surfaces. Alongside, we introduce the notion of a covering and the monodromy operation.

Chapter 3 is dedicated to the concept of automorphic functions and automorphic forms. We define them and present some examples. Using automorphic functions it is possible to relate a finite index subgroup of a Fuchsian group to a rational covering. This covering is defined over the projective line and branched over at most three points.

Triangle groups are the topic of the chapter 4. We define the notion of these groups and calculate an embedding of the hyperbolic triangle groups in $\mathrm{PSL}_2(\mathbb{R})$. The Hecke groups are defined as a special case of triangle groups. Furthermore, we state and proof a result about finitely presented groups: There is a relation between the finite index subgroups of a given finitely presented group and certain permutation tuples. We will use this theorem to describe subgroups of triangle groups. Since we embedded the hyperbolic triangle group in $\mathrm{PSL}_2(\mathbb{R})$, we need an algorithm to decide if a given matrix is in a given subgroup of a triangle group. The algorithm which solves this problem involves the solution of the word problem for triangle groups. Inspired by the classical solution to the word problem of $\mathrm{PSL}_2(\mathbb{Z})$, we present an algorithm to solve the word problem for a general triangle group.

In chapter 5 we introduce Belyĭ functions and dessins d'enfants. We give the definition of these objects and their relation to each other. They are in a strong relation with subgroups of triangle groups. We explain this relation. At the end of this chapter we mention a method to calculate the Belyĭ function of a given dessin.

To be able to handle finite index subgroups of Hecke groups, we introduce the concept of generalized Farey symbols in chapter 6. Although we use these symbols mainly as a technical tool to handle these subgroups, they have a rich structure themselves. As an example, we present a generalization of the Stern-Brocot tree. Farey symbols work as follows: To each subgroup, we can associate a certain fundamental domain – a *special polygon*. These special polygons can be described by a sequence of algebraic numbers, together with a pairing. It is used to calculate geometric invariants like the genus. In this chapter, we define the notion of a generalized Farey symbol, present the algorithms which we need later, and end with a detailed example.

Chapter 7 is about conformal mappings. We develop the theory of conformal mappings, the Schwarzian derivative, and calculate the hauptmodul with the help of the Schwarzian derivative. Furthermore, we introduce the concept of the Picard-Fuchs equations. In the end of this chapter, we discuss an example that this theory does not suffice to find the hauptmodul for an arbitrary Fuchsian group.

We present in chapter 8 numerical methods to find modular functions and modular forms. In the first part of this chapter, we explain an approach using series expansion of modular forms. These ideas are generalized to find an approximation of the hauptmodul. In the second part we present a new method. Now, we want solve the Laplace equation on a fundamental domain with certain boundary conditions. An approximation of this solution is found using a finite element solver. The precision of the solution is improved by Newton's method – used on equations from the theory of dessin d'enfants. The exact

coefficients are found using continued fraction expansion or the LLL algorithm.

In chapter 9 we present some results which we calculated using the methods described in the previous chapters. We analyze “Hsu’s examples” and the groups related to the sporadic groups M_{12} and M_{11} .

We finish the thesis in chapter 10 where we suggest further improvements of the methods. We state some open questions and generalizations. Especially we sketch how to generalize the notion of the Farey symbols to general triangle groups.

In the appendix we give some details on the implementations of the algorithms.

Notations and terminology

We denote by \mathbb{Z} , \mathbb{Q} , \mathbb{R} , and \mathbb{C} the *integer*, *rational*, *reals*, and the *complex* numbers. The non-negative real numbers are denoted by

$$\mathbb{R}_{\geq 0} := \{x \in \mathbb{R} \mid x \geq 0\}.$$

Analog to this we use $\mathbb{Z}_{<0}$ for negative integer numbers and analog constructions. With Re and Im we denote the *real and the imaginary part* of a complex number or function. The complex conjugated of a number $z \in \mathbb{C}$ is denoted by \bar{z} .

For a field k the *projective n -space* is denoted by $\mathbb{P}^n(k)$. It is defined as the quotient space of $k^{n+1} \setminus \{0\}$ by the following equivalence relation:

$$(x_0, \dots, x_n) \sim (y_0, \dots, y_n) \Leftrightarrow \exists \lambda \in k^\times : \forall i : x_i = \lambda y_i.$$

We write a representative of an equivalence class as homogenous coordinates: $[x_0 : \dots : x_n]$. The projective line $\mathbb{P}^1(\mathbb{C})$ will sometimes be written as $\mathbb{C} \cup \{\infty\}$ using the identification:

$$[x_0 : x_1] = \begin{cases} \frac{x_0}{x_1} & \text{if } x_1 \neq 0 \\ \infty & \text{if } x_1 = 0. \end{cases} \quad (1.1)$$

We use the same identification for $\mathbb{P}^1(\mathbb{Q})$.

For a ring R we write R^\times for the *unit group* of R and $M_n(R)$ for the set of all $n \times n$ *matrices with entries in R* . Furthermore, we write

$$\begin{aligned} \operatorname{GL}_n(R) &= \{A \in M_n(R) \mid \det(A) \in R^\times\}, \\ \operatorname{SL}_n(R) &= \{A \in M_n(R) \mid \det(A) = 1\}. \end{aligned}$$

for the *general and the special linear group*. The *trace* of a matrix A is denoted by $\operatorname{tr}(A)$ and the *determinant* by $\det(A)$. The *projective special linear group* $\operatorname{PSL}_n(R)$ is the quotient of $\operatorname{SL}_n(R)$ by its center $\{\pm \begin{pmatrix} 1 & 0 \\ 0 & 1 \end{pmatrix}\}$.

For an element $A \in \operatorname{PSL}_n(R)$ we usually write down an element $A \in \operatorname{SL}_n(R)$, meaning the equivalence class represented by A .

If G is a group and $g_1, \dots, g_n \in G$ are elements in the group, we denote by $\langle g_1, \dots, g_n \rangle$ the subgroup of G generated by these elements. For the *symmetric group on n letters*, the full permutation group on n letters, we write \mathfrak{S}_n .

If $A \subseteq X$ is a subset of a topological space X , we write the *interior* of the set A as $\overset{\circ}{A}$ and the *closure* as \bar{A} . The *boundary* of A is denoted by ∂A .

Chapter 2.

Hyperbolic geometry and Fuchsian groups

He had said that the geometry of the dream-place he saw was abnormal, non-Euclidean, and loathsomely redolent of spheres and dimensions apart from ours.

(H. P. Lovecraft)

This chapter is about the basics of hyperbolic geometry and Fuchsian groups. It is based on the books of Katok (Fuchsian groups [Kat92]), Maskit (Kleinian groups [Mas04]), Beardon (The Geometry of Discrete Groups [Bea95]) and Ratcliffe (Foundations of Hyperbolic Manifolds [Rat05]). The model of hyperbolic geometry we are using is the Poincaré upper half plane model. We state the necessary definitions and the central theorems. Especially we present the group of automorphisms of the upper half plane which is $\mathrm{PSL}_2(\mathbb{R})$. Furthermore, we introduce the notion of a Fuchsian group as discrete subgroup of $\mathrm{PSL}_2(\mathbb{R})$ and their basic properties. For this we refer in addition to the books by Ford (Automorphic forms [For51]) and Shimura (Introduction to the theory of automorphic functions [Shi71]). As subgroups of the group of automorphism of the upper half plane, Fuchsian groups operate on the upper half plane as well. Hence, we look at the quotient of this operation. It turns out that this quotient is a Riemann surface which we compactify if the group is a Fuchsian group of the first kind. For a subgroup of finite index of a Fuchsian groups, we construct a branched covering of the corresponding Riemann surfaces.

Introduction to hyperbolic geometry

The classical axioms of a geometry were first stated by Euclid in his famous book “Euclid’s Elements”. He used five axioms to define the Euclidian geometry. One of these axioms is the *parallel postulate*.

That, if a straight line falling on two straight lines make the interior angles on the same side less than two right angles, the two straight lines, if produced indefinitely, meet on that side on which are the angles less than the two right angles.” (Euclid, translated by Heath [Euc08, pp. 195-202]).

In the 19th century, mathematicians started to develop theories of geometry where all axioms of the Euclidian geometry hold, but not the parallel postulate. Lobachevsky and Bolyai developed independently a model of a *non-Euclidian geometry*. This geometry is nowadays called “hyperbolic geometry”. They substituted the parallel postulate by the following axiom.

For each line and for each point not on the line there are at least two different lines through the point and not intersecting the line.

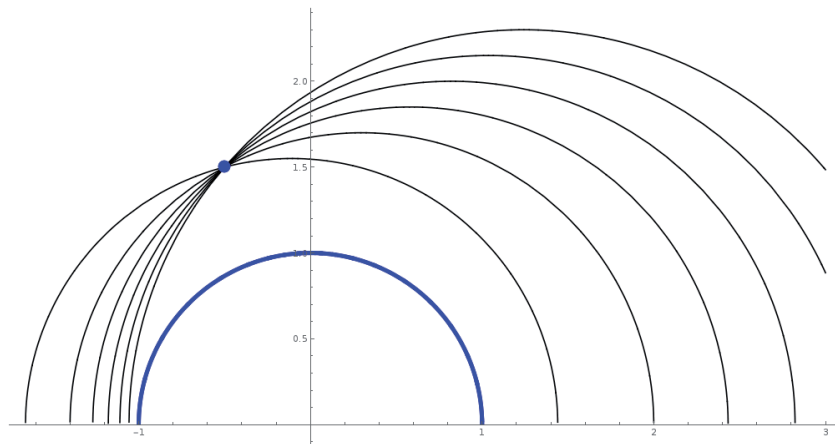


Figure 2.1.: “Parallel” lines in hyperbolic geometry

The model of the hyperbolic geometry we use in this thesis is called the *Poincaré half plane model*. Together with the hyperbolic length (formula (2.1)) it is a two-dimensional model of hyperbolic geometry. Other such models include the Poincaré disk model, the Lorentz model [Kil80], and the Gans model [Gan66]. All of these models are isomorphic, but for our purposes it turns out that the upper half plane model is the most useful. We start with the definition of the upper half plane as well as its closure in $\mathbb{P}^1(\mathbb{C})$

$$\begin{aligned}\mathbb{H} &:= \{z = x + iy \in \mathbb{C} \mid y > 0\}, \\ \overline{\mathbb{H}} &:= \mathbb{H} \cup \mathbb{P}^1(\mathbb{R}) = \{z = x + iy \in \mathbb{C} \mid y \geq 0\} \cup \{\infty\}.\end{aligned}$$

We equip \mathbb{H} with the metric

$$ds = \frac{\|dz\|}{\text{Im}(z)} = \frac{\sqrt{dx^2 + dy^2}}{y}.$$

We call this metric the *hyperbolic metric* on the upper half plane. For a piecewise differentiable path $\gamma: [0, 1] \rightarrow \mathbb{H}$, $t \mapsto x(t) + iy(t)$, with $x(t)$ the real and $y(t)$ the imaginary part, the hyperbolic length $l(\gamma)$ is defined using the hyperbolic metric

$$l(\gamma) := \int_0^1 \frac{\sqrt{\left(\frac{dx}{dt}\right)^2 + \left(\frac{dy}{dt}\right)^2}}{y(t)} dt. \quad (2.1)$$

We define the hyperbolic distance $d(z_1, z_2)$ between two points $z_1, z_2 \in \mathbb{H}$ in the upper half plane as the infimum over all curves joining z_1 and z_2 in \mathbb{H} . We call a path in \mathbb{H} which actually taking this infimum a *geodesic*. A geodesic starting and ending in the boundary $\mathbb{P}^1(\mathbb{R}) = \partial\overline{\mathbb{H}} \subseteq \overline{\mathbb{H}}$ is called a *complete geodesic*. These geodesics are described easily.

2.2 Theorem ([Kat92], Theorem 1.2.1). *The complete geodesics in $\overline{\mathbb{H}}$ are semicircles and straight lines orthogonal to the real axis \mathbb{R} in the sense of the Euclidian geometry.*

Proof. See [Kat92, Theorem 1.2.1]. □

This is used to calculate a formula for the hyperbolic distance between two points.

2.3 Theorem ([Kat92], Theorem 1.2.6, Part (ii)). *Let $z_1 = x_1 + iy_2 \in \mathbb{H}$ and $z_2 = x_2 + iy_2 \in \mathbb{H}$ two points in the upper half plane. Then, the hyperbolic distance is*

$$d: \mathbb{H} \times \mathbb{H} \rightarrow \mathbb{R}_{\geq 0},$$

$$d(x_1 + iy_1, x_2 + iy_2) = \operatorname{arcosh} \left(1 + \frac{(x_2 - x_1)^2 + (y_2 - y_1)^2}{2y_1y_2} \right). \quad (2.4)$$

In addition, this extends to a distance on the closed upper half plane $\overline{\mathbb{H}}$: $d: \overline{\mathbb{H}} \times \overline{\mathbb{H}} \rightarrow \mathbb{R} \cup \{\infty\}$

Proof. See [Kat92, Theorem 1.2.6]. □

Note that the topology induced by the hyperbolic metric is the same as the topology induced by the Euclidean metric on the upper half plane, see [Kat92, Theorem 1.3.3].

Hyperbolic trigonometry

A central object of our interest is the hyperbolic triangle. In chapter 4 we will look at a tessellation by hyperbolic triangles of the upper half plane. The symmetry group of such a tessellation is the main object of our interest. To construct the necessary triangles as well as the symmetry operation, we need some hyperbolic geometry. In this subsection, we collect the definitions and theorems we need for this.

Definition. A *hyperbolic n -sided polygon* is a closed set $P \subseteq \overline{\mathbb{H}}$, bounded by n geodesic segments which intersect in at most one point and do not belong to the same complete geodesic. We call these geodesic segments the *edges* of the polygon and if the intersection of two edges belongs to the boundary ∂P , we call it a *vertex* of the polygon.

A hyperbolic 3-sided polygon is also called a *hyperbolic triangle*.

Example. In figure 2.2 we show a hyperbolic 6-sided polygon and in figure 2.3 a hyperbolic triangle.

2.5 Theorem. *Let P be a hyperbolic triangle with angles α, β and γ . Let A be the length of the edge opposite of α , B the length of the edge opposite of β , and the length of the edge opposite γ is denoted by C . Then, the following holds.*

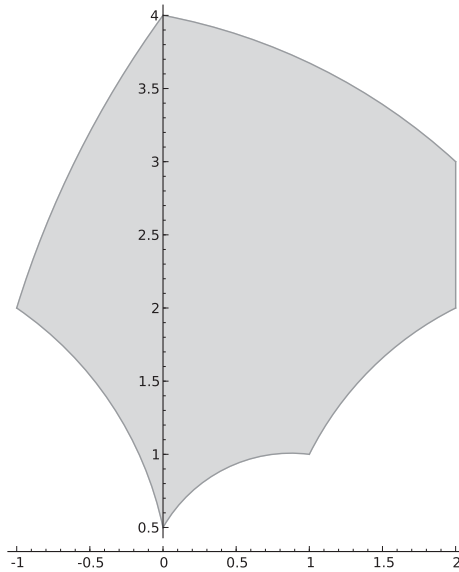


Figure 2.2.: A hyperbolic 6-sided polygon

- The hyperbolic area of the triangle $\mu(P)$ is

$$\mu(P) = \pi - \alpha - \beta - \gamma.$$

- The sine rule holds

$$\frac{\sinh A}{\sin \alpha} = \frac{\sinh B}{\sin \beta} = \frac{\sinh C}{\sin \gamma}.$$

- The two Cosine rules hold

$$\cosh C = \cosh A \cosh B - \sinh A \sinh B \cos \gamma,$$

$$\cosh C = \frac{\cos \alpha \cos \beta + \cos \gamma}{\sin \alpha \sin \beta}.$$

Proof. See [Kat92]: Theorem 1.4.2 and Theorem 1.5.2. □

Isometries

The group $\mathrm{GL}_2(\mathbb{R})$ operates on the complex, projective line naturally as

$$\begin{aligned} \mathrm{GL}_2(\mathbb{R}) \times \mathbb{P}^1(\mathbb{C}) &\rightarrow \mathbb{P}^1(\mathbb{C}), \\ \left(\begin{pmatrix} a & b \\ c & d \end{pmatrix}, [x_0 : x_1] \right) &\mapsto [ax_0 + bx_1 : cx_0 + dx_1]. \end{aligned}$$

Using the identification $\mathbb{P}^1(\mathbb{C}) = \mathbb{C} \cup \{\infty\}$, this transformation become the famous *Möbius transformation*

$$\begin{aligned} \mathrm{GL}_2(\mathbb{R}) \times (\mathbb{C} \cup \{\infty\}) &\rightarrow (\mathbb{C} \cup \{\infty\}), \\ \left(\begin{pmatrix} a & b \\ c & d \end{pmatrix}, z \right) &\mapsto \frac{az + b}{cz + d}. \end{aligned}$$

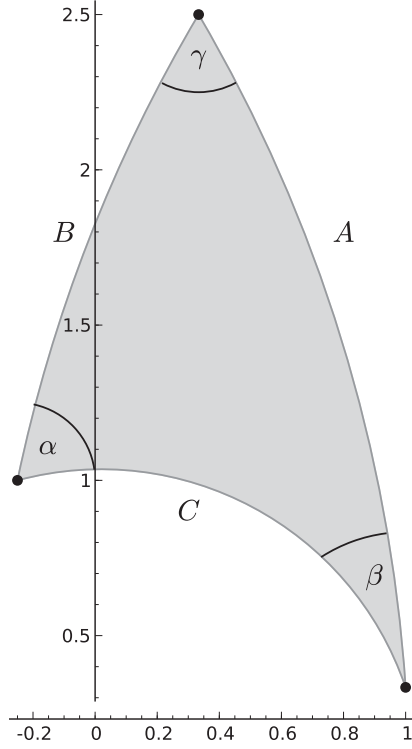


Figure 2.3.: A hyperbolic triangle

For a point $z = x + iy \in \mathbb{H}$ on the upper half plane and a matrix $\begin{pmatrix} a & b \\ c & d \end{pmatrix} \in \text{GL}_2(\mathbb{R})$, we calculate the real and the imaginary part of this operation.

$$\frac{a(x + iy) + b}{c(x + iy) + d} = \frac{ac(x^2 + y^2) + 2adx + bd - \det(A)x}{c^2y^2 + (cx + d)^2} + i \cdot \frac{\det(A)y}{c^2y^2 + (cx + d)^2}.$$

If the determinant of the matrix A is greater than zero, this operation maps the closure of the upper half plane to itself. Especially we obtain the Möbius transformation as an operation of the special linear group on the closed upper half plane. Since the center of $\text{SL}_2(\mathbb{R})$ operates trivially, this operation descends to an operation of the projective linear group $\text{PSL}_2(\mathbb{R})$.

$$\begin{aligned} \text{PSL}_2(\mathbb{R}) \times \overline{\mathbb{H}} &\rightarrow \overline{\mathbb{H}}, \\ (A, \tau) = \left(\begin{pmatrix} a & b \\ c & d \end{pmatrix}, \tau \right) &\mapsto A.\tau := \frac{a\tau + b}{c\tau + d}. \end{aligned}$$

One can check that this is actually a group operation.

We extend the group $\text{PSL}_2(\mathbb{R})$ by the additional operation $z \mapsto (\bar{z})^{-1}$ and call the resulting group the *extended group of Möbius transformations* $\text{PSL}_2^*(\mathbb{R})$.

An automorphism of the upper half plane (or more general of a Riemann surface) is an holomorphic mapping from the surface to itself. An isometry of a metric space

is a distance preserving mapping from the surface to itself. Such an isometry is not necessary a holomorphic mapping. For example the complex conjugation $z \mapsto \bar{z}$ is distance preserving, but anti-holomorphic.

2.6 Theorem.

- (i) The group $\mathrm{PSL}_2(\mathbb{R})$ operates transitively on the upper half plane.
- (ii) The group of automorphisms of the upper half plane $\mathrm{Aut}(\mathbb{H})$ is isomorphic to $\mathrm{PSL}_2(\mathbb{R})$.
- (iii) The group of isometries of the upper half plane $\mathrm{Isom}(\mathbb{H})$ is isomorphic to $\mathrm{PSL}_2^*(\mathbb{R})$.
- (iv) The operation of the group $\mathrm{PSL}_2(\mathbb{R})$ on the upper half plane preserves the cross-ratio $\frac{(z_1 - z_2)}{(z_2 - z_3)} \cdot \frac{(z_3 - z_4)}{(z_1 - z_4)}$ of four points $z_1, \dots, z_4 \in \mathbb{H}$.

Proof. For the first part see [Miy06], Theorem 1.1.3. The statement is equivalent to the statement that for every $z = x + iy \in \mathbb{H}$, there is an $\alpha \in \mathrm{PSL}_2(\mathbb{R})$, such that $\alpha i = z$. We choose this α as follows.

$$\alpha = \begin{pmatrix} \sqrt{y} & \frac{x}{\sqrt{y}} \\ 0 & \frac{1}{\sqrt{y}} \end{pmatrix}.$$

We choose the positive roots in this matrix. Using this, a matrix that maps $z_1 = x_1 + iy_1 \in \mathbb{H}$ to $z_2 = x_2 + iy_2 \in \mathbb{H}$ is given as follows

$$\begin{pmatrix} \sqrt{\frac{y_2}{y_1}} & \frac{x_2 y_1 - x_1 y_2}{\sqrt{y_1 y_2}} \\ 0 & \sqrt{\frac{y_1}{y_2}} \end{pmatrix}.$$

The second part is also [Miy06, theorem 1.1.3].

The third part is [Kat92, theorem 1.3.1]. The last part is proven by direct calculations. For $A = \begin{pmatrix} a & b \\ c & d \end{pmatrix} \in \mathrm{PSL}_2(\mathbb{R})$ and $z_1, \dots, z_4 \in \mathbb{H}$ we need do show

$$\frac{(A.z_1 - A.z_2)}{(A.z_2 - A.z_3)} \cdot \frac{(A.z_3 - A.z_4)}{(A.z_1 - A.z_4)} = \frac{(z_1 - z_2)}{(z_2 - z_3)} \cdot \frac{(z_3 - z_4)}{(z_1 - z_4)}.$$

□

Remark. To construct a Möbius map, which maps three given points $x_1, x_2, x_3 \in \partial\overline{\mathbb{H}} = \mathbb{P}^1(\mathbb{R})$ to another set of three points $z_1, z_2, z_3 \in \partial\overline{\mathbb{H}}$, we use part (iv). Since Möbius map $f: \overline{\mathbb{H}} \rightarrow \overline{\mathbb{H}}$, with $f(x_i) = z_i$, for $i = 1, 2, 3$ preserves the cross ratio, it needs to fulfill

$$\frac{(x_1 - x_2)}{(x_2 - x_3)} \cdot \frac{(x_3 - x)}{(x_1 - x)} = \frac{(z_1 - z_2)}{(z_2 - z_3)} \cdot \frac{(z_3 - f(x))}{(z_1 - f(x))}.$$

We solve this equation for $f(x)$ and obtain a Möbius transformation with the desired properties.

In addition, this also works for general points in $\overline{\mathbb{H}}$, but the resulting Möbius transformation can have complex coefficients in this case.

Later, we will map hyperbolic triangles using Möbius transformations. Hence, we need to know how geodesics and the hyperbolic area behaves under these transformations.

2.7 Theorem.

(i) Any map in $\mathrm{PSL}_2(\mathbb{R})$ of the upper half plane maps geodesics into geodesics.

(ii) The hyperbolic area is invariant under all transformations in $\mathrm{PSL}_2(\mathbb{R})$.

Proof. See [Kat92], Theorem 1.2.4 and Theorem 1.4.1. □

Fuchsian groups

The main result of this thesis is to present an algorithm to calculate rational coverings and modular functions for finite index subgroups of Hecke groups. To define the notion of modular function of triangle groups, we introduce the more general concept of Fuchsian groups. We will see in chapter 4 that the triangle groups – as well as the even more special Hecke groups – are examples of Fuchsian groups. Also the next chapter, chapter 3, uses the more general notion of Fuchsian groups to define modular function. Starting with chapter 4 we specialize on the triangle groups.

In this section we start with the following definition.

Definition. We call a discrete subgroup $\Delta \subseteq \mathrm{PSL}_2(\mathbb{R})$ a *Fuchsian group*.

There is an equivalent definition of the notion of a Fuchsian group. This notion uses the operation of the group $\mathrm{PSL}_2(\mathbb{R})$, respectively its subgroups, on the upper half plane. Note that subgroups of $\mathrm{PSL}_2(\mathbb{R})$ act on the upper half plane in the same way on the upper half plan as $\mathrm{PSL}_2(\mathbb{R})$ does. To give the alternative description, we need the following definition.

Definition. Let Δ be a group acting on a topological space X . We call the group action *properly discontinuously* if for any two points $x, y \in X$, there exist neighborhoods U of x and V of y , such that the following set is finite

$$\{g \in \Delta \mid gU \cap V \neq \emptyset\}.$$

2.8 Theorem. A subgroup of $\mathrm{PSL}_2(\mathbb{R})$ is a Fuchsian group if and only if it acts properly discontinuously on the upper half plane.

Proof. See [Kat92, theorem 2.2.1] or [Miy06, theorem 1.5.2]. □

Example. The most famous examples is the modular group

$$\mathrm{PSL}_2(\mathbb{Z}) := \left\{ \begin{pmatrix} a & b \\ c & d \end{pmatrix} \mid a, b, c, d \in \mathbb{Z}, \det \left(\begin{pmatrix} a & b \\ c & d \end{pmatrix} \right) = ad - bc = 1 \right\} / \left\{ \pm \begin{pmatrix} 1 & 0 \\ 0 & 1 \end{pmatrix} \right\}.$$

This group is generated by the matrices

$$S = \begin{pmatrix} 0 & -1 \\ 1 & 0 \end{pmatrix} \quad \text{and} \quad R = \begin{pmatrix} 0 & -1 \\ 1 & -1 \end{pmatrix}.$$

The matrix S is of order two and R is of order three. One can also show that this group is the free product $\mathbb{Z}/2\mathbb{Z} \star \mathbb{Z}/3\mathbb{Z}$ of the cyclic group of order two and three. For a more detailed discussion we refer to [Apo90, Section 2.2].

Furthermore, we give two examples from the book of Miyake [Miy06].

$$\Gamma_1 = \left\langle \left(\begin{array}{cc} 1 & 1 \\ 0 & 1 \end{array} \right) \right\rangle = \left\{ \left(\begin{array}{cc} 1 & n \\ 0 & 1 \end{array} \right) \mid n \in \mathbb{Z} \right\}, \quad (2.9)$$

$$\Gamma_2 = \left\langle \left(\begin{array}{cc} \cos \frac{\pi}{3} & \sin \frac{\pi}{3} \\ -\sin \frac{\pi}{3} & \cos \frac{\pi}{3} \end{array} \right) \right\rangle. \quad (2.10)$$

Later we see that the modular group is different from the groups Γ_1 and Γ_2 . The groups Γ_1 and Γ_2 are *Fuchsian groups of the second kind* whereas the modular group is a *Fuchsian groups of the first kind*.

The elements of a Fuchsian group are classified according to their trace.

Definition. Let $g = \begin{pmatrix} a & b \\ c & d \end{pmatrix} \in \mathrm{PSL}_2(\mathbb{R})$. We call g

- (i) *elliptic* if $\mathrm{tr}(g)^2 < 4$,
- (ii) *parabolic* if $\mathrm{tr}(g)^2 = 4$, and
- (iii) *hyperbolic* if $\mathrm{tr}(g)^2 > 4$.

Since the group $\mathrm{PSL}_2(\mathbb{R})$ operates on the closed upper half plane via Möbius transformations, the subgroups of $\mathrm{PSL}_2(\mathbb{R})$ do as well. Hence, the Fuchsian group operate on the upper half plane. We use the classification of elements of Fuchsian groups, to define special points on the upper half plane.

Definition. Let Δ be a Fuchsian group and $z \in \overline{\mathbb{H}}$ be a point on the closed upper half plane. We call z an *elliptic*, *parabolic*, or *hyperbolic* point for Δ if it is the fix point of a elliptic, non trivial parabolic or hyperbolic element of Δ .

Furthermore, we call a parabolic point in $\overline{\mathbb{H}}$ a *cusps*. Two cusps $p_1, p_2 \in \overline{\mathbb{H}}$ are equivalent if there is an element $\gamma \in \Delta$ such that $p_1 = \gamma.p_2$.

Example. As we have seen, the modular group $\mathrm{PSL}_2(\mathbb{Z})$ is a Fuchsian group. The generator $R = \begin{pmatrix} 0 & -1 \\ 1 & -1 \end{pmatrix}$ is an elliptic element, since the square of the trace is one. Solving the equations $z = R.z$ for z , we see that there are two fixed points in the complex plane: $z = \frac{1}{2} \pm \frac{\sqrt{3}}{2}i$ – one of the point is actually in the upper half plane. Hence, the point $\frac{1}{2} + \frac{\sqrt{3}}{2}i$ is an elliptic point for the modular group.

We claim that each rational point $\frac{a}{b}$ is a cusp for the modular group. A short calculation shows that the matrix

$$P = \begin{pmatrix} 1 - ab & a^2 \\ -b^2 & 1 + ab \end{pmatrix}$$

has the following properties. It has determinant one and trace two. Therefore, it is a parabolic element of the modular group. The matrix P also maps the rational point $\frac{a}{b}$ to itself, making it a cusp.

When we construct the Riemann surface corresponding to a Fuchsian group in the next section, we start by defining a non-compact Riemann surface which is compactified by adding the cusps. For this, we need to know to possible positions of the cusps.

2.11 Theorem. *Let $A \in \mathrm{PSL}_2(\mathbb{R})$ be a non-trivial element. Then,*

A is parabolic $\Leftrightarrow A$ has only one fixed point on $\mathbb{P}^1(\mathbb{R})$.

A is elliptic $\Leftrightarrow A$ has one fixed point in \mathbb{H} and one in the lower half plane.

A is hyperbolic $\Leftrightarrow A$ has two fixed points on $\mathbb{P}^1(\mathbb{R})$.

Proof. See [Shi71, proposition 1.13]. □

2.12 Corollary. *Let Δ be a Fuchsian group and $z \in \overline{\mathbb{H}}$ a cusp of Δ . Then, z lies in $\mathbb{P}^1(\mathbb{R})$.*

Proof. If $z \in \overline{\mathbb{H}}$ is a cusp, there is a parabolic matrix $A \in \Delta$, such that $A.z = z$. From the proposition we see that this fixed point need to lie in $\mathbb{P}^1(\mathbb{R})$. □

Fundamental domains and Riemann surfaces

To study a Fuchsian group Δ , we study the Riemann surface $\Delta \backslash \mathbb{H}$ and its compactification. To describe this surface, we use the concept of the fundamental domain of a group operation. In this section define the notion of a fundamental domain and construct a compact Riemann surface for certain Fuchsian groups.

Fundamental domains

The concept of a fundamental domain works in the context of an arbitrary group operation on a topological space and we give the definition in this generality.

Definition. Let G be a group acting on a topological space X . We call a closed subset $\mathfrak{F} \subseteq X$ of X a *fundamental domain* for this group operation if

(i) $X = \bigcup_{g \in G} g\mathfrak{F}$,

(ii) $g\mathring{\mathfrak{F}} \cap \mathring{\mathfrak{F}} = \emptyset$ for all $g \neq 1$.

Furthermore, we call the family $\{g\mathfrak{F} \mid g \in G\}$ a *tessellation* of X .

In this definition there are some important subtleties concerning the boundary $\partial\mathfrak{F}$ of the fundamental domain. We do not require that the intersection of $g\mathfrak{F} \cap \mathfrak{F}$, for all $g \in G \setminus \{1\}$, is the empty set. In fact, for the Fuchsian groups we are interested in, there are elements of the group that map one part of the boundary of the fundamental domain onto another.

The first part of the definition implies that for every point $x \in X$ in the topological space X , there is one $g \in G$, such that $g^{-1}x$ is in $\mathring{\mathfrak{F}}$. The second part of the definition claims that this g is unique if $g^{-1}x \in \mathring{\mathfrak{F}}$.

Example. Let $G = D_4$ the dihedral group of order 8, the symmetry group of a square. This group operates on a square. In figure 2.4 we give a fundamental domain of this operation and in 2.5 the corresponding tessellation.

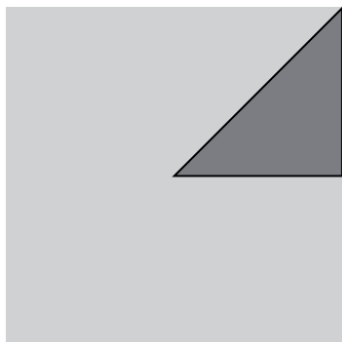


Figure 2.4.: Fundamental domain of a D_4

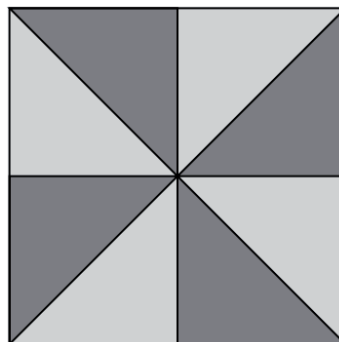


Figure 2.5.: Tessellation of the square

Example. Another important example is the operation of the modular group $\text{PSL}_2(\mathbb{Z})$ on the upper half plane. The corresponding tessellation is called the *Dedekind tessellation*. A discussion of this example is in standard textbooks about modular forms – for example [Apo90, section 2.3]. In figure 2.6 you find in red a fundamental domain. The

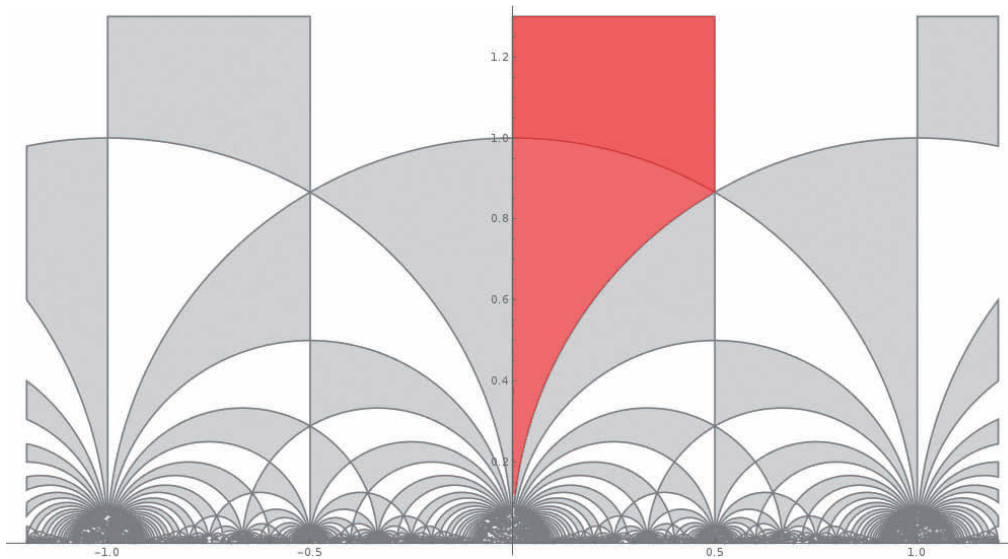


Figure 2.6.: The Dedekind tessellation of the upper half plane and a fundamental domain (in red)

red part is the domain bounded by the following geodesics

$$\begin{aligned} B_1 &= \{it \mid t \in [0, 1]\}, \\ B_2 &= \{it \mid t \in [1, \infty]\}, \\ B_3 &= \left\{t + i\sqrt{1 - (t-1)^2} \mid t \in [0, \frac{1}{2}]\right\}, \\ B_4 &= \left\{\frac{1}{2} + it \mid t \in [\frac{\sqrt{3}}{2}, \infty]\right\}. \end{aligned}$$

As we mention before, there are elements in the group which map one part of the boundary to another part. Here we explicitly give these elements. The matrix $S = \begin{pmatrix} 0 & -1 \\ 1 & 0 \end{pmatrix}$ maps B_1 to B_2 and vice versa. The second generator $R = \begin{pmatrix} 0 & -1 \\ 1 & -1 \end{pmatrix}$ maps B_4 to B_3 and its second power (or its inverse) $R^2 = R^{-1}$ maps B_3 to B_4 .

A fundamental domain is neither unique, nor does it have a priori any nice properties. For a Fuchsian group it is always possible to find a connected, polygonal fundamental domain. In chapter 4 we construct such a domain for the triangle groups and in chapter 6 for subgroups of Hecke groups.

If we know a fundamental domain $\mathfrak{F} \subseteq \overline{\mathbb{H}}$ for a Fuchsian group Δ , we construct a fundamental domain for any finite index subgroup $\Gamma \subseteq \Delta$ in the following way. Let c_1, \dots, c_r be coset representatives of $\Gamma \backslash \Delta$. Then, $c_1^{-1}(\mathfrak{F}) \cup \dots \cup c_r^{-1}(\mathfrak{F})$ is a fundamental domain for Γ . The sets $c_i^{-1}(\mathfrak{F})$ are defined as follows $c_i^{-1}(\mathfrak{F}) = \{c_i^{-1}.z \in \overline{\mathbb{H}} \mid z \in \mathfrak{F}\}$. For a proof, see [Kat92, Theorem 3.1.2]. The resulting domain depends of course on the choice of the coset representatives. In the generic setting, it is not a connected domain. In various settings it is possible to find coset representatives, such that the resulting domain is actually connected. See for example for subgroups of the modular group $\mathrm{PSL}_2(\mathbb{Z})$ the fundamental domain drawer by Verrill [Ver] or in the more general context of Shimura curves [KV03].

The Riemann surface for Fuchsian groups

In this section we use the theory of (compact) Riemann surfaces to study Fuchsian groups. For the definition of a Riemann surface, we refer to the books by Springer (Introduction to Riemann surfaces [Spr57]), Farkas and Kra (Riemann surfaces [FK80]), and Jost (Compact Riemann surfaces [Jos97]). The Riemann surfaces we are interested in, are the quotients of the upper half plane by a Fuchsian group.

$$Y(\Delta) := \Delta \backslash \mathbb{H}.$$

This space is a Riemann surface. But in general it needs not to be compact. In fact, if this surface $Y(\Delta)$ is compact, then the group Δ has no cusps – see [Miy06, Chapter 1.8].

To construct a compactification of this surface, we add the cusps. We denote with $P_\Delta \subseteq \overline{\mathbb{H}}$ the set of all cusps of Δ . Due to corollary 2.12, we know that all the cusps lie

on the boundary of $\overline{\mathbb{H}}$. Hence, $P_\Delta \subseteq \mathbb{P}^1(\mathbb{R})$. We define the *extended upper half plane*.

$$\mathbb{H}_\Delta^* = \mathbb{H}^* := \mathbb{H} \cup P_\Delta \subseteq \overline{\mathbb{H}}. \quad (2.13)$$

The topology on \mathbb{H}^* is defined as follows: For every $\tau \in \mathbb{H}$ we take as fundamental set of open neighborhoods the usual one in \mathbb{H} . For a fundamental system of open neighborhoods for a cusp τ , we take the following sets:

$$\{\tau\} \cup \{\text{the interior of an area bounded by a geodesic in } \mathbb{H} \text{ with the center } \tau\}$$

. With this extended plane, we define another Riemann surface

$$X(\Delta) := \Delta \backslash \mathbb{H}_\Delta^*.$$

If this surface is compact, we call Δ a *Fuchsian group of the first kind*. If $X(\Delta)$ is not compact, Δ is a *Fuchsian group of the second kind*. From now on, whenever we talk about a Fuchsian group, we always mean a Fuchsian group of the first kind.

We collect some facts about this Riemann surface $X(\Delta)$ for a Fuchsian group Δ . Most of this is contained in standard text books, like Miyake (Modular forms [Miy06]) or Shimura (Introduction to the arithmetic theory of automorphic functions [Shi71]).

First of all, we remark that the topological space $X(\Delta)$ we constructed is actually a compact Riemann surface and a locally compact Hausdorff space. There is a natural projection map from the extended upper half plane to this surface

$$\pi = \pi_\Delta: \mathbb{H}^* \rightarrow X(\Delta).$$

The definition of elliptic points and cusps is pushed forward to describe special points on the Riemann surface $X(\Delta)$.

Definition. Let Δ be a Fuchsian group and $X(\Delta)$ the corresponding Riemann surface as constructed above.

- A point $z \in X(\Delta)$ is a *cusps* if there is a point $x \in \pi^{-1}(z) \subseteq \mathbb{H}^*$ in the fiber such that x is a cusp for Δ .
- A point $z \in X(\Delta)$ is an *elliptic point*, if there is a point $x \in \pi^{-1}(z) \subseteq \mathbb{H}^*$ in the fiber such that x is an elliptic point for Δ .
- The *genus* of the Fuchsian group is the genus of the Riemann surface $X(\Delta)$.

Remark. If one point in the fiber is a cusp, respectively an elliptic point, all points in the fiber are. In fact, let $x \in \pi^{-1}(z)$ be a cusp which means there is a parabolic element $P \in \Delta$ fixing $x = P.x$. If y is another point in the fiber, there is an element $D \in \Delta$ mapping x to y : $D.x = y$. Now, the element DPD^{-1} fixes y and is parabolic since the trace is invariant under conjugation.

Let Δ be a Fuchsian group and $\mathfrak{F} = \mathfrak{F}_\Delta \subseteq \overline{\mathbb{H}^*}$ a fundamental domain for Δ . We restrict the projection map to the fundamental domain,

$$\pi|_{\mathfrak{F}}: \mathfrak{F} \rightarrow X(\Delta).$$

Due to the definition of \mathfrak{F} the map is still surjective. Furthermore, if we restrict this map to the interior $\overset{\circ}{\mathfrak{F}}$, it is also injective. On the boundary, the fiber of a point can (and in general will) contain more than one point. The quotient map identifies these points. These identifications of the borders are called the *side pairings*. The following theorem is crucial for chapter 6.

2.14 Theorem. *Let Δ be a Fuchsian group and \mathfrak{F} a fundamental domain of Δ , bounded by geodesics. Then, the side pairings generate the group Δ .*

Proof. See [Kat92], Section 3.2 to 3.5 – especially theorem 3.5.4 or [Bea95, theorem 9.2.7]. \square

Coverings

We have seen that for a subgroup of finite index $\Gamma \subseteq \Delta$ of a Fuchsian group, we can construct a fundamental domain for Γ from a fundamental domain of Δ using the cosets of $\Gamma \backslash \Delta$. In terms of the corresponding Riemann surfaces, we obtain a commutative diagram.

$$\begin{array}{ccc}
 & \Gamma \backslash \mathbb{H}^* & \\
 \nearrow \pi_\Gamma & & \downarrow \varphi \\
 \mathbb{H}^* & & \Delta \backslash \mathbb{H}^* \\
 \searrow \pi_\Delta & &
 \end{array} \tag{2.15}$$

First of all, we must remark that $\mathbb{H}^* = \mathbb{H}_\Delta^* = \mathbb{H}_\Gamma^*$. The two extensions of the upper half plane coincide. This is due to the fact that the cusps of the finite index subgroup Γ coincide with that of Δ – see [Miy06, corollary 1.5.5]. Hence, the maps π_Γ and π_Δ are the projections from the same extended upper half plane. The map φ maps a Γ -orbit of a point $z \in \mathbb{H}^*$ to the corresponding Δ -orbit. This map is well defined. If $z' \in \mathbb{H}^*$ is another point in \mathbb{H}^* representing the same orbit, there is a matrix $\gamma \in \Gamma$ such that $z = \gamma.z'$. Since $\Gamma \subseteq \Delta$, the point z and z' also represent the same Δ -orbit. The map φ turns out to be a branched covering of Riemann surfaces. So we start with the definition of a covering.

Definition. Let X be a topological space. A *covering space* of X is a topological space E together with a continuous, surjective map $p: E \rightarrow X$, such that for every point $x \in X$, there is a neighborhood U_x of x , such that the inverse image $p^{-1}(U_x)$ of U_x is isomorphic to a disjoint union of copies of U_x .

Remark. If the base space X is connected, locally path-connected and semi-locally simply connected, it can be shown that there is always a simply connected covering. This covering is called the *universal covering*. See [Hat01, p. 59] for the construction.

The map φ described in (2.15) is not a covering according to the previous definition. If we have for example an elliptic point on the Riemann surface $X(\Delta)$, the fiber over this point has a different cardinality than a generic point. Therefore, we need to loosen the definition of the covering and introduce branched coverings.

Definition. We call a map f between Riemann surfaces $f: X \rightarrow Y$ a *branched covering* if there is a finite set $S \subseteq X$, such that the map $f|_{X \setminus S}: X \setminus S \rightarrow Y \setminus f(S)$ is a covering. If we choose S to be the minimal set with this property, we call a point in S *singular point* and a point in $f(S) \subseteq Y$ a *branching point*.

This definition fits our purposes and we show that the map we defined is such a branched covering.

2.16 Lemma. *Let Δ be a Fuchsian group and $\Gamma \subseteq \Delta$ a subgroup of finite index. Then, we have an induced map on the quotients, respectively on the corresponding Riemann surfaces*

$$\begin{aligned} \varphi: X(\Gamma) &\rightarrow X(\Delta), \\ \Gamma z &\mapsto \Delta z. \end{aligned}$$

This map is a well defined, branched covering. It is branched over the elliptic and parabolic points of Δ .

Proof. We already saw that the map is well defined. Using diagram (2.15), we calculate the fibers of the map φ . We fix one point $z \in \mathbb{H}^*$ on the extended upper half plane.

$$\begin{aligned} \varphi^{-1}(\Delta z) &= \pi_{\Gamma} \left(\pi_{\Delta}^{-1}(z) \right) \\ &= \pi_{\Gamma} (\{ \delta z \mid \delta \in \Delta \}) \\ &= \{ \Gamma \delta z \mid \delta \in \Delta \}. \end{aligned}$$

Two elements $\Gamma A z$ and $\Gamma A' z$ in this set are equal if and only if there is a $\gamma \in \Gamma$ such that $A z = \gamma A' z$. If we now assume that z is neither an elliptic point nor a cusp, we obtain the condition that there exists a $\gamma \in \Gamma$ such that $A = \gamma A'$. Since this is the defining relation for the cosets $\Gamma \backslash \Delta$, we describe the fiber as follows. Let c_1, \dots, c_r be coset representative of $\Gamma \backslash \Delta$, then

$$\varphi^{-1}(\Delta z) = \{ \Gamma c_1 z, \dots, \Gamma c_r z \}.$$

Since we assume that z is neither an elliptic point nor a cusp, all of these elements are distinguished. Hence, the map φ is a covering with possible branching over the elliptic point and the cusps. \square

Later, we will define subgroups of certain Fuchsian groups, using the monodromy representation. To understand this notion, we give the general definition of monodromy. To do this, we start with the definition of the fundamental group of a topological space – see also [Hat01, p.26f] or [For77, section 3.8]. For this definition, we need the unit sphere, denoted by \mathbb{S}^1

$$\mathbb{S}^1 = \left\{ (x, y) \in \mathbb{R}^2 \mid x^2 + y^2 = 1 \right\} \subseteq \mathbb{R}^2.$$

We fix a point on the sphere which we call the north pole $N = (0, 1)$.

Definition. Let X be a topological space, $x_0 \in X$ a point and the unit circle equipped with the Euclidian topology. Then, we define the fundamental group as loops on the point x_0 up to homotopy

$$\pi_1(X, x_0) := \left\{ f: X \rightarrow \mathbb{S}^1 \mid f \text{ continuous and } f(x_0) = N \right\} / \sim.$$

The equivalence relation \sim is the homotopy. Two loops f and g are homotopy equivalent if there is a homotopy $H: [0, 1] \times X \rightarrow \mathbb{S}^1$, such that H is continuous, $H(0, x) = f(x)$, $H(1, x) = g(x)$ and $H(t, x_0) = N$ for all $t \in [0, 1]$.

We define on the set $\pi_1(X, x_0)$ a group structure by the composition of loops.

Example. As before, we denote by \mathbb{S}^1 the unit circle. Then, one shows that for every $x_0 \in \mathbb{S}^1$ the following holds

$$\pi_1(\mathbb{S}^1, x_0) = \mathbb{Z}.$$

This is proven for example in [Hat01, p.26ff].

It is possible to calculate the fundamental group of an arbitrary compact Riemann surface. To do this, one should first see that any compact Riemann surface is homeomorphic to a sphere which g handles where g is the genus of the surface. Then, we can proof the following theorem.

2.17 Theorem. *Let X be a compact Riemann surface of genus g . Then, for any base point x_0 , we have that the fundamental group $\pi_1(X, x_0)$ is a free group on the generators $a_1, b_1, \dots, a_g, b_g$ divided out by the subgroup generated by $[a_1, b_1] \cdot \dots \cdot [a_g, b_g]$ where $[\cdot, \cdot]$ is the commutator.*

Proof. See [Jos97, theorem 2.4.3]. In this source, you also find a geometric interpretation of the elements $a_1, \dots, a_g, b_1, \dots, b_g$. □

Since for a Fuchsian group Δ the Riemann surface $X(\Delta)$ is compact, we apply this theorem and obtain its fundamental group.

Now, we introduce the monodromy. Therefore, we consider the following setting. Let X be a topological space and $p: E \rightarrow X$ a covering. We fix a base point $x_0 \in X$ and denote the fundamental group with $\pi_1(X, x_0)$. There is an operation of this fundamental group on the fiber $p^{-1}(x_0)$, defined in the following way. Let $e_0 \in p^{-1}(x_0)$ be a point

in the fiber and $\gamma \in \pi_1(X, x_0)$ a loop in X . This loop is lifted to a unique path in E starting in e_0 . Denoting this path with $\tilde{\gamma}_{e_0}$ and the end point with $e_1 = \tilde{\gamma}_{e_0}(1) \in p^{-1}(x_0)$, we obtain a permutation of the points in the fiber, via $e_0 \mapsto e_1$. Altogether, we have a map with n the degree of the map p

$$\begin{aligned} \pi_1(X, x_0) &\rightarrow \text{Aut}(p^{-1}(x_0)) \cong S_n \\ \gamma &\mapsto (e_0 \mapsto \tilde{\gamma}_{e_0}(1)). \end{aligned}$$

We call the image of this homomorphism the *monodromy group* of the covering.

Chapter 3.

Automorphic forms and functions

There are five elementary, arithmetical operations: addition, subtraction, multiplication, division, and ... modular forms.

(Matrin Eichler)

Around 1750 Giulio Carlo Fagnano dei Toschi and Leonhard Euler looked at the problem of calculating the circumference of an ellipse. The result is now known as the complete elliptic integral of the second kind. They continued to calculate the arc length of an ellipse. This is nowadays known as an incomplete elliptic integral. Several years later, around 1825, Niels Henrik Abel had the idea of looking at the *inverse* functions of the elliptic integral to get a better understanding of them. These functions are the elliptic functions.

Another central contribution came from Karl Weierstrass by introducing the *Weierstrass's elliptic function*. All elliptic functions can be described using this function and its derivative. Carl Gustav Jakob Jacobi improved this theory – he introduced the notion of the theta functions. These theta functions and generalizations of them are still under investigation and not yet fully understood.

In the book *Vorlesungen über das Ikosaeder und die Auflösung der Gleichungen vom 5ten Grade* by Felix Klein [Kle84], he started to investigate the automorphic properties and set out a theory of *automorphic forms*. What now became important are the transformation properties of the functions we mentioned before.

At this point the question arose, whether it is possible to calculate a function with a given automorphic property. A partial answer gave Erich Hecke by introducing the concept of *Hecke operators* ([Hec36] and [Hec37]). These operators operate on automorphic forms and make it possible to actually find automorphic forms. Up to now, it was only possible to find these Hecke operators for the *congruence subgroups*. Although it was possible to calculate automorphic form for some special cases ([FHL⁺10], [LLY05a]), it is still an open problem, how to calculate automorphic forms efficiently. There were some attempts to write down Hecke operators for non-congruence subgroup, but these definitions did not yield the desired results – see for example [Ber94]. For automorphic functions we will give an algorithm how to solve this problem numerically.

In this chapter we introduce the concept of automorphic forms and automorphic functions for a general Fuchsian group. Aside from the definitions, we state some examples and formulate the central properties which we will need later. A priori these functions

are functions on the upper half plane. Nevertheless, they can also be defined in terms of the Riemann surface $X(\Delta)$ for a Fuchsian group Δ . Finally, we use a special automorphic function, the *hauptmodul*, to lift the branched covering (2.15) from the previous chapter to a covering $\mathbb{P}^1(\mathbb{R}) \rightarrow \mathbb{P}^1(\mathbb{R})$ which will be a rational function. It will be necessary that the involved groups have genus zero.

As in the previous chapter, we continue to write Fuchsian group, whenever we mean a Fuchsian group of the first kind.

Automorphic forms

An automorphic form is a function on the upper half plane, with a certain transformation behavior under a given Fuchsian group. To describe this behavior we introduce the slash operator.

Definition. Let $\Gamma \subseteq \mathrm{PSL}_2(\mathbb{R})$ a Fuchsian group. We define a right action of Γ , the *slash operator of weight k* , on the set of all functions $f: \mathbb{H} \rightarrow \mathbb{C}$. For $\gamma = \begin{pmatrix} a & b \\ c & d \end{pmatrix} \in \mathrm{PSL}_2(\mathbb{R})$ we let

$$(f|_k \gamma)(z) := (cz + d)^{-k} f(\gamma z).$$

This operation is actually a group operation [Miy06, p. 37]. It is also possible to generalize this operation to an operation of the group $\mathrm{GL}_2^+(\mathbb{R})$, the group of invertible matrices with positive determinant. For this group we introduce a factor on the right-hand side

$$(f|_k \gamma)(z) := \det(\gamma)^{\frac{k}{2}} (cz + d)^{-k} f(\gamma z).$$

In the last chapter we have introduced the extended upper half plane \mathbb{H}_Δ^* for a Fuchsian group Δ – equation (2.13). For automorphic forms we require in addition to the transformation property a smoothness conditions.

Definition. Let Δ be a Fuchsian group acting on the extended upper half plane \mathbb{H}_Δ^* and $k \in \mathbb{Z}$. Then, we define

- (i) The space of *meromorphic, automorphic forms of weight k*

$$A_k(\Delta) := \left\{ f: \mathbb{H}_\Delta^* \rightarrow \mathbb{C} \mid f \text{ is meromorphic and } \forall \gamma \in \Delta : f|_k \gamma = f \right\}.$$

A meromorphic, automorphic forms of weight 0 is also called an *automorphic function*.

- (ii) The space of *automorphic forms of weight k*

$$G_k(\Delta) := \left\{ f: \mathbb{H}_\Delta^* \rightarrow \mathbb{C} \mid f \text{ is holomorphic and } \forall \gamma \in \Delta : f|_k \gamma = f \right\}.$$

(iii) The set of *cuspidal forms of weight k*

$$S_k(\Delta) := \left\{ f: \mathbb{H}_\Delta^* \rightarrow \mathbb{C} \mid f \text{ is holomorphic, } \forall \gamma \in \Delta: f|_k \gamma = f \text{ and } f \text{ vanishes at all cusps} \right\}.$$

We define the space of *all meromorphic, automorphic forms* by

$$A(\Delta) := \bigoplus_{k=-\infty}^{\infty} A_k(\Delta).$$

Analog to this, we define the space of *all automorphic forms* and *all cuspidal forms* in the following way.

$$G(\Delta) := \bigoplus_{k=-\infty}^{\infty} G_k(\Delta), \quad S(\Delta) := \bigoplus_{k=-\infty}^{\infty} S_k(\Delta).$$

We have the following inclusions of these spaces

$$A_k(\Delta) \supseteq G_k(\Delta) \supseteq S_k(\Delta).$$

3.1 Theorem. *Let Δ be a Fuchsian group. Then, the following holds.*

- (i) *If Δ has no cusps, then $G_k(\Delta) = S_k(\Delta)$ for all $k \in \mathbb{Z}$.*
- (ii) *If k is odd, then $A_k(\Delta) = \{0\}$.*
- (iii) *If $f \in A_k(\Delta)$, then $1/f \in A_{-k}(\Delta)$.*
- (iv) *If $f \in A_k(\Delta)$ and $g \in A_l(\Delta)$, then $fg \in A_{k+l}(\Delta)$.*
- (v) *If $f \in G_k(\Delta)$ and $g \in G_l(\Delta)$, then $fg \in G_{k+l}(\Delta)$.*
- (vi) *If $f \in G_k(\Delta)$ and $g \in S_l(\Delta)$, then $fg \in S_{k+l}(\Delta)$.*
- (vii) *The rings $A(\Delta)$, $G(\Delta)$, and $S(\Delta)$ are graded rings.*

Proof. See [Miy06, section 2.1]. □

This theorem shows that the space of automorphic functions $A_0(\Delta)$ is actually a field under the multiplication of functions. From a geometric point of view this field can be interpreted as follows. The condition for being an automorphic function is on the one hand being meromorphic on the upper half plane and the cusps. On the other hand the transformation condition needs to be satisfied.

$$\begin{aligned} j \in A_0(\Delta) &\Rightarrow \forall \gamma \in \Delta: \forall z \in \mathbb{H}^*: \left(f|_0 \gamma \right) (z) = j(z) \\ &\Leftrightarrow \forall \gamma \in \Delta: \forall z \in \mathbb{H}^*: j(\gamma z) = j(z). \end{aligned}$$

The transformation condition for automorphic function is the condition that the function is invariant under the operation of the underlying Fuchsian group. Hence, this function factors through a meromorphic function on the Riemann surface $X(\Delta)$.

$$\begin{array}{ccc}
 \mathbb{H}^* & \xrightarrow{j} & \mathbb{P}^1(\mathbb{C}) \\
 & \searrow \pi_\Delta & \nearrow f \\
 & & X(\Delta)
 \end{array} \tag{3.2}$$

Here, f is a meromorphic function on $X(\Delta)$, an element of the function field $K(X(\Delta))$. Conversely, for such a function f in the function field, we lift f to a function $j \in A_0(\Delta)$, via $j = f \circ \pi_\Delta$. Hence, we have shown the following lemma.

3.3 Lemma. *Let Δ be a Fuchsian group. Then, the function field $K(X(\Delta))$ of $X(\Delta)$ is isomorphic to the ring of meromorphic functions $A_0(\Delta)$, via the following isomorphism*

$$K(X(\Delta)) \rightarrow A_0(\Delta) \quad f \mapsto j = f \circ \pi_\Delta.$$

To write down automorphic forms and functions we make the following remark, see Shimura [Shi71, section 1.5 and 2.1]. Let Δ be a Fuchsian group with a cusp $p \in \mathbb{H}_\Delta^*$. We find a map $R \in \text{PSL}_2(\mathbb{R})$, such that $R.p = \infty$: theorem 2.6, part (i). Then, we write the stabiliser $\Delta_p = \{A \in \Delta \mid A.p = p\}$ as follows

$$R \Delta_p R^{-1} \cdot \{\pm 1\} = \left\{ \pm \begin{pmatrix} 1 & w \\ 0 & 1 \end{pmatrix}^m \mid m \in \mathbb{Z} \right\},$$

where $w = w_p \in \mathbb{R}_{>0}$ is a positive real number. We call w the *cuspidal width* of the cusp p . Now let $f \in A_k(\Delta)$ be a meromorphic, automorphic function. Due to the transformation condition of f the function $f|_k R^{-1}$ is invariant under all $A \in R \Delta_p R^{-1}$.

$$(f|_k R^{-1})|_k A = f|_k R^{-1}.$$

Since $\begin{pmatrix} 1 & w \\ 0 & 1 \end{pmatrix} \in R \Delta_p R^{-1}$, the function $f|_k R^{-1}$ is invariant under $z \mapsto z + w$. Due to this periodicity condition, we write the function $f|_k R^{-1}$ as follows.

$$f|_k R^{-1} = \sum_{n \geq n_0} c_n e^{2\pi i n \tau / w} = \sum_{n \geq n_0} c_n q^n. \tag{3.4}$$

We call this the *Fourier expansion of f at the cusp p* and the numbers c_n the *Fourier coefficients of f* . We use the common abbreviation $q = q_w = \exp(2\pi i \tau / w)$. The expansion (3.4) is sometimes also called the q -series of f at p . If we take about the q -series, we mean the series at $p = \infty$.

Examples of automorphic forms and automorphic functions

The first examples that we give are from the article *Elliptic modular forms and Their Applications* by Zagier [Zag08]. Starting with a vector space V with group operation (of a finite group G) there is an elementary way of finding invariant vectors. For an arbitrary vector $v \in V$ we take the sum $\sum_{g \in G} g.v$, where $g.v$ is the group operation. If the vector v is already invariant under a subgroup $H \subseteq G$, it suffices to sum only over a set of coset representatives $H \backslash G$: $\sum_{g \in H \backslash G} g.v$. However, a Fuchsian group is not finite, we still would like to use this. Here, the vector space is the of functions on \mathbb{H}^* and the group operation is the slash operator. This results in the *Poincaré series* - see [Kol95, chapter 5].

To obtain a concrete example, we look at the modular group $\mathrm{PSL}_2(\mathbb{Z})$. The subgroup we choose to be the stabiliser of ∞ : $\Gamma_\infty = \langle \begin{pmatrix} 1 & n \\ 0 & 1 \end{pmatrix} \rangle$. According to theorem 3.1, there are no automorphic forms, if k odd. Hence, we assume k to be even. We calculate the cosets of this subgroup. They are parameterized by the pairs $(c, d) \in \mathbb{Z}^2$ with (c, d) coprime. For each such pair there is exactly one pair (a, b) , such that $\begin{pmatrix} a & b \\ c & d \end{pmatrix} \in \mathrm{PSL}_2(\mathbb{Z})$. Using this, we introduce the *Eisenstein series of weight k for $\mathrm{PSL}_2(\mathbb{Z})$* for $k \in \mathbb{Z} > 2$

$$E_k(z) = \sum_{\gamma \in \Gamma_\infty \backslash \Gamma} 1|_k \gamma = \frac{1}{2} \sum_{\substack{(c,d) \in \mathbb{Z}^2 \\ (c,d)=1}} \frac{1}{(cz+d)^k}.$$

It is possible to calculate the q -series of the Eisenstein series.

3.1 Proposition. *Let $E_k(z)$ the Eisenstein series as defined before for $k > 2$ and $\zeta(s) = \sum_{i=1}^n \frac{1}{i^s}$ the Riemann zeta function. We renormalize the Eisenstein series by*

$$\mathbb{E}_k(z) = \frac{(2\pi i)^k}{\zeta(k)(k-1)!} E_k(z).$$

Then, the series $\mathbb{E}_k(z)$ has the following Fourier expansion.

$$\mathbb{E}_k(z) = -\frac{B_k}{2k} + \sum_{n=1}^{\infty} \sigma_{k-1}(n) q^n,$$

where B_k is the k th Bernoulli number and $\sigma_{k-1}(n)$ for $n \in \mathbb{N}$ denotes the sum of the $(k-1)$ st power of the positive divisors of n .

Proof. See [Zag08, Proposition 5]. □

As an example of an automorphic function, we give the first terms of the q -series of the *modular invariant* or *Klein's j -invariant*.

$$j(z) = \frac{1}{q} + 744 + 196884q + 21493760q^2 + 864299970q^3 + \mathcal{O}(q^4).$$

This function is an automorphic function for $\mathrm{PSL}_2(\mathbb{Z})$ and every automorphic function is a rational function of this function [Apo90, theorem 2.8]. Inspired by this example, we define the notion of a *hauptmodul*.

Definition. Let Δ be a Fuchsian group of genus zero and at least one cusp. Furthermore, let the expansion parameter at the cusp infinity be q . We call an automorphic function $j: \mathbb{H}^* \rightarrow \mathbb{P}^1(\mathbb{C})$ a *hauptmodul*, if

- (i) $j = \frac{1}{q} + \mathcal{O}(q)$ and
- (ii) the corresponding function in the function field $K(X(\Delta))$ generates the function field.

Such a hauptmodul is unique: [CY95]. Sometimes we will also call the corresponding function in the function field the hauptmodul of the Fuchsian group.

Dimension formulas

In this short passage, we cite the dimensions of the space of automorphic forms. We call two elliptic point $\tau_1, \tau_2 \in \mathbb{H}$ equivalent under a Fuchsian group Δ , if there is a $\delta \in \Delta$, such that $\tau_1 = \delta.\tau_2$. These dimension formulas are deduced by using the Riemann-Roch theorem. For detail we refer to the book by Shimura [Shi71]. In this reference you also find the definition *regular* and *irregular* cusps, which are necessary to state these theorems but we will not use them in this thesis later on.

3.5 Theorem. *Let Δ be a Fuchsian group of genus g . The number of inequivalent cusps is m and e_1, \dots, e_r the orders of the inequivalent elliptic elements of \mathbb{H}^* .*

- (i) *The dimension of the space of automorphic forms $G_k(\Delta)$, for an even integer k , is*

$$\dim G_k(\Delta) = \begin{cases} (k-1)(g-1) + m\frac{k}{2} + \sum_{i=1}^r \frac{k(e_i-1)}{2e_i} & \text{for } k > 2, \\ g + m - 1 & \text{for } k = 2, m > 0, \\ g & \text{for } k = 2, m = 0, \\ 1 & \text{for } k = 0, \\ 0 & \text{for } k < 0. \end{cases}$$

- (ii) *Suppose that $-1 \notin \Delta$ and let u be the number of regular cusps and u' the number of irregular cusps. The dimension of the space of automorphic forms $G_k(\Delta)$, for an odd integer k , is*

$$\dim G_k(\Delta) = \begin{cases} (k-1)(g-1) + u\frac{k}{2} + u'\frac{k-1}{2} + \sum_{i=1}^r \frac{k(e_i-1)}{2e_i} & \text{for } k \geq 3, \\ 0 & \text{for } k < 0. \end{cases}$$

If we do not assume that $-1 \notin \Delta$ in part two of the theorem, we know from 3.1, part 2 that there are no forms. The second theorem is the analog theorem for cusp forms.

3.6 Theorem. *Let Δ be a Fuchsian group of genus g . The number of inequivalent cusps is m and e_1, \dots, e_r the orders of the inequivalent elliptic elements of \mathbb{H}^* .*

(i) The dimension of the space of cusp forms $S_k(\Delta)$, for an even integer k , is

$$\dim S_k(\Delta) = \begin{cases} (k-1)(g-1) + m\left(\frac{k}{2} - 1\right) + \sum_{i=1}^r \frac{k(e_i-1)}{2e_i}, & \text{for } k > 2, \\ g & \text{for } k = 2, \\ 1 & \text{for } k = 0, m = 0, \\ 0 & \text{for } k = 0, m > 0, \\ 0 & \text{for } k < 0. \end{cases}$$

(ii) Suppose that $-1 \notin \Delta$ and let u be the number of regular cusps and u' the number of irregular cusps. The dimension of the space of cusp forms $S_k(\Delta)$, for an odd integer k , is

$$\dim S_k(\Delta) = \begin{cases} (k-1)(g-1) + u\frac{k-2}{2} + u'\frac{k-1}{2} + \sum_{i=1}^r \frac{k(e_i-1)}{2e_i} & \text{for } k \geq 3, \\ 0 & \text{for } k < 0. \end{cases}$$

The rational covering R_Γ

We fix a Fuchsian group Δ and a subgroup of finite index Γ – both of genus zero and with at least one cusp. As we have seen, an automorphic function for the Fuchsian group Δ is equivalent to an element of the function field of the corresponding Riemann surface $K(X(\Delta))$. Hence, we find for the hauptmodul j_Δ of Δ a function $f_\Delta: X(\Delta) \rightarrow \mathbb{P}^1(\mathbb{C})$ (formula (3.2)). Analog for Γ we find a function $f_\Gamma: X(\Gamma) \rightarrow \mathbb{P}^1(\mathbb{C})$. For the Riemann surfaces we calculated a covering $\varphi: X(\Gamma) \rightarrow X(\Delta)$ (formula (2.15)). This covering lifts to a branched covering $R_\Gamma: \mathbb{P}^1(\mathbb{C}) \rightarrow \mathbb{P}^1(\mathbb{C})$. It branches over the images of the elliptic and parabolic points of $X(\Gamma)$.

$$\begin{array}{ccccc} & & X(\Gamma) & & \\ & \nearrow \pi_\Gamma & \downarrow & \searrow f_\Gamma & \\ \mathbb{H}^* & \xrightarrow{j_\Gamma} & \mathbb{P}^1(\mathbb{C}) & & \\ & & \downarrow \varphi & & \\ & & X(\Delta) & & \\ & \nearrow \pi_\Delta & \downarrow & \searrow f_\Delta & \\ \mathbb{H}^* & \xrightarrow{j_\Delta} & \mathbb{P}^1(\mathbb{C}) & & \\ & & & & \downarrow R_\Gamma \\ & & & & \mathbb{P}^1(\mathbb{C}) \end{array} \quad (3.7)$$

This function R_Γ is a rational function in j_Γ . In fact, j_Δ is also invariant under Γ and therefore, an element of the function field. The hauptmodul j_Γ generates this function field which implies that R_Γ is a rational function since $j_\Delta = R_\Gamma(j_\Gamma)$.

Chapter 4.

Triangle groups

If people do not believe that mathematics is simple, it is only because they do not realize how complicated life is.

(John von Neumann)

This chapter is about triangle groups and Hecke groups. We define them as finitely presented groups and give a geometric interpretation of them as symmetry groups of a triangle tessellation. Using this tessellation, we calculate an embedding of the hyperbolic triangle groups into $\mathrm{PSL}_2(\mathbb{R})$ making the Fuchsian groups. We classify the finite index subgroups of the triangle groups and solve the word problem.

Introduction to triangle groups

Definition. Let $a, b, c \in \mathbb{Z}_{\geq 2} \cup \{\infty\}$ with $a \leq b \leq c$. The *triangle group* $\Delta(a, b, c)$ is the following finitely presented group.

$$\begin{aligned}\Delta(a, b, c) &:= \langle \delta_a, \delta_b, \delta_c \mid \delta_a^a = \delta_b^b = \delta_c^c = \delta_a \delta_b \delta_c = 1 \rangle \\ \Delta(a, b) &:= \Delta(a, b, \infty) = \langle \delta_a, \delta_b, \delta_c \mid \delta_a^a = \delta_b^b = \delta_a \delta_b \delta_c = 1 \rangle.\end{aligned}$$

We call the triangle group $\Delta(a, b, c)$

- (i) *spherical* if $\frac{1}{a} + \frac{1}{b} + \frac{1}{c} > 1$,
- (ii) *euclidian* if $\frac{1}{a} + \frac{1}{b} + \frac{1}{c} = 1$,
- (iii) *hyperbolic* if $\frac{1}{a} + \frac{1}{b} + \frac{1}{c} < 1$,

where we define $\frac{1}{\infty}$ to be zero. Furthermore, the Hecke groups are the triangle groups

$$\Delta_n := \Delta(2, n) = \Delta(2, n, \infty).$$

4.1 Proposition. *The classification of the triangle groups is the following.*

- (i) *The spherical groups are $\Delta(2, 3, 3)$, $\Delta(2, 3, 4)$, $\Delta(2, 3, 5)$, and $\Delta(2, 2, n)$ for $2 \leq n < \infty$.*
- (ii) *The Euclidian groups are $\Delta(2, 2, \infty)$, $\Delta(2, 3, 6)$, $\Delta(2, 4, 4)$, and $\Delta(3, 3, 3)$.*

(iii) All other triangle groups are hyperbolic.

Proof. See for example Klug et. al [KMSV14] or [Rat05, Chapter 7.2]. \square

Before we explain why these groups are called the triangle groups, we introduce the extended triangle groups.

Definition. Let $a, b, c \in \mathbb{Z}_{\geq 2} \cup \{\infty\}$ with $a \leq b \leq c$. The *extended triangle group* $\Delta^*(a, b, c)$ is the following finitely presented group.

$$\begin{aligned} \Delta^*(a, b, c) &:= \langle \tau_a, \tau_b, \tau_c \mid \tau_a^2 = \tau_b^2 = \tau_c^2 = (\tau_c \tau_b)^a = (\tau_a \tau_c)^b = (\tau_b \tau_a)^c = (\tau_c \tau_b \tau_a)^2 = 1 \rangle, \\ \Delta^*(a, b) &:= \Delta^*(a, b, \infty) = \langle \tau_a, \tau_b, \tau_c \mid \tau_a^2 = \tau_b^2 = \tau_c^2 = (\tau_c \tau_b)^a = (\tau_a \tau_c)^b = (\tau_c \tau_b \tau_a)^2 = 1 \rangle, \\ \Delta_n^* &= \Delta^*(2, n) = \Delta^*(2, n, \infty). \end{aligned}$$

The triangle groups $\Delta(a, b, c)$ are subgroups of index 2 in the extended triangle groups $\Delta^*(a, b, c)$. We embed them via

$$\Delta(a, b, c) \rightarrow \Delta^*(a, b, c), \quad \delta_a = \tau_c \tau_b, \quad \delta_b = \tau_a \tau_c, \quad \delta_c = \tau_b \tau_a. \quad (4.1)$$

These groups have a nice geometric interpretation – see [Mag74]. Let F be a triangle with angles $\frac{\pi}{a}$, $\frac{\pi}{b}$, and $\frac{\pi}{c}$. We define the angle $\frac{\pi}{\infty}$ to be zero. This triangle is spherical, Euclidian, respectively hyperbolic, if the triangle group $\Delta(a, b, c)$ is spherical, Euclidian, respectively hyperbolic. Then, the generators τ_a, τ_b , and τ_c of the extended triangle group are reflections at the three sides of the triangle.

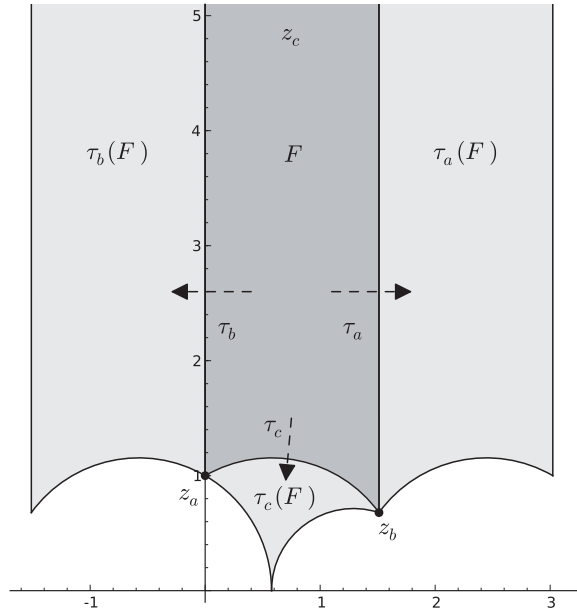


Figure 4.1.: Reflections on a hyperbolic triangle with angles $\frac{\pi}{3}$, $\frac{\pi}{5}$, and 0

Note that these operations are anti-holomorphic and orientation-reversing. If we fix such a triangle, we obtain a tessellation of the sphere for the spherical triangle groups,

of the Euclidean plane for the Euclidean ones and for the upper half plane for the hyperbolic groups. This tessellation of the underlying space will be drawn with gray and white triangles. Each of those triangles is a fundamental domain for the extended triangle group operating on this space. For a fundamental domain of the triangle group we have to join exactly one white and one gray triangle.

Rotations of the triangles around the vertices generate the triangle group. These rotations are products of two reflections.

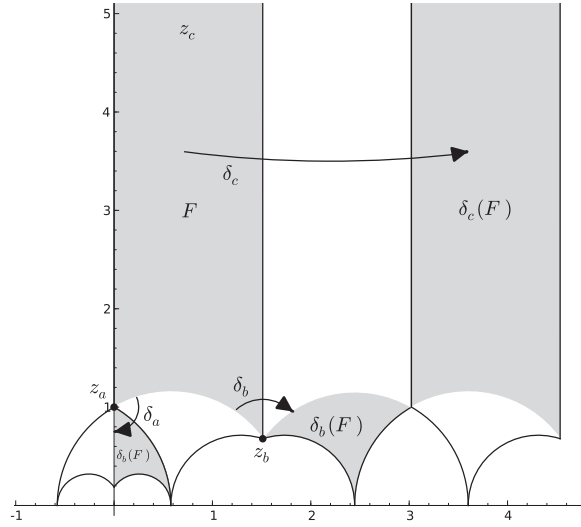


Figure 4.2.: Rotations on a hyperbolic triangle with angles $\frac{\pi}{3}$, $\frac{\pi}{5}$, and 0

Since there is just a finite number of Euclidean triangle groups, we present them in figure 4.3 to 4.6. For the spherical groups, we give one example of the family $\Delta(2, 2, n)$, figure 4.7 and $\Delta(2, 3, 4)$, figure 4.8.

Geometric realizations of the triangle groups

$\Delta(a, b, \infty)$

We focus on the non-compact, hyperbolic triangle groups $\Delta(a, b, \infty)$. We show that these groups are actually Fuchsian groups by giving an explicit embedding into $\text{PSL}_2(\mathbb{R})$. We start by constructing a triangle with given angles and use this to write down matrices in $\text{PSL}_2(\mathbb{R})$ which represent the elements in the triangle group.

The construction of the triangle and the embedding of the triangle groups in $\text{PSL}_2(\mathbb{R})$ are inspired by the article *Numerical Calculation of three-point branched covers of the projective line* by Klug et. al [KMSV14]. In this article they did the analog construction for the compact triangle groups $\Delta(a, b, c)$, where $c < \infty$.

Let $\Delta(a, b)$ be a hyperbolic triangle group. Then, we define the angles $\alpha = \frac{\pi}{a}$, $\beta = \frac{\pi}{b}$,

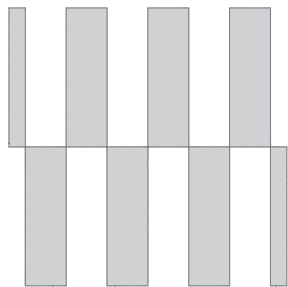


Figure 4.3.: $\Delta(2, 2)$

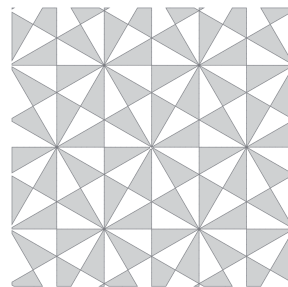


Figure 4.4.: $\Delta(2, 3, 6)$

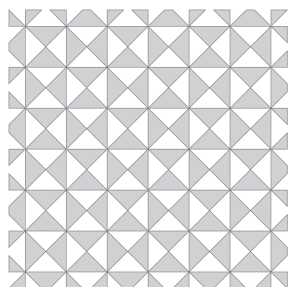


Figure 4.5.: $\Delta(2, 4, 4)$

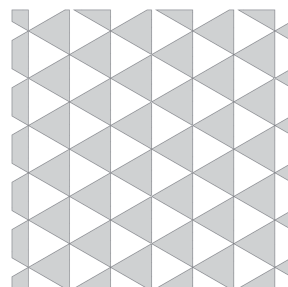


Figure 4.6.: $\Delta(3, 3, 3)$



Figure 4.7.: $\Delta(2, 2, 6)$



Figure 4.8.: $\Delta(2, 3, 4)$

and $\gamma = \frac{\pi}{\infty} = 0$. Recall that the hyperbolic distance in upper half plane \mathbb{H} is (see (2.1))

$$d: \mathbb{H} \times \mathbb{H} \rightarrow \mathbb{R}_{\geq 0},$$

$$d(x_1 + iy_1, x_2 + iy_2) = \operatorname{arcosh} \left(1 + \frac{(x_2 - x_1)^2 + (y_2 - y_1)^2}{2y_1y_2} \right).$$

Due to the same arguments as in [KMSV14], we assume $z_a = i$ and $z_c = \mu i$ for some $\mu \in \mathbb{R}_{>1} \cup \{\infty\}$ and $\operatorname{Re}(z_b) > 0$. We start with any triangle and since $\operatorname{PSL}_2(\mathbb{R})$ operates transitively, we may choose $z_a = i$. Then, we rotate the triangle around i and may assume $z_c = \mu i$, for some $\mu \in \mathbb{R}_{>1}$. Finally, we reflect the triangle at the imaginary axis and assume $\operatorname{Re}(z_b) > 0$.

We find μ by using the law of cosines from hyperbolic geometry (2.5). Let B be the

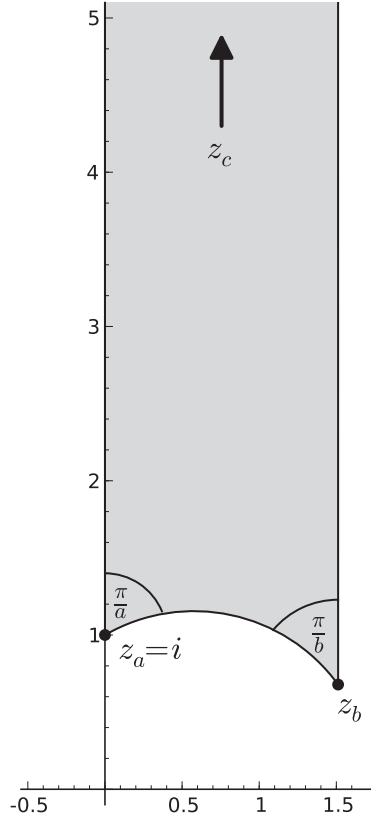


Figure 4.9.: Triangle with angles $\frac{\pi}{a}$, $\frac{\pi}{b}$, and $\frac{\pi}{\infty} = 0$

length of the side opposite the point z_b .

$$\begin{aligned} \cosh(B) &= \frac{\cos \frac{\pi}{a} \cos \frac{\pi}{c} + \cos \frac{\pi}{b}}{\sin \frac{\pi}{a} \sin \frac{\pi}{c}} \\ &= \frac{\cos \frac{\pi}{a} \cos \frac{\pi}{c} + \cos \frac{\pi}{b}}{\sin \frac{\pi}{a} \sin \frac{\pi}{c}} \longrightarrow \infty \text{ as } c \rightarrow 0. \end{aligned}$$

The formula for the hyperbolic distance (2.4) gives us

$$d(i, \mu i) = \operatorname{arcosh} \left(\frac{(\mu - 1)^2}{2\mu} + 1 \right).$$

To find a value of μ , such that this distance becomes infinitely large, we set the distance equal to $t \in \mathbb{R}$, solve the distance for μ and let $t \rightarrow \infty$.

$$\begin{aligned} t &= d(i, \mu^{(t)} i) = \operatorname{arcosh} \left(\frac{(\mu^{(t)} - 1)^2}{2\mu^{(t)}} + 1 \right). \\ \Rightarrow \mu_{1,2}^{(t)} &= \exp(\pm t) \\ \lim_{t \rightarrow \infty} \mu_1^{(t)} &= \lim_{t \rightarrow \infty} \exp(t) = \infty \\ \lim_{t \rightarrow \infty} \mu_2^{(t)} &= \lim_{t \rightarrow \infty} \exp(-t) = 0. \end{aligned}$$

Hence, we have two choices for the triangle. Since we assumed $\mu > 1$, we define $z_c = i \cdot \infty$. Finding the point z_b is more effort than in the compact case. Now, we need to use the two angles $\frac{\pi}{a}$ and $\frac{\pi}{b}$. We first calculate a geodesic going through the point $z_a = i$, such that the angle between this geodesic and the line from i to $i\infty$ is equal to $\frac{\pi}{a}$. Then, we have to find a point on this geodesic, such that the angle between the line z_b to $i\infty$ and the geodesic is equal to $\frac{\pi}{b}$. To perform the calculations, we use the fact that geodesics in upper half plane model of hyperbolic geometry are actually circles in Euclidian geometry with a real center. Hence, the first task – finding a geodesic through z_a with a certain angle – is the same as to find a circle with this property. With $x \in \mathbb{R}$ and $y \in \mathbb{R}_{\geq 0}$ we denote the coordinates in the upper half plane $\tau = x + iy$.

If r is the radius and m the (real) midpoint of the circle in question, we write it as $F(x, y) := (x - r)^2 + y^2 - r^2 = 0$. Asking for z_a to lie on the circle translates to $F(0, 1) = 0$. This gives the following relation between r and m

$$\begin{aligned} 0 &= F(0, 1) \\ &= 1 + m^2 - r^2 \\ \Rightarrow r &= \sqrt{1 - m^2}. \end{aligned}$$

We choose the positive root of this equation – the radius of the circle should be positive. To adjust the midpoint of this circle to have the right angle at z_a we calculate the tangent at the point. For this purpose we use the representation of the circle in parametric form

$$P(\varphi) := \begin{pmatrix} \sqrt{1 + m^2} \cos(\varphi) + m \\ \sqrt{1 + m^2} \sin(\varphi) \end{pmatrix} \quad \text{for } \varphi \in [0, 2\pi].$$

The function P takes at $\varphi_0 = \arccos\left(\frac{-m}{\sqrt{1+m^2}}\right)$ the value $(0, 1)$ which corresponds to i in the upper half plane. Using the derivative of P and inserting φ_0 , we obtain the slope in this point.

$$P'(\varphi_0) = \begin{pmatrix} -1 \\ -m \end{pmatrix}.$$

Hence, the angle in question gives us the following condition which results in a formula for the midpoint m

$$\begin{aligned} \frac{1}{m} &= \tan \frac{\pi}{a} \\ \Rightarrow m &= \cot \frac{\pi}{a} \\ \Rightarrow r &= \sqrt{1 + \cot^2 \frac{\pi}{a}} = \frac{1}{\sin \frac{\pi}{a}} = \csc \frac{\pi}{a}. \end{aligned}$$

In the second step, we need to find a point (which will be z_b) on this circle, such that the angle between the line to infinity and this circle is $\frac{\pi}{b}$. This point should have the

slope $-\tan\left(\frac{\pi}{b}\right)$. We need the minus sign since we are now looking at the supplementary angle.

$$\begin{aligned} P'(\varphi) &= \begin{pmatrix} -\csc\frac{\pi}{a}\sin\varphi \\ \csc\frac{\pi}{a}\cos\varphi \end{pmatrix} = -\tan\frac{\pi}{b} \\ \Rightarrow \varphi_b &= \frac{\pi}{b} \\ \Rightarrow P(\varphi_b) &= P\left(\frac{\pi}{a}\right) = \begin{pmatrix} \cot\frac{\pi}{a} + \cos\frac{\pi}{b}\csc\frac{\pi}{a} \\ \csc\frac{\pi}{a}\sin\frac{\pi}{b} \end{pmatrix} \\ \Rightarrow z_b &= \cot\frac{\pi}{a} + \cos\frac{\pi}{b}\csc\frac{\pi}{a} + i\left(\csc\frac{\pi}{a}\sin\frac{\pi}{b}\right). \end{aligned}$$

We summarize the result of this calculations in the following lemma.

4.2 Lemma. *The hyperbolic triangle with the edges*

$$\begin{aligned} z_a &= i, \\ z_b &= \cot\frac{\pi}{a} + \cos\frac{\pi}{b}\csc\frac{\pi}{a} + i\left(\csc\frac{\pi}{a}\sin\frac{\pi}{b}\right), \\ z_c &= i\infty. \end{aligned}$$

has the angles $\frac{\pi}{a}$, $\frac{\pi}{b}$, and 0.

Remark. For the modular group $\Delta(2, 3, \infty) = \text{PSL}_2(\mathbb{Z})$ we obtain the triangle in the Dedekind tessellation with the edges $\{i, \frac{1}{2} + i\frac{\sqrt{3}}{2}, i\infty\}$.

Since we now have constructed a triangle which has the given angles, we write down the generators of the extended triangle group τ_a, τ_b , and τ_c . For visualization we refer to picture 4.1 earlier in this chapter. From the construction of the triangle F , we see that τ_b is a reflection on the axes $\text{Re}(z) = 0$. Hence,

$$\tau_b(z) = -\bar{z}.$$

Let $\xi = \text{Re}(z_b) = \cot\frac{\pi}{a} + \cos\frac{\pi}{b}\csc\frac{\pi}{a}$ the real part of the point z_b . The map τ_a is a reflection the line $\text{Re}(z) = \xi$

$$\tau_a(z) = \xi - \overline{(z - \xi)} = 2\xi - \bar{z} = 2\left(\cot\frac{\pi}{a} + \cos\frac{\pi}{b}\csc\frac{\pi}{a}\right) - \bar{z}.$$

Finally, the map τ_c is a reflection at the circle going through z_a and z_b . As we have seen before, its midpoint is at $m = \cos\frac{\pi}{a}$ and it has the radius $r = \csc\frac{\pi}{a}$. Therefore, we have

$$\tau_c(z) = m + \frac{r^2}{\bar{z} - m} = \frac{1 + \bar{z}\cot\frac{\pi}{a}}{\bar{z} - \cot\frac{\pi}{a}}.$$

These three maps generate the extended triangle group $\Delta^*(a, b)$.

4.3 Lemma. *The extended hyperbolic triangle groups $\Delta^*(a, b)$ are realized as the following functions on $\overline{\mathbb{H}}$.*

$$\begin{aligned}\tau_a(z) &= 2 \left(\cot \frac{\pi}{a} + \cos \frac{\pi}{b} \csc \frac{\pi}{a} \right) - \bar{z}, \\ \tau_b(z) &= -\bar{z}, \\ \tau_c(z) &= \frac{1 + \bar{z} \cot \frac{\pi}{a}}{\bar{z} - \cot \frac{\pi}{a}}.\end{aligned}$$

A fundamental domain of this operation on the upper half plane is the hyperbolic triangle with edges z_a, z_b , and z_c as described in lemma 4.2.

In the beginning of this section we showed how the triangle groups $\Delta(a, b)$ are embedded into the extended ones: formula (4.1). We use this, to construct an explicit representation of the groups $\Delta(a, b)$.

$$\begin{aligned}\delta_a(z) &:= \tau_c(\tau_b(z)) = \frac{-z \cot \frac{\pi}{a} + 1}{-z - \cot \frac{\pi}{a}} \\ &= \frac{z \cos \frac{\pi}{a} - \sin \frac{\pi}{a}}{z \sin \frac{\pi}{a} + \cos \frac{\pi}{a}}, \\ \delta_b(z) &:= \tau_a(\tau_c(z)) = 2 \csc \frac{\pi}{a} \left(\cos \frac{\pi}{a} + \cos \frac{\pi}{b} \right) + \frac{z \cot \frac{\pi}{a} + 1}{z - \cot \frac{\pi}{a}} \\ &= \frac{z \left(\cos \frac{\pi}{a} + 2 \cos \frac{\pi}{b} \right) - 2 \cot \frac{\pi}{a} \left(\cos \frac{\pi}{a} + \cos \frac{\pi}{b} \right) - \sin \frac{\pi}{a}}{z \sin \frac{\pi}{a} - \cos \frac{\pi}{a}}, \\ \delta_c(z) &:= \tau_b(\tau_a(z)) = z - 2 \left(\cos \frac{\pi}{a} + \frac{\pi}{b} \right) \csc \frac{\pi}{a}.\end{aligned}$$

We see that the maps δ_a, δ_b , and δ_c are actually Möbius transformations. Therefore, we write them as projective, real 2×2 matrix. Note that we reduced the fractions in such a way that the resulting matrices have determinant one. For a visualization see figure 4.2.

4.4 Theorem. *Let $\Delta(a, b)$ be a hyperbolic triangle group. Then, we have an embedding*

$$\begin{aligned}\Delta(a, b) &\rightarrow \text{PSL}_2(\mathbb{R}), \\ \delta_a &\mapsto \begin{pmatrix} \cos \frac{\pi}{a} & -\sin \frac{\pi}{a} \\ \sin \frac{\pi}{a} & \cos \frac{\pi}{a} \end{pmatrix}, \\ \delta_b &\mapsto \begin{pmatrix} \cos \frac{\pi}{a} + 2 \cos \frac{\pi}{b} & -2 \left(\cos \frac{\pi}{a} + \cos \frac{\pi}{b} \right) \cot \frac{\pi}{a} - \sin \frac{\pi}{a} \\ \sin \frac{\pi}{a} & -\cos \frac{\pi}{a} \end{pmatrix}, \\ \delta_c &\mapsto \begin{pmatrix} 1 & -2 \left(\cos \frac{\pi}{a} + \cos \frac{\pi}{b} \right) \csc \frac{\pi}{a} \\ 0 & 1 \end{pmatrix}.\end{aligned}$$

The embedding actually maps into the group $\text{PSL}_2(R)$, where R is the ring

$$\mathbb{Z} \left[\cos \frac{\pi}{a}, \sin \frac{\pi}{a}, \csc \frac{\pi}{a}, 2 \cos \frac{\pi}{b} \right].$$

A fundamental domain of this operation on the upper half plane is the union of the triangle in lemma 4.2 and one image of this triangle under one arbitrary reflection of lemma 4.3.

With this explicit description, we describe the Riemann surface $X(\Delta(a, b))$ as we constructed it in chapter 2 as follows. The fundamental domain for group operation is, according to the theorem, the triangle described in lemma 4.2 together with the image under one reflection. We use the reflection τ_c and obtain the quadrilateral with the vertices $i\infty, i, \cot\left(\frac{\pi}{a}\right)$, and $\rho_{a,b}$. To obtain the Riemann surface, we identify the following edges. The edges from $i\infty$ to i with the edge from i to $\cot\left(\frac{\pi}{a}\right)$ using the map δ_a and the edges from $i\infty$ to $\rho_{a,b}$ with the edge from $\rho_{a,b}$ to $\cot\left(\frac{\pi}{a}\right)$ using δ_b . From this, we see that the genus of the Riemann surface $X(\Delta(a, b))$ is zero. Furthermore, this surface has one cusp – the image under projection map $\pi_{\Delta(a,b)}$ of $i\infty$ and two elliptic points: The image of i with order a and the image of $\rho_{a,b}$ of order b .

Notations and examples

For the use in the later chapters, we define some symbols. When we work with the triangle groups, we often use the following generators.

$$\begin{aligned} S = S_a &:= \delta_a = \begin{pmatrix} \cos \frac{\pi}{a} & -\sin \frac{\pi}{a} \\ \sin \frac{\pi}{a} & \cos \frac{\pi}{a} \end{pmatrix}, \\ R = R_{a,b} &:= -\delta_b^{-1} = \begin{pmatrix} \cos \frac{\pi}{a} & -2\left(\cos \frac{\pi}{a} + \cos \frac{\pi}{b}\right) \cot \frac{\pi}{a} - \sin \frac{\pi}{a} \\ \sin \frac{\pi}{a} & -\cos \frac{\pi}{a} - 2\cos \frac{\pi}{b} \end{pmatrix}, \\ T = T_{a,b} &:= \delta_c^{-1} = \begin{pmatrix} 1 & 2\left(\cos \frac{\pi}{a} + \cos \frac{\pi}{b}\right) \csc \frac{\pi}{a} \\ 0 & 1 \end{pmatrix} = \begin{pmatrix} 1 & \omega \\ 0 & 1 \end{pmatrix}. \end{aligned} \quad (4.5)$$

The value $\omega := 2\left(\cos \frac{\pi}{a} + \cos \frac{\pi}{b}\right) \csc \frac{\pi}{a}$ is the cusp width of ∞ in the triangle group $\Delta(a, b)$. The matrix S is of order a and the matrix R is of order b . Furthermore, $T^n = 1$ if and only if $n = 0$. Note that the sign in the definition of R is actually irrelevant since we are working in projective space. When we are working with the fundamental domain of (extended) triangle groups, we refer to the vertex z_b as ρ

$$\begin{aligned} \rho = \rho_{a,b} &:= z_b = \cot \frac{\pi}{a} + \cos \frac{\pi}{b} \csc \frac{\pi}{a} + i \left(\csc \frac{\pi}{a} \sin \frac{\pi}{b} \right) \\ &= \csc \frac{\pi}{a} \left(\cos \frac{\pi}{a} + e^{i\frac{\pi}{b}} \right). \end{aligned} \quad (4.6)$$

Example. The first example the modular group $\text{PSL}_2(\mathbb{Z})$. It is the triangle group for $a = 2$ and $b = 3$. The underlying ring is \mathbb{Z} , since $\cos \frac{\pi}{2} = 0$ and $\sin \frac{\pi}{2} = \csc \frac{\pi}{2} = 2 \cos \frac{\pi}{3} =$

1. The matrices $S, R,$ and T become

$$\begin{aligned} S &= \begin{pmatrix} 0 & -1 \\ 1 & 0 \end{pmatrix}, \\ R &= \begin{pmatrix} 0 & -1 \\ 1 & -1 \end{pmatrix}, \\ T &= \begin{pmatrix} 1 & 1 \\ 0 & 1 \end{pmatrix}. \end{aligned}$$

As we have seen in chapter 2, the matrices S and R generate the full modular group. Hence, the modular group is isomorphic to the triangle group $\Delta(2, 3)$.

Later, we will focus on *Hecke groups*. The following matrices generate these groups.

$$\begin{aligned} S &= \begin{pmatrix} 0 & -1 \\ 1 & 0 \end{pmatrix}, \\ R_n = R_{2,n} &= \begin{pmatrix} 0 & -1 \\ 1 & -2 \cos\left(\frac{\pi}{n}\right) \end{pmatrix}, \\ T_n = T_{2,n} &= \begin{pmatrix} 1 & 2 \cos\left(\frac{\pi}{n}\right) \\ 0 & 1 \end{pmatrix} = \begin{pmatrix} 1 & \omega_n \\ 0 & 1 \end{pmatrix}. \end{aligned}$$

Again $\omega_n = 2 \cos\left(\frac{\pi}{n}\right)$ is the cusp width of ∞ in the Hecke group Δ_n .

Subgroups and permutations

Up to now, we worked with the triangle groups themselves. In the next step, we start working with finite index subgroups of triangle groups. The first question we will address is how to describe or classify these subgroups. In this thesis we present two methods to do this. In this section we classify them using finite groups or more precise, equivalence classes of permutation tuples. The second description is the notion of the *generalized Farey symbols* and we discuss it in detail in chapter 6. The idea of the classification based on permutation tuples works more general in the context of finitely generated groups. With \mathfrak{S}_μ we denote the symmetric group on μ letters. Furthermore, we mark one letter and call it 1.

Definition. Let $G = \langle (x_i)_{i=1}^n \mid (r_j)_{j=1}^s \rangle$ be a finitely presented group with n generators and s relations. Let $\underline{\sigma} = (\sigma_1, \dots, \sigma_n) \in \mathfrak{S}_\mu^n$ be a n -tuple of permutations, such that $\langle \sigma_1, \dots, \sigma_n \rangle$ is a transitive group. If the map

$$\begin{aligned} \beta_{\underline{\sigma}}: G &\rightarrow \mathfrak{S}_\mu, \\ x_i &\mapsto \sigma_i. \end{aligned}$$

satisfies $\beta_{\underline{\sigma}}(r_j) = 1$ for all $1 \leq j \leq s$, we call it a *G-pairing*. We define two G -pairings $\beta_{\underline{\sigma}}, \beta_{\underline{\tau}}$ to be equivalent if there is an element $\pi \in \mathfrak{S}_\mu$, such that $\pi(1) = 1$ and for all $\pi^{-1} \cdot \sigma_i \pi = \tau_i$ for all i .

We use these G -pairings to describe the subgroups of a finitely presented group.

4.7 Theorem. *Let $G = \langle (x_i)_{i=1}^n \mid (r_j)_{j=1}^s \rangle$ be a finitely presented group. There is for each subgroup a G -pairing and vice versa*

$$\left(\begin{array}{c} \Gamma \subseteq G \\ \text{subgroup of} \\ \text{index } \mu \end{array} \right) \leftrightarrow \left(G\text{-pairings} \right) / \text{equivalence.}$$

Proof. Starting with a subgroup $\Gamma \subseteq G$ of index μ :

Let $\Gamma c_1, \dots, \Gamma c_\mu$ be coset representatives of $\Gamma \backslash \Delta$. Then, we define the following permutation representation.

$$\begin{aligned} \beta: G &\longrightarrow \mathfrak{S}_\mu, \\ \beta(g)(i) = j &\iff \Gamma c_i g^{-1} = \Gamma c_j. \end{aligned}$$

This map is actually a homomorphism, since

$$\begin{aligned} \beta(g_1 g_2)(i) &= j \\ \iff \Gamma c_i (g_1 g_2)^{-1} &= \Gamma c_j \\ \iff \Gamma c_i g_2^{-1} g_1^{-1} &= \Gamma c_j \\ \iff \Gamma c_i g_2^{-1} = \Gamma c_k \text{ and } \Gamma c_k g_1^{-1} &= \Gamma c_j \\ \iff \beta(g_2)(i) = k \text{ and } \beta(g_1)(k) &= j \\ \iff \beta(g_2)(\beta(g_1)(i)) &= j. \end{aligned}$$

Using this map, we define the G -pairing as

$$\sigma_i := \beta(x_i),$$

where x_i are the generators of G . Being a homomorphism implies that $\beta(r_i) = 1$ what is required to be a pairing.

If we start with a pairing β_σ :

We define a subgroup Γ of G as the stabiliser of 1

$$\Gamma := \left\{ g \in G \mid \beta_\sigma(g)(1) = 1 \right\}.$$

□

As a special case we obtain a classification of finite index subgroups of triangle groups. This version can also be found in [KMSV14]. Since we used this frequently, we cite the definition and the corresponding theorem for triangle groups. A first version of this for the modular group is due to Millington [Mil69a], [Mil69b]. The version we cite now is in [KMSV14].

Definition. Let X be a finite set of μ letters and $x_1 \in X$ a fixed element. A (a, b) -pairing $(\sigma_a, \sigma_b)_{x_1}$ is an equivalence class of a pair of permutations of X with the following properties.

- (i) $\sigma_a^a = \sigma_b^b = 1$.
- (ii) The group $G = \langle \sigma_a, \sigma_b \rangle$ operates transitively on X .

The equivalence relation between two pairs is the “exchange of letters”. Formally,

$$\begin{aligned}
 & (\sigma_a, \sigma_b)_{x_1} \sim (\tau_a, \tau_b)_{x_1}, \\
 & \text{if and only if there exists a } \pi \in S_X \text{ such that} \\
 & \pi^{-1} \sigma_a \pi = \tau_a, \pi^{-1} \sigma_b \pi = \tau_b, \pi(x_1) = x_1.
 \end{aligned}$$

We call this representation of a subgroup of finite index the *monodromy representation*. We now explain where this name comes from. In the second chapter we constructed a branched covering of Riemann surfaces. Let $\Gamma \subseteq \Delta$ be a finite index subgroup of a triangle group $\Delta = \Delta(a, b)$. Then, we have a commutative diagram.

$$\begin{array}{ccc}
 & \mathbb{H}^* & \\
 \pi_\Gamma \swarrow & & \searrow \pi_\Delta \\
 X(\Gamma) = \Gamma \backslash \mathbb{H}^* & \xrightarrow{\varphi} & X(\Delta) = \Delta \backslash \mathbb{H}^*
 \end{array}$$

Here, φ is a covering map, branched over the elliptic points and the cusps of Δ . In the embedding we constructed, the point $\pi_\Delta(i)$ is the only elliptic point of order a and $\pi_\Delta(\rho_{a,b})$ the only elliptic point of order b . There is exactly one cusp which is $i\infty$. Apart from these points, the map φ does not branched. We fix one point \tilde{z} on the upper half plane which is neither an elliptic point nor a cusp. Let c_1, \dots, c_r be a set of coset representatives for the quotient $\Gamma \backslash \Delta$. Then, the fiber of φ of a point $z = \pi_\Delta(\tilde{z}) \in X(\Delta)$ is $\pi_\Gamma(c_1 \cdot \tilde{z}), \dots, \pi_\Gamma(c_r \cdot \tilde{z})$.

If we remove the points $i, \rho_{a,b}, i\infty$, and their images under Δ in the extended upper half plane and map the result using π_Δ , we obtain topologically a sphere without three points. The fundamental group of this is the finitely presented group $\langle s_0, s_1, s_2 \mid s_0 s_1 s_2 = 1 \rangle$. The loop s_0 is a loop around the image of i , the loop s_1 the loop around ρ and s_2 around $i\infty$. This finitely presented group is isomorphic to the free group on two generators. From the topology this can be seen as follows. A sphere without one point is homeomorphic to a disc. Hence, a sphere without three points is homeomorphic to a disc without two points. Since the fundamental group is invariant under homeomorphisms, we need to calculate the fundamental group of a two punctured sphere, which is known to be the free group on two generators. These two generators are loops around the images of i and ρ . We obtain the two generators of the fundamental group of the Riemann surface without three points.

Using this description, we find the monodromy of this covering. We defined the monodromy as the operation of the fundamental group of Δ on the fiber. We described the points in the fiber as images under the cosets of \tilde{z} . Furthermore, the endpoints of a loop corresponded to the operation using R , respectively S . Hence, the permutation of the cosets induced by multiplication with R , respectively S is the monodromy.

Membership test based on permutations

For a given matrix $A \in \Delta \subseteq \mathrm{PSL}_2(\mathbb{R})$ we need to decide, if this matrix is in a subgroup $\Gamma \subseteq \Delta$ of a triangle group given by permutations. We now give an algorithm to check this. We recall the map from the previous section

$$\beta_{(\sigma_a, \sigma_b)}: \Delta \rightarrow \mathfrak{S}_n, \quad \delta_i \mapsto \sigma_i \text{ for } i \in \{a, b\}.$$

Algorithm 1 (Membership test). Let $\Gamma \subseteq \Delta(a, b)$ a finite index subgroup of a triangle group, defined by two permutations (σ_a, σ_b) . For a matrix $A \in \Delta(a, b)$, the following algorithm decides, whether $A \in \Gamma$.

- (i) Solve the word problem for A in $\Delta(a, b)$ and write $A = \prod_{i \in I} \delta_i$. Here, $I \subseteq \{a, b\}^s$ for some $s \in \mathbb{N}$.
- (ii) Calculate $\beta_{(\sigma_a, \sigma_b)}(A)$ which is given by $\prod_{i \in I} \sigma_i =: \sigma$.
- (iii) The matrix A is in Γ if and only $\sigma(1) = 1$.

Proof. This works due to the description of the group as permutations. The subgroup Γ consists exactly of those matrices which fix the 1 which is the coset of the neutral element. \square

To implement this algorithm in a computer, we need to solve the word problem in the triangle groups.

Solving the word problem

To implement algorithm 1 we have to solve the word problem for the triangle groups. Inspired by the classical solution of the word problem for $\mathrm{PSL}_2(\mathbb{Z})$, we give an algorithm which solves this problem. We first recall the definitions from (4.5).

$$T = \begin{pmatrix} 1 & 2 \left(\cos\left(\frac{\pi}{a}\right) + \cos\left(\frac{\pi}{b}\right) \right) \csc\left(\frac{\pi}{a}\right) \\ 0 & 1 \end{pmatrix} = \begin{pmatrix} 1 & \omega \\ 0 & 1 \end{pmatrix},$$

$$S = \begin{pmatrix} \cos\left(\frac{\pi}{a}\right) & -\sin\left(\frac{\pi}{a}\right) \\ \sin\left(\frac{\pi}{a}\right) & \cos\left(\frac{\pi}{a}\right) \end{pmatrix}.$$

Multiplying the μ -th power of the matrices with an arbitrary matrix does the following

$$T^\mu \cdot \begin{pmatrix} x_{11} & x_{12} \\ x_{21} & x_{22} \end{pmatrix} = \begin{pmatrix} x_{11} + x_{21} \cdot \mu\omega & x_{12} + x_{22} \cdot \mu\omega \\ x_{21} & x_{22} \end{pmatrix},$$

$$S^\mu \cdot \begin{pmatrix} x_{11} & x_{12} \\ x_{21} & x_{22} \end{pmatrix} = \begin{pmatrix} x_{11} \cos\left(\mu \cdot \frac{\pi}{a}\right) - x_{21} \sin\left(\mu \cdot \frac{\pi}{a}\right) & x_{12} \cos\left(\mu \cdot \frac{\pi}{a}\right) - x_{22} \sin\left(\mu \cdot \frac{\pi}{a}\right) \\ x_{21} \cos\left(\mu \cdot \frac{\pi}{a}\right) + x_{11} \sin\left(\mu \cdot \frac{\pi}{a}\right) & x_{22} \cos\left(\mu \cdot \frac{\pi}{a}\right) + x_{12} \sin\left(\mu \cdot \frac{\pi}{a}\right) \end{pmatrix}.$$

We now focus on the left column of the matrices. The matrix T adds $x_{21} \cdot \omega$ to the first entry and S rotates the vector $\begin{pmatrix} x_{11} \\ x_{21} \end{pmatrix}$. Now the idea is to decrease the absolute values of x_{21} in every step. For a formal proof of the correctness of this algorithm, one looks at the image of the point $2i \in \mathbb{H}$.

Algorithm 2. Let $A = \begin{pmatrix} x_{11} & x_{12} \\ x_{21} & x_{22} \end{pmatrix} \in \Delta(a, b)$ be a matrix in a triangle group. The following algorithm computes a decomposition into the generators S and T .

- (i) While $x_{21} \neq 0$ do:
 - a) While $|x_{11}| \leq |\omega \cdot x_{21}|$ do:
 - If $\text{sgn}(x_{11}) = -\text{sgn}(x_{21})$: $A = T \cdot A$.
 - If $\text{sgn}(x_{11}) = \text{sgn}(x_{21})$: $A = T^{-1} \cdot A$.
 - b) Find i , such that $|(S^i \cdot A)_{2,1}|$ is minimal. Set $A = S^i \cdot A$.
- (ii) After the previous step, we assume $A = \begin{pmatrix} x_{11} & x_{12} \\ 0 & x_{22} \end{pmatrix}$. We define $p = \frac{x_{12}}{\omega x_{22}}$. Then, $\begin{pmatrix} 1 & 0 \\ 0 & 1 \end{pmatrix} = T^p \cdot A$.

Chapter 5.

Dessins d'enfants

Als ich so alt war [wie diese Kinder], konnte ich malen wie Raphael. Aber ich brauchte ein Leben lang um so zu malen wie die Kinder.

(Pablo Picasso - Nachdem er eine Ausstellung mit Kinderzeichnungen besucht hatte)

In this chapter we introduce the notion of dessins d'enfants. These are bipartite graphs on Riemann surfaces and can be used to describe certain functions, the Belyĭ functions. Their first version appeared in the work of Hamilton [Ham56] and Felix Klein [Kle79]. In the year 1983, Grothendieck wrote a proposal (*Esquisse d'un Programme*, [Gro97]) in which he proposed these dessins d'enfants as a method to understand the absolute Galois group $\text{Gal}(\overline{\mathbb{Q}}/\mathbb{Q})$. Sadly, this proposal got rejected – Le Bruyn called it the best rejected proposal ever [Bru07]. These dessins are in a strong relation with the subgroups of triangle groups. We use this relation to calculate Hauptmoduls of finite index subgroups of genus zero of triangle groups with a cusp.

Belyĭ functions

In this section we present the notion of the Belyĭ functions which we need to describe dessins d'enfants. Wolfart has written some introductions to this topic: [Wol06] and [Wol01], as well as Zvonkin [Zvo08], [LZ04]. Furthermore, one should mention the article by Schneps [Sch94].

Definition. Let X be a Riemann surface. We call a non-constant mapping $f: X \rightarrow \mathbb{P}^1(\mathbb{C})$, branched over at most three points, a *Belyĭ function*.

For a Riemann surface X let $f: X \rightarrow \mathbb{P}^1(\mathbb{C})$ be a Belyĭ function which is branched over the points x_0, x_1 , and x_2 . Let $\varphi: \mathbb{P}^1(\mathbb{C}) \rightarrow \mathbb{P}^1(\mathbb{C})$ be a Möbius transformation which maps the branching points x_0, x_1 , and x_2 to the points z_1, z_2 , and z_3 . Such a map can always be found – we described a method for this in the remark after theorem 2.6. The composite map $\varphi \circ f$ is also a Belyĭ function, but branched over z_1, z_2 , and z_3 . Hence, we can choose arbitrary three branching points. A common choice is $z_1 = 0, z_2 = 1$, and $z_3 = \infty$. For our application it turns out that $z_1 = 0$ and $z_3 = \infty$ are eligible. We choose the third point different for each triangle group, for example for the modular

group $\Delta(2, 3)$ we will find $z_2 = 1728$ to be eligible. This choice was already known to Klein when he calculated his j -invariant.

One of the reasons why Belyĭ functions are important is that they provide a relation between algebraic curves and subgroups of finite index of triangle groups. Furthermore, this connection can be extended to the notion of the dessin d'enfants.

5.1 Theorem (Belyĭ's theorem). *Let X be a smooth algebraic curve in $\mathbb{P}^n(\mathbb{C})$. Then, the following are equivalent.*

- (i) *There exists a Belyĭ function on X .*
- (ii) *There is a subgroup Γ of finite index of a triangle group Δ , such that $X \cong \Gamma/\mathbb{H}$.*
- (iii) *X is defined over a number field.*

Proof. Belyĭ gave the first proof in [Bel79] and improved it in [Bel02]. Parts of the proof were also known to Grothendieck [Gro97]. A more elementary version is contained in the article by Wolfart [Wol06] or the book by Gironde and González-Diez [GGD12]. \square

Dessins d'enfants

Let X be a smooth algebraic curve defined over a number field and $f: X \rightarrow \mathbb{P}^1(\mathbb{C})$ a Belyĭ function on X which is branch over $0, 1$, and ∞ . Such a map exists due to Belyĭ's theorem 5.1. We use this function to construct a bipartite graph on X . We define the preimages of 0 as *black vertices* and the preimages of 1 as *white vertices*. The edges of this graph are defined as the preimages of the interval $[0, 1]$ and each edge connects a black and a white vertex. This construction results in a graph on X . In this graph is the branching behavior of the function f encoded. We call such a graph a dessin d'enfant.

Definition. We call a bipartite graph \mathcal{D} on a connected Riemann surface X a *dessin d'enfants* or sometimes a *dessin* if the complement X/\mathcal{D} consists of finitely many simply connected components.

To see some examples, we need a method to find the dessin for a given Belyĭ function. In the article [Sch94, Chapter II, §1], Schneps gives such a procedure. Furthermore, we wrote a short Mathematica program which gives an approximation how the dessin looks. In the appendix, section A, we give the source of this program. A similar program can be found in the Wolfram demonstrations project, see [Goi].

Example. (i) $f(z) = z^n$ results in a star, figure 5.1.

(ii) The Chebyshev polynomials $T_n(z) = \cos(n \arccos(x))$ branch over $\{-1, 1, \infty\}$ and their dessin is a line with $n + 1$ vertices, figure 5.2.

(iii) It is possible, to find Belyĭ functions, such that the corresponding dessins are platonic solids – see figure 5.3 to 5.5. These Belyĭ functions are

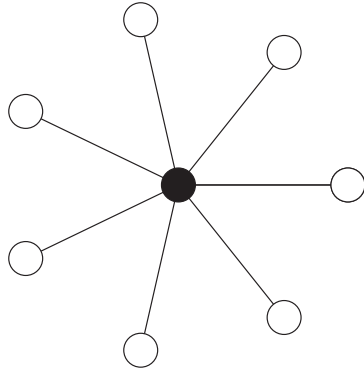


Figure 5.1.: The dessin for $f(z) = z^7$

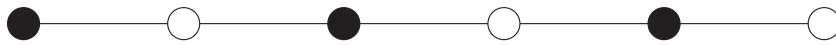


Figure 5.2.: The dessin for $f(z) = \frac{1}{2}(1 + T_5(x))$

a) for the tetrahedron $-\frac{64z^3(z^3 - 1)^3}{(8z^3 + 1)^3},$

b) for the cube $\frac{(z^8 + 14z^4 + 1)^3}{108z^4(z^4 - 1)^4},$

c) for the dodecahedron $\frac{(z^{20} + 228z^{15} + 494z^{10} - 228z^5 + 1)^3}{1728z^5(z^{10} - 11z^5 - 1)^5}.$

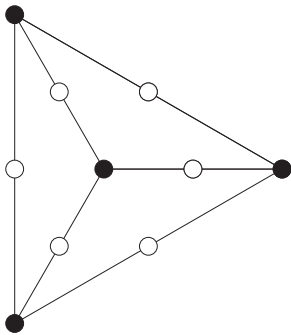


Figure 5.3.: Tetrahedron

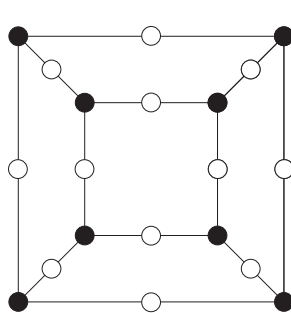


Figure 5.4.: Cube

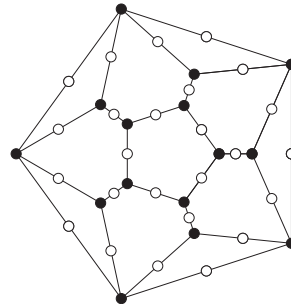


Figure 5.5.: Dodecahedron

- (iv) In the article [MZ00] of Magot and Zvonkin, they present some operations to create new dessins out of old ones. These techniques are used to construct Belyı̆ function which have the Archimedean solids as dessins. For example the map $f_{\text{truc}}(z) = -27 \frac{z^2}{(z-4)^3}$ truncates the Dessin when composed with a Belyı̆ map.
- (v) Similar to this, in the article [SZ94] Shabat and Zvonkin introduce a method to compose certain Belyı̆ function and their dessins.

Permutations and dessins

Another way of describing dessins is the use of permutations. Each dessin corresponds to a triple of permutations of n letters where n is the number of edges of the graph. We orient all edges of the graph from black to white vertices. Then, we label all edges of the graph with consecutive numbers. This label is placed on the left of the edge, with respect to the orientation. The first permutation consists of b cycles where b is the number of black vertices. For each black vertex, we collect the labels of the edges while going counterclockwise around this vertex. The product of all of these cycles is the first permutation which we call σ_0 . The order of the cycles does not matter. The cycles are disjoint since the graph is bipartite. By using the same method for the white vertices we end up with another permutation σ_1 . To define the third permutation σ_∞ we go counterclockwise around each face of the graph and collect all labels on the face. Only every second edge is marked with a label, due to their placement. Note that going around the outer face counterclockwise means going around the graph clockwise.

These three permutations have the property that $\sigma_0\sigma_1\sigma_\infty = 1$. Therefore, it suffices to calculate σ_0 and σ_1 .

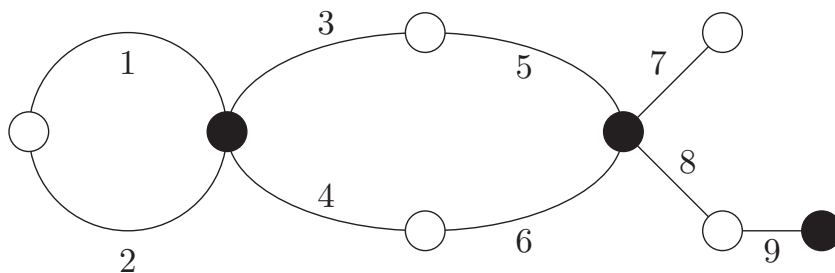


Figure 5.6.: A dessin d'enfant with labels

Example. We labeled the dessin in figure 5.6 according to the rules we used described. It corresponds to the permutations

$$\begin{aligned}\sigma_0 &= (1\ 2\ 4\ 3)(5\ 6\ 8\ 7)(9), \\ \sigma_1 &= (1\ 2)(3\ 5)(4\ 6)(7)(8\ 9), \\ \sigma_\infty &= (1)(2\ 3\ 7\ 8\ 9\ 6)(4\ 5).\end{aligned}$$

Subgroups of triangle groups

In this section, we take a look at the relation between dessin d'enfants and subgroups of finite index of triangle groups. We fix a triangle group $\Delta = \Delta(a, b)$ and a subgroup $\Gamma \subseteq \Delta$ of finite index. We assume that Γ has genus zero. As we have seen in chapter 3, we obtain a rational covering $R_\Gamma: \mathbb{P}^1(\mathbb{C}) \rightarrow \mathbb{P}^1(\mathbb{C})$ branching over the elliptic and parabolic points. Since the triangle groups have two elliptic points and one cusp, the map R_Γ branches over at most three points and is thereby a Belyi function. The branching

points depend on the normalization of the hauptmodul of the triangle group Δ . In chapter 7 we will calculate a hauptmodul which maps the fundamental domain of the extended triangle group to the upper half plane. This results in the branching points to be ∞ (as the value at the cusp 0), 0 (as the value at the elliptic point z_b of order b), and some value $\eta \in \mathbb{R}$ (as the value at the elliptic point z_a of order a). The value of η depends on the triangle group. We give the exact expression in chapter 7, formula (7.2).

From the subgroup Γ we directly compute the corresponding dessin. First note that the interval $[0, \eta]$ is mapped on the circle going through the elliptic points z_a and z_b on the upper half plane. We choose a connected fundamental domain for Γ composed from copies of the fundamental of Δ – see section *Fundamental domains and Riemann surfaces* in chapter 2. The images of the two elliptic points and the images of the circle connecting these two define a graph on the upper half plane. Identifying the points elliptic points on the boundaries, using the side pairings, results in the dessin for the Belyĭ function R_Γ .

Example. As an example we look at the following subgroup of the modular group $\mathrm{PSL}_2(\mathbb{Z})$.

$$\Gamma_0(6) = \left\{ \begin{pmatrix} a & b \\ c & d \end{pmatrix} \in \mathrm{PSL}_2(\mathbb{Z}) \mid c \equiv 0 \pmod{6} \right\}.$$

We draw a fundamental domain, figure 5.7, and apply the procedure we described above, figures 5.8 to 5.10 and the end of this chapter. If we apply the methods we will develop later, we can also calculate the Belyĭ function. This function is

$$R_{\Gamma_0(6)}(x) = \frac{(12x + 1)^3 (15552x^3 + 3888x^2 + 252x + 1)^3}{x(8x + 1)^2(9x + 1)^3}.$$

This result coincide also with the result by other authors, see for example [Mai09].

The other direction is also possible. If we start with a dessin, we can build up a fundamental domain using the dessin. From this fundamental domain, we can read off the side pairings. As we have seen in chapter 2, these side pairings generate the group. For a more detailed discussion for the modular group, see [Car09].

Computation of Belyĭ functions

In this section, we will address the question how to compute equations, whose solution determinate the Belyĭ function of a given dessin. It turns out that the solution of this problem is hard and no solution for large graphs is known. The article *On computing Belyĭ maps*, by Sijling and Voight [SV14], provides a good overview of the existing methods. Furthermore, we like to mention the article *Belyĭ functions for hyperbolic hypergeometric-to-Heun transformations*, by van Hoeij and Vidunas [vHV12], provides a large source of examples.

The methods, we present in this thesis to compute hauptmoduls for finite index subgroups of genus zero of Hecke groups, can be modified to calculate a Belyĭ function for a

given dessin d'enfants. First construct the corresponding subgroups and then construct the rational covering.

To find the “general structure” of the Belyĭ function, we do the following. It is a rational function over \mathbb{C} . Therefore, we can take about the numerator and the denominator.

We obtain the numerator in the following way. For each black vertex of valence ν we take a factor $(x - \alpha_i)^\nu$ with an unknown coefficient $\alpha_i \in \mathbb{C}$. We obtain such a factor for each black vertex, which a different α_i . Multiplying all of these, yields the numerator. To obtain a more “simple” result we do the following. If we have n_i vertices of valence i for $i = 1, 2, \dots$ the numerator is as follows.

$$p(x) = \prod_i p_i(x)^i,$$

$$\text{with } p_i(x) = \sum_{\nu=0}^{n_i} a_{i\nu} x^\nu,$$

and for all i : $a_{in_i} = 1$.

Here, the $a_{i\nu} \in \mathbb{C}$ are unknown coefficients which we have to determinate. Other normalizations are also possible, for example we can ask for $a_{i0} = 1$. The coefficients a_{ij} will satisfy certain algebraic equations. Hence, they are lying in a number field. In the second approach, the degree of this number field is in general smaller than in the first one.

Note that the permutation σ_0 gives the natural number n_i as the number of cycles of length i . Hence, a factorisation of the the polynomial $p(x)$ can be calculated just from the knowledge of σ_0 .

To obtain the full Belyĭ function we also need information on the denominator. The denominator encodes the behavior at the singularities. The singularities in the dessin correspond to the cycles of the graph. If there are m_i circles of length $2i$, we write down exactly the same polynomial as in the numerator, but with different coefficients.

$$q(x) = \prod_i q_i(x)^i,$$

$$\text{with } q_i(x) = \sum_{\mu=0}^{m_i} b_{i\mu} x^\mu,$$

and for all i : $b_{im_i} = 1$.

Again, the coefficients $b_{i\nu} \in \mathbb{C}$ are unknown and we have to determinate them. We can extract the structure from the permutations, analog to the numerator, except we now use the permutation σ_∞ . The resulting Belyĭ function is $p(x)/q(x)$.

To determinate the unknown coefficients of this function we need some more information. Up to now, we just used the information coming from the black vertices and faces of the graph. To calculate the Belyĭ function, we also need to include the information coming from the white vertices. We do this in the same way we did it with the black vertices. We denote the number of vertices of valence i with \tilde{n}_i and obtain a polynomial

with unknown coefficients $\tilde{a}_{i\nu} \in \mathbb{C}$.

$$\tilde{p}(x) = \prod_i \tilde{p}_i(x)^{i},$$

$$\text{with } \tilde{p}_i(x) = \sum_{\nu=0}^{\tilde{n}_i} \tilde{a}_{i\nu} x^\nu,$$

$$\text{and for all } i: \tilde{a}_{i\tilde{n}_i} = 1.$$

We treat the points at infinity in the same way. Hence, there is another Belyĭ function which is $\tilde{p}(x)/q(x)$. This Belyĭ function results in the same dessin as $p(x)/q(x)$, but with the black and white vertices exchanged.

This gives us a relation between these two functions. If we want the branching points to lie over 0, $\eta \in \mathbb{Q}$, and ∞ , we get the condition $p(x)/q(x) = \eta + \tilde{p}(x)/q(x)$ or equivalent

$$0 = \eta \cdot q(x) + \tilde{p}(x) - p(x) =: G(x). \quad (5.2)$$

The right-hand side is a polynomial in x of degree number of edges of the dessin. This polynomial should vanish. Therefore, all coefficients must vanish. The coefficients of $G(x)$ are polynomial expression over \mathbb{Q} in the unknowns $a_{i\nu}$, $\tilde{a}_{i\nu}$, and $b_{i\mu}$. This gives us a system of algebraic equations. The solutions of this system results in the Belyĭ function and its Galois orbits. It is also possible to obtain so called ‘‘parasitic solutions’’: These are solutions to the equations, where the corresponding dessins do not have the correct cycle type. The right Belyi function is found by calculating the dessin for each possible result.

If the degree of this polynomial $G(x)$ is small, the solution of this system can be calculated by using methods like Gröbner bases. But for larger degree, this does not work anymore. In the next chapters, we present a different approach to find a solution of this system.

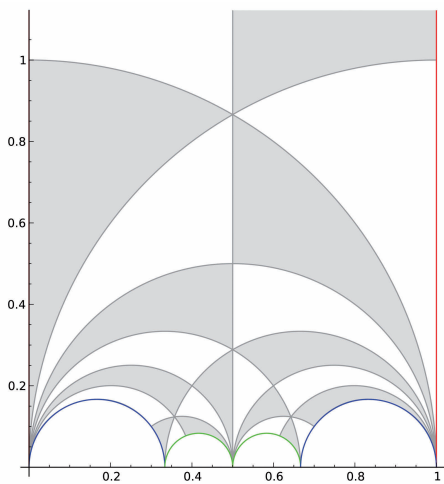


Figure 5.7.: A fundamental domain for $\Gamma_0(6)$

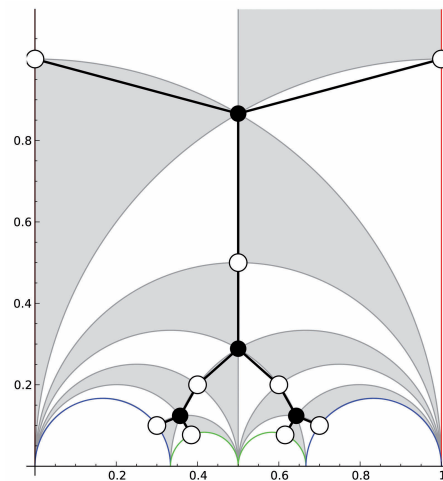


Figure 5.8.: A fundamental domain with marked points

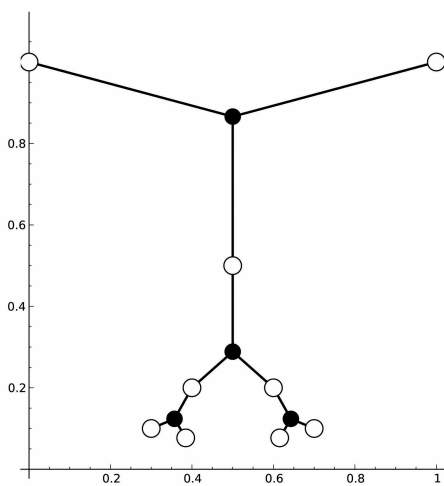


Figure 5.9.: The dessin without identification

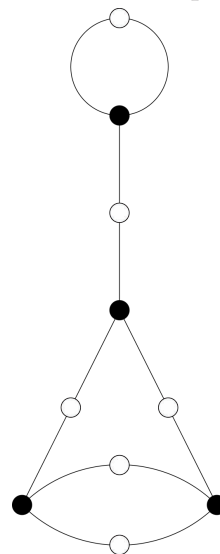


Figure 5.10.: The dessin for the Belyi function of $\Gamma_0(6)$

Chapter 6.

Generalized Farey symbols

Obsessed by a Farey tale, we spent our lives searching for a magic door and a lost kingdom of peace.

(More or less Eugene O'Neill)

To describe a subgroup of a triangle group we presented in chapter 4 a method using finite groups and permutations. In this chapter we present a different approach to this classification for the Hecke groups Δ_n . The advantage of this method is that it is possible to calculate invariants of the subgroup, such as coset representatives, generators, genus, etc efficiently.

In the year 1991, Kulkarni presented a powerful tool to study subgroups of the modular group [Kul91]. Nowadays, we call this tool the *Farey symbols*. There are partial implementations of these methods in Sage [KL08], [Kur09], magma [MAG], and gap [GAP]. A complete and efficient implementation in *C++*, with an interface to interact with Sage [SAG], became only recently available – published by Monien [Mon11].

The idea of Kulkarni is to describe a subgroup of the modular group by a certain fundamental domain with additional information, a *special polygon*. These special polygons are polygons in the hyperbolic plane with vertices in $\mathbb{P}^1(\mathbb{Q})$. Furthermore, these vertices form a sequence which satisfies a certain arithmetic property. It is a generalized Farey sequence. We equipped this sequence with additional information from the special polygon, the *pairings*. A Farey sequence equipped with pairings, is a Farey symbol.

In this chapter we generalize this concept to the Hecke groups. Lang, Lim, and Tan [LLT95b] started to generalize this notion to the Hecke groups and introduced the notion of a *Hecke-Farey symbol*. The ideas of Kulkarni also work in this more general context, but with some differences. In the classical setting of the modular group, the Farey sequence and the edges of the special polygon are rational numbers. For the Hecke groups, we need to work over number fields. We present an approach which is more general since Lang, Lim, and Tan focused on the Hecke groups Δ_q where q prime. In this more general setting, we need to generalize the notion of the pairings. Many of the algorithms which were introduced by Kulkarni, work in this more general context – for example the calculation of the genus or the cusps of the underlying group.

We give a short discussion about Farey symbols for general non-compact triangle groups in chapter 10. Here, more work needs to be done.

We continue using the notion from chapter 4 and start by introducing the concept of

the special polygons.

Special polygons

To define the notion of a special polygon, we need to name certain points and geodesics on the upper half plane. The point $\rho = \rho_{a,b} = \csc \frac{\pi}{a} \left(\cos \frac{\pi}{a} + e^{i\frac{\pi}{b}} \right)$ is the same as we defined it in chapter 4.

Definition. Let Δ_n be a hyperbolic Hecke group and Δ_n^* the corresponding extended triangle group. Then, we define

- (i) The elements in the Δ_n^* -orbit of i are called *even vertices*.
- (ii) The elements in the Δ_n^* -orbit of ρ are called *odd vertices*.
- (iii) The elements in the Δ_n^* -orbit of the edge joining ∞ and i are called *even edges*.
- (iv) The elements in the Δ_n^* -orbit of the edge joining ∞ and ρ are called *odd edges*.
- (v) The elements in the Δ_n^* -orbit of the edge joining i and ρ are called *f-edges*.

6.1 Theorem. *Let Δ_n be hyperbolic Hecke group. Then, if*

(i) *n is even:*

- a) *The even edges come in pairs, each pair forming a complete hyperbolic arc. Each geodesic contains one even vertex. The group Δ_n acts transitive on these geodesics.*
- b) *The odd edges come in pairs, each pair forming a complete hyperbolic arc. Each geodesic contains one odd vertex. The group Δ_n acts transitive on these geodesics.*
- c) *The f-edges come in infinity families, each family forming a complete hyperbolic arc. Each geodesic contains a (naturally sorted) set of vertices. In this natural ordering an even vertex follows an odd one and vice versa.*

(ii) *n is odd:*

- a) *The even edges come in pairs, each pair forming a complete hyperbolic arc. Each geodesic contains one even vertex. The group Δ_n acts transitive on these geodesics.*
- b) *A pair of odd edges and a pair of f-edges form a complete hyperbolic geodesic. The group Δ_n acts transitive on these geodesics.*

Proof. (i) Let n be even:

-
- a) Since the even edges are the images of the line from ∞ to i , each even edge needs to end in an even vertex, e.g. the image of the point i . The other end needs to be a image of ∞ which in $\mathbb{P}^1(\mathbb{R})$. Since n is even, through every even vertex there are $\frac{n}{2}$ even lines passing. Hence, the even edges come in pairs and form a complete hyperbolic geodesic.
 - b) Since the first parameter of the Hecke group, which is 2, is even, the same argumentation holds as in part *a*.
 - c) We start in an arbitrary even or odd point. Without loss of generality, we assume starting in an even point. Due to the construction, there are two outgoing f -edges. We choose an arbitrary one and find an odd point at the end of this line. Now, there are n outgoing f -edges attached to this point. Since n is even, the continuation of the geodesic we came from is again a f edge. We follow this new one and find another even point. Now we continue with this process and find an infinite, naturally ordered family of f -edges (if we also continue this process at the other edge going out of our starting point). This procedure lasts infinitely long (in both directions): It ends, if we come to a point, where we have no further (unused) outgoing edge or a vertex opposite of the incoming one. There is one vertex with this property; the one we started with. In this case, we produced a circle which is also not possible.
- (ii) If n is odd, a similar argument is possible. Although Kulkarni [Kul91] gave the argument only for the modular group, the same argument holds for general Hecke groups Δ_n , if n is odd.

□

Example. As an example, we look at the triangle group Δ_4 . In figure 6.1 and 6.2 we show a part of the tessellation, mark the even vertices respectively the even edges in red and the odd vertices, respectively the odd edges in blue. The f -edges are shown in green.

Definition. A $(2, n)$ -special polygon (or n -special polygon for short) is a convex hyperbolic polygon P , such that the boundary ∂P is a union of even and odd edges, together with a marking of its edges, the *side-pairings*. The following conditions must be satisfied:

- S_1) 0 and ∞ are vertices of the polygon P .
- S_2) The even edges in ∂P come in pairs, each pair forming a complete hyperbolic arc.
- S_3) The odd edges in ∂P come in pairs, each pair meets an odd vertex making an internal angle of $\frac{2\pi}{d}$ where $d \neq 1$ is a divisor of n .

The side pairing is a map from the set of edges to the set of edges, such that it fixes no edge. The following should hold.

- S_4) An odd edge e paired with another odd edge f making an internal angle $\frac{2\pi}{d}$, where $d \neq 1$ is a divisor of n .

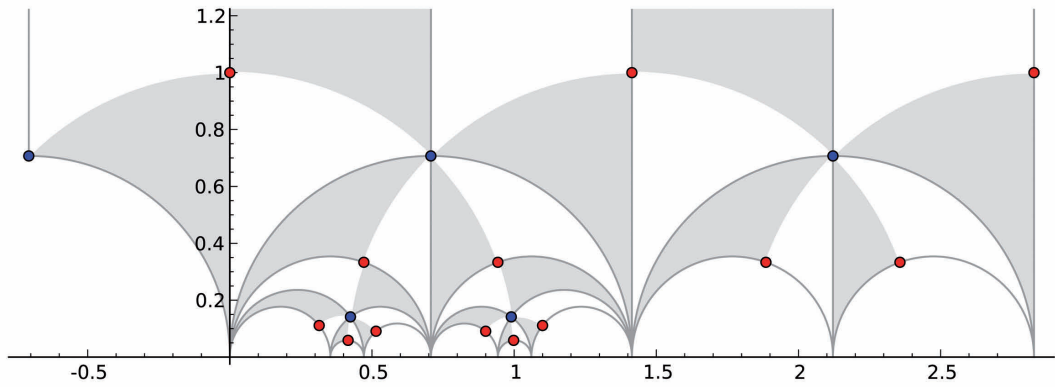


Figure 6.1.:
 ●: even vertex
 ●: odd vertex

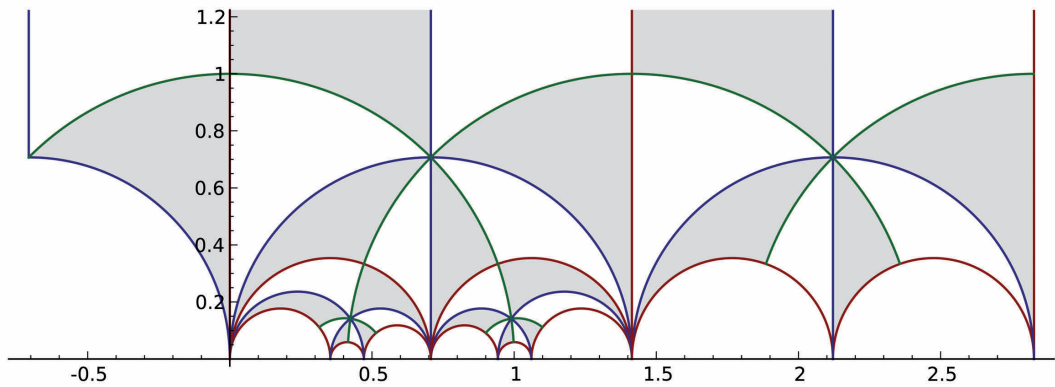


Figure 6.2.:
 — : even edge
 — : odd edge
 — : f -edge

S_5) Let e, f be a pair of even edges. Then either e is paired to f or there is other pairing e', f' of even edges, such that e is paired the f' and f is paired with e' .

Before we give an example of the special polygon, we make some comments about the definition.

Remark. (i) The notion of being a *convex* polygon is meant in the hyperbolic sense. The polygons we are looking at, are not convex in the Euclidian sense.

(ii) Note that this definition is similar to the notion of a special polygon for $\text{PSL}_2(\mathbb{Z})$ – see for example Kulkarni, Kurth or Lang, Lim, and Tang.

The main difference in this generalization is that there are more possible pairings for the odd edges. There is one type for each divisor $d \neq 1$ of n . In the cited

articles, the authors have been working with $\mathrm{PSL}_2(\mathbb{Z})$ corresponding to $n = 3$. Since this number is prime, there is only one divisor larger than 1. Hence, we have only one type of odd pairing.

- (iii) If we choose n to be a prime number, the odd edges can just be paired in one way, such that they meet in internal angle of $\frac{2\pi}{n}$. Assuming this, the definition coincides with the one by Lim, Lang, and Tam [LLT95b]. Due to the existence of elliptic points of order d , where d is a divisor of n , we need to include these more general pairings.

Examples of special polygons

In figure 6.3, we see a typical example of a 4-special polygon. The colors indicate the pairings. Sides with the same color are paired with each other. If there is no color, we identify the left part of the arc with the right part and vice versa. As we will see in

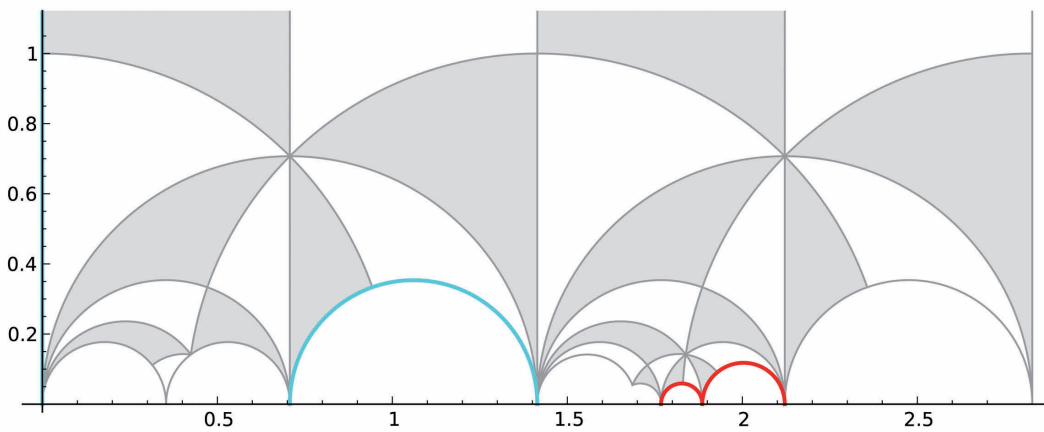


Figure 6.3.: Example of a 4-special polygon.

the next paragraph, each special polygon is the fundamental domain of a subgroup of a triangle group. The subgroup which belongs to this special polygon has the monodromy representation

$$\begin{aligned}\sigma_2 &= (1, 4)(2, 15)(3, 9)(5, 7)(8, 13)(11, 12) \in S_{15}, \\ \sigma_4 &= (1, 13, 4, 11)(2, 15, 9, 5)(3, 10, 14, 12)(6, 8) \in S_{15}\end{aligned}$$

and is a subgroup of the triangle group $\Delta(2, 4)$.

Subgroups and special polygons

As we just mentioned, there is a connection between the subgroups of finite index of the Hecke groups Δ_n and n -special polygons. For each special polygon there is such a subgroup which has this special polygon as a fundamental domain.

Let P be a special polygon. Note that P is equipped with a canonical orientation, by using the induced orientation from \mathbb{H} . This gives a canonical orientation on each of its sides. If e and f are two sides which are paired, then there is a unique element in Δ_n which maps e into f in an orientation-reversing manner. We call the elements of Δ_n obtained in the way the *side-pairing transformations* of P .

Generalized Farey symbols

In this section we generalize the notion of the classical Farey symbols, introduced by Kulkarni. These generalized Farey symbols allow us to do efficient calculations with subgroups of the Hecke groups Δ_n . For $n = 3$ the Farey symbols are based upon the notion of Farey sequences. These are increasing sequences of rational numbers. For $n = 3$ the corresponding triangle group is $\mathrm{PSL}_2(\mathbb{Z})$, a matrix group where the coefficients are integer numbers. If we generalize this to higher triangle groups, we need to consider more general rings.

$(2, n)$ -Farey sequences

Definition. We call a sequence $\{\frac{-1}{0}, \frac{a_0}{b_0} = x_0, \dots, \frac{a_\nu}{b_\nu} = x_\nu, \frac{1}{0}\}$ in $\mathbb{P}^1(\mathbb{R})$ a *complete $(2, n)$ -Farey sequence*, if

- (i) a_i and b_i are in the ring $\mathbb{Z}\left[2\cos\left(\frac{\pi}{n}\right)\right]$,
- (ii) the sequence is increasing,
- (iii) for all $i = 0, \dots, \nu$

$$g\left(\frac{a_i}{b_i}, \frac{a_{i+1}}{b_{i+1}}\right) = g(x_i, x_{i+1}) := |a_i b_{i+1} - a_{i+1} b_i| = 1. \quad (6.2)$$

It will be convenient to set $x_{-1} = \frac{-1}{0} = \infty = \frac{1}{0} = x_{\nu+1}$ and consider the x_i as forming a cyclic order.

A sequence $F = \{\frac{-1}{0}, x_0 = \frac{a_0}{b_0}, \dots, x_\nu = \frac{a_\nu}{b_\nu}, \frac{1}{0}\}$ is called a *partial $(2, n)$ -Farey sequence* or a just *n -sequence*, if it can be extended to a complete $(2, n)$ -Farey sequence by inserting no or $d - 1$ additional fractions between each two consecutive numbers in the sequence. Here, $d \neq n$ is a divisor of n and it varies for each insertion point. These points, where we need to insert points to obtain a complete $(2, n)$ -Farey sequence are called a *hole in the sequence*. We call the divisor d the *length of the hole* and it can be computed from the hole itself – see lemma 6.3.

Although we write the elements as fractions, it would be formally correct, to write them as an ordered pair, since we do not allow the cancellation of a common factor of the numerator and the denominator. The cancellation of such a factor modifies the third condition of the definition.

Examples and remarks

Before we equip these sequences with the additional structure needed to define the notion of the generalized Farey symbols, let us take a look at this definition. We start with some examples.

Example. The first examples we look at are the ones for $n = 3$. We obtain the classical notion of a Farey symbol. It is not possible, to have a hole in the sequence, since 3 is a prime number.

So the first new examples appear for $n = 4$. A typical sequence looks like this

$$\left\{ \frac{-1}{0}, \frac{0}{1}, \frac{1}{2\sqrt{2}}, \frac{\sqrt{2}}{3}, \frac{3}{4\sqrt{2}}, \frac{2\sqrt{2}}{5}, \frac{1}{\sqrt{2}}, \frac{\sqrt{2}}{1}, \frac{1}{0} \right\}.$$

This sequence is a complete $(2, 4)$ -Farey sequence. We obtain a partial one by omitting some of the terms. The possible divisor of 4 is 2, hence we omit $1 = 2 - 1$ term.

$$\left\{ \frac{0}{1}, \frac{1}{2\sqrt{2}}, \frac{\sqrt{2}}{3}, \frac{3}{4\sqrt{2}}, \frac{1}{\sqrt{2}}, \frac{\sqrt{2}}{1} \right\}.$$

These sequences have properties which are similar to the ones from the original Farey sequences. To give an idea, how the structure generalize to higher Farey sequences, we introduce the *insertion operators*. Later we show how to calculate these operators – see lemma 6.6.

$$I_\mu \left(\frac{a_i}{b_i}, \frac{a_j}{b_j} \right) := \frac{\csc \left(\frac{\pi}{n} \right) \left(a_j \sin \left(\mu \frac{\pi}{n} \right) + a_i \sin \left((1 + \mu) \frac{\pi}{n} \right) \right)}{\csc \left(\frac{\pi}{n} \right) \left(b_j \sin \left(\mu \frac{\pi}{n} \right) + b_i \sin \left((1 + \mu) \frac{\pi}{n} \right) \right)}, \quad \mu = 0, \dots, n - 1.$$

Remark. Although it is possible to cancel out the term $\csc \left(\frac{\pi}{n} \right)$, we must not do this to obtain the right result.

The insertion operators work as follows. We start with a complete $(2, n)$ -Farey sequence $\left\{ \frac{-1}{0}, x_0 = \frac{a_0}{b_0}, \dots, x_\nu = \frac{a_\nu}{b_\nu}, \frac{1}{0} \right\}$ and choose two consecutive numbers $\frac{a_i}{b_i}$ and $\frac{a_{i+1}}{b_{i+1}}$. Then, we apply the insertion operators $I_\mu \left(\frac{a_i}{b_i}, \frac{a_{i+1}}{b_{i+1}} \right)$ for $\mu = 1, \dots, n - 2$ and obtain a new, extended n -Farey sequence.

$$\left\{ \frac{-1}{0}, \frac{a_0}{b_0}, \dots, \frac{a_i}{b_i} = I_0 \left(\frac{a_i}{b_i}, \frac{a_{i+1}}{b_{i+1}} \right), I_1 \left(\frac{a_i}{b_i}, \frac{a_{i+1}}{b_{i+1}} \right), \dots \right. \\ \left. \dots, I_{n-2} \left(\frac{a_i}{b_i}, \frac{a_{i+1}}{b_{i+1}} \right), I_{n-1} \left(\frac{a_i}{b_i}, \frac{a_{i+1}}{b_{i+1}} \right) = \frac{a_{i+1}}{b_{i+1}}, \dots, \frac{a_\nu}{b_\nu}, \frac{1}{0} \right\}.$$

A partial $(2, n)$ -Farey sequence is obtained by omitting some insertion operators. Starting again with the complete sequence $\left\{ \frac{-1}{0}, x_0 = \frac{a_0}{b_0}, \dots, x_\nu = \frac{a_\nu}{b_\nu}, \frac{1}{0} \right\}$, we choose two consecutive numbers $\frac{a_i}{b_i}$ and $\frac{a_{i+1}}{b_{i+1}}$, where we want to insert a hole of length d . Now, we do not apply all operators, only I_1, \dots, I_{n-d-1} . We call the pair (x_i, x_j) the *support of the hole*. We continue to extend this sequence by applying the procedure above (full and partial insertion) but now we are not allowed inserting numbers in the hole, between I_{n-d-1} and $x_j = I_{n-1}$.

Example. Since the index of the insertion operators runs from 1 to $n - 2$, there are no non-trivial operators for $n \leq 2$. From a geometric point of view, $n = 2$ corresponds to the Hecke group Δ_2 which is not a hyperbolic but an Euclidian triangle group. Hence, the first non-trivial insertion operator occurs for $n = 3$.

- $n = 3$: The non-trivial operator I_1 is well known from the theory of Farey fractions

$$I_1\left(\frac{a_i}{b_i}, \frac{a_j}{b_j}\right) = \frac{a_i + a_j}{b_i + b_j}.$$

- $n = 4$: Now, we have two non-trivial operators

$$I_1\left(\frac{a_i}{b_i}, \frac{a_j}{b_j}\right) = \frac{a_i + \sqrt{2}a_j}{b_i + \sqrt{2}b_j},$$

$$I_2\left(\frac{a_i}{b_i}, \frac{a_j}{b_j}\right) = \frac{\sqrt{2}a_i + a_j}{\sqrt{2}b_i + b_j}.$$

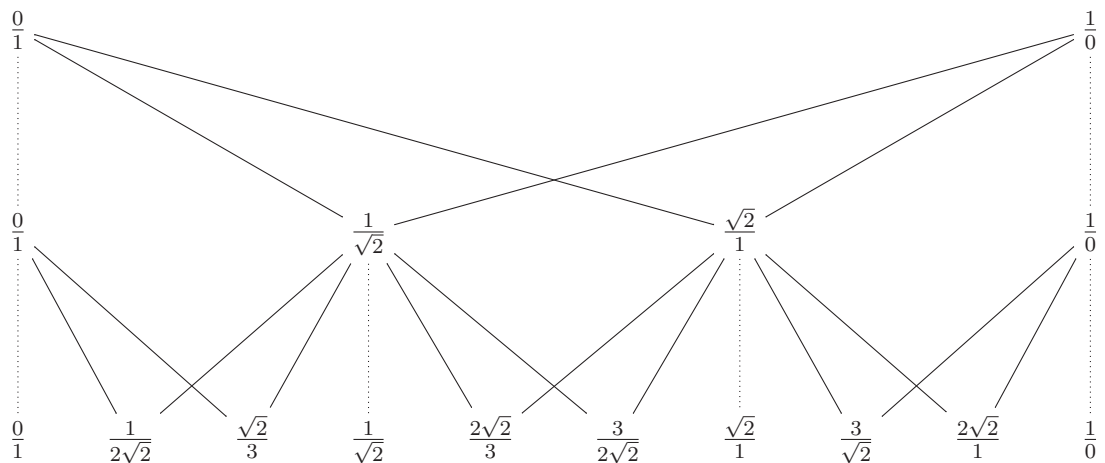
- $n = 6$: There are 4 insertion operators, we just list the first two. The remaining two operators are obtained by exchanging the role of a_i and a_j , respectively b_i and b_j .

$$I_1\left(\frac{a_i}{b_i}, \frac{a_j}{b_j}\right) = \frac{a_i + \sqrt{3}a_j}{b_i + \sqrt{3}b_j},$$

$$I_2\left(\frac{a_i}{b_i}, \frac{a_j}{b_j}\right) = \frac{\sqrt{3}a_i + 2a_j}{\sqrt{3}b_i + 2b_j}.$$

Using these operators, we construct a generalization of the Stern-Brocot tree. We start with the fractions $\frac{0}{1}$ and $\frac{1}{0}$. Then, we apply the insertion operators to obtain a new level. For the classical Stern-Brocot tree, we insert exactly one fraction for each level and every fraction is a rational number. In this generalization, we insert more than one fraction for each level, $n - 2$ fractions. Furthermore, the resulting fractions are not rational numbers anymore. As we see from the definition of the insertion operators, we now have to work over number fields.

Example. $n = 4$:



In the light of these operators, we see that an actual hole in a sequence only appears, if n is not a prime number. If n is a prime number, we only insert $n - 1 - 1 = n - 2$ points to obtain a complete Farey sequence. Since we have seen that there are for each pair of fractions $n - 2$ insertion operators, we end up again with a complete Farey sequence, if we insert $n - 2$ fractions.

In the definition of a complete $(2, n)$ -Farey sequence we asked for the determinant of two consecutive number to be one. For a hole in the partial $(2, n)$ -Farey sequence, this does not hold. We use the insertion operators to calculate the determinant for a hole.

6.3 Lemma. *If (x_i, x_{i+1}) is a hole in a $(2, n)$ -Farey sequence, we have*

$$g(x_i, x_{i+1}) = \frac{\sin\left(\frac{\pi d}{n}\right)}{\sin\left(\frac{\pi}{n}\right)}.$$

Here, d is the length of the hole.

Proof. If (x_i, x_{i+1}) is a hole in a sequence, it is obtained by the use of the insertion operators I_1, \dots, I_{n-d-1} on the support of the hole. We define the fractions $\tilde{x}_i = \frac{a_i}{b_i}$ and $\tilde{x}_j = \frac{a_j}{b_j}$ to be this support. Hence, the hole appears between the operators $x_i = I_{n-d-1}(\tilde{x}_i, \tilde{x}_j)$ and $x_{i+1} = I_{n-1}(\tilde{x}_i, \tilde{x}_j)$. Therefore, we need to calculate the following determinant

$$\begin{aligned} & g\left(I_{n-d-1}\left(\frac{a_i}{b_i}, \frac{a_j}{b_j}\right), I_{n-1}\left(\frac{a_i}{b_i}, \frac{a_j}{b_j}\right)\right) \\ &= g\left(\frac{\csc\left(\frac{\pi}{n}\right)\left(a_j \sin\left(\frac{d\pi}{n}\right) + a_i \sin\left((1+d)\frac{\pi}{n}\right)\right)}{\csc\left(\frac{\pi}{n}\right)\left(b_j \sin\left(\frac{d\pi}{n}\right) + b_i \sin\left((1+d)\frac{\pi}{n}\right)\right)}, \frac{a_j}{b_j}\right) \\ &= \left| \csc\left(\frac{\pi}{n}\right) \sin\left(\frac{d\pi}{n}\right) a_i b_j - \csc\left(\frac{\pi}{n}\right) \sin\left(\frac{d\pi}{n}\right) a_j b_i \right| \\ &= \underbrace{|a_i b_j - a_j b_i|}_{=1} \frac{\sin\left(\frac{\pi d}{n}\right)}{\sin\left(\frac{\pi}{n}\right)}. \end{aligned}$$

□

$(2, n)$ -Farey symbols

Now, we equip the $(2, n)$ -Farey sequences with additional information which we call the pairings. This is the analog of the pairings in the special polygons. Inspired by Kulkarni, we start with a special polygon P which has $\left\{\frac{0}{1}, x_0, x_1, \dots, x_\nu, \frac{1}{0}\right\}$ as $(2, n)$ -sequence formed by its vertices.

If (x_i, x_{i+1}) is a hole in the sequence, we know that there are two paired odd edges, one starting at x_i and the other starting at x_{i+1} , meeting at an internal angle $\frac{2\pi}{d}$ where

$d \neq 1$ is a divisor of n . We call this a n/d -odd pairing and indicate this information by

$$x_i \overset{\text{---}}{\underset{(n/d,n)}{\curvearrowright}} x_{i+1}.$$

Remark. In figure 6.4 we see a part of a special polygon which corresponds to a n/d -odd pairing. In this example, we have $n = 6$ and $d = 3$ resulting in a 2-odd pairing. Note that at the elliptic point, $\frac{n}{d}$ triangle meet. The order of the stabilizer of this point is d .

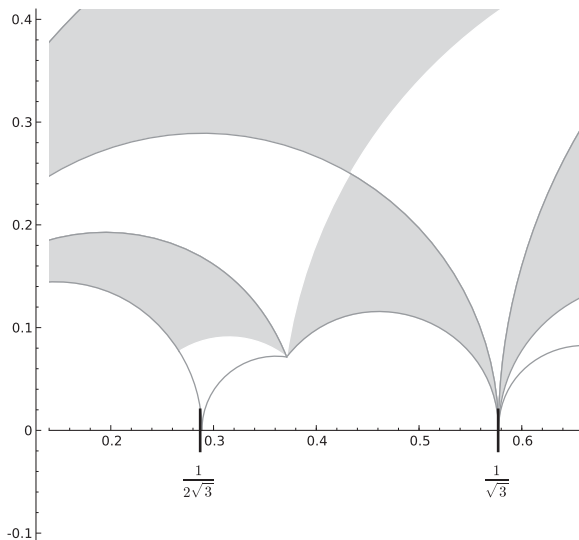


Figure 6.4.: This is the following pairing

$$\frac{1}{2\sqrt{3}} \overset{\text{---}}{\underset{(2,6)}{\curvearrowright}} \frac{1}{\sqrt{3}}.$$

If (x_i, x_{i+1}) is not a hole in the Farey sequence, there are three possibilities. The complete hyperbolic arc from x_i to x_{i+1} can be paired with itself. The first possibility is a special case of the n/d -odd pairing, when $d = n$.

The second possibility is the *even pairing* – we indicate it with

$$x_i \overset{\text{---}}{\underset{\circ}{\curvearrowright}} x_{i+1}.$$

The last possibility is that the complete hyperbolic arc from x_i to x_{i+1} is a part of a *free pairing*. There is a $j \neq i$, such that the arc x_i to x_{i+1} is paired with the arc x_j to x_{j+1} . We indicate this kind of pairings with

$$x_i \overset{\text{---}}{\underset{a}{\curvearrowright}} x_{i+1} \quad \cdots \quad x_j \overset{\text{---}}{\underset{a}{\curvearrowright}} x_{j+1},$$

where a is a positive integer number which is different for each different free pairing.

Definition. A *generalized Farey symbol* is a n -Farey sequence, such that every pair (x_i, x_{i+1}) of consecutive numbers of the sequence is equipped with information we described above.

Example. In the section about special polygons we presented a typical 4-special polygon, figure 6.3. The corresponding $(2, 4)$ -Farey symbol is the following

$$\frac{-1}{0} \underset{1}{\frown} \frac{0}{1} \underset{\circ}{\frown} \frac{1}{2\sqrt{2}} \underset{(2,4)}{\frown} \frac{1}{\sqrt{2}} \underset{1}{\frown} \frac{\sqrt{2}}{1} \underset{(1,4)}{\frown} \frac{5}{2\sqrt{2}} \underset{2}{\frown} \frac{4\sqrt{2}}{3} \underset{2}{\frown} \frac{3}{\sqrt{2}} \underset{\circ}{\frown} \frac{2\sqrt{2}}{1} \underset{\circ}{\frown} \frac{1}{0}.$$

Algorithms for generalized Farey symbols

In this section we explain, how one does calculations using the generalized Farey symbols. Most of the algorithms work similar to $\text{PSL}_2(\mathbb{Z})$ [Kul91], [Kur09]. Especially we show that it is possible to construct a generalized Farey symbol for every subgroup of a Hecke group of finite index.

Before we start with the actual algorithms, we introduce the *standard maps* which help us to construct pairing matrices and coset representatives.

Definition. Let $x_i = \frac{a_i}{b_i}$ and $x_j = \frac{a_j}{b_j}$ be two real numbers, such that $g(x_i, x_j) = 1$. Then, we define the *standard map* as follows

$$\Lambda_{(x_i, x_j)} = \begin{pmatrix} a_j & a_i \\ b_j & b_i \end{pmatrix}.$$

6.4 Lemma. Let $x_i = \frac{a_i}{b_i}$ and $x_j = \frac{a_j}{b_j}$ be two real numbers, such that $g(x_i, x_j) = 1$. Then, the standard map $\Lambda_{(x_i, x_j)}$ has the following properties.

- (i) $\det(\Lambda_{(x_i, x_j)}) = 1$.
- (ii) $\Lambda_{(x_i, x_j)}(0) = x_i$.
- (iii) $\Lambda_{(x_i, x_j)}(\infty) = x_j$.
- (iv) $\Lambda_{(x_i, x_j)}(\rho_n) = \frac{a_i b_i + a_j b_j + (a_j b_i + a_i b_j) \cos\left(\frac{\pi}{n}\right)}{2b_i b_j \cos\left(\frac{\pi}{n}\right) + b_i^2 + b_j^2} + i \cdot \frac{\sin\left(\frac{\pi}{n}\right)}{2b_i b_j \cos\left(\frac{\pi}{n}\right) + b_i^2 + b_j^2}$.
- (v) Let $\tilde{\rho}_n = -\bar{\rho}_n = S\rho_n$, with $S = \begin{pmatrix} 0 & -1 \\ 1 & 0 \end{pmatrix}$. Then,

$$\Lambda_{(x_i, x_j)}(\tilde{\rho}_n) = \frac{a_i b_i + a_j b_j - (a_j b_i + a_i b_j) \cos\left(\frac{\pi}{n}\right)}{b_i^2 + b_j^2 - 2b_i b_j \cos\left(\frac{\pi}{n}\right)} + i \cdot \frac{\sin\left(\frac{\pi}{n}\right)}{b_i^2 + b_j^2 - 2b_i b_j \cos\left(\frac{\pi}{n}\right)}.$$

- (vi) The standard map $\Lambda_{(x_i, x_j)}$ maps the fundamental domain described in chapter 4, lemma 4.2 of the triangle group Δ_n to a hyperbolic triangle with edges given by the formulas above. If (x_i, x_{i+1}) is a part of a complete $(2, n)$ -Farey sequence, the resulting triangle is a part of the corresponding tessellation of the upper half plane. One edge coincides with the geodesic from x_i to x_{i+1} and from the two possibilities it is the one with the smaller imaginary part.

Proof. The proof of this is straight forward. A direct calculation confirms the points (i) to (v). The last point works as follows. From (ii) and (iii) follows, using the fact that Möbius transformations maps circles to circles, that the line from 0 to ∞ maps to a hyperbolic arc from x_i to x_{i+1} . The standard map is a member in the triangle group. Hence, it maps the fundamental domain to a part of the tessellation. Since there are two triangles, with the line from x_i to x_{i+1} , we have to verify that it maps to the lower one. We do this by comparing the imaginary parts of (iv) and (v). \square

Pairing matrices

Now, we write down the pairing matrices. The idea is that we pull the triangle in question back to the standard fundamental domain, using the standard map. Then, we apply the pairing matrix for this domain and push it back.

6.5 Lemma. Let $\mathcal{F}_n = \left\{ \frac{-1}{0}, x_0, x_1, \dots, x_\nu, \frac{1}{0} \right\}$ be a $(2, n)$ -Farey symbol and P the corresponding special polygon. Then, we have the following pairing matrices.

- (i) For an even pairing

$$x_i \overset{\frown}{\underset{\circ}{x_{i+1}}}$$

we have the pairing matrix:

$$E_{(x_i, x_{i+1})} := \begin{pmatrix} a_i b_i + a_{i+1} b_{i+1} & -a_i^2 - a_{i+1}^2 \\ b_i^2 + b_{i+1}^2 & -a_i b_i - a_{i+1} b_{i+1} \end{pmatrix}.$$

- (ii) For a n/d -odd pairing between \tilde{x}_i and \tilde{x}_{i+1} with support (x_i, x_{i+1})

$$\tilde{x}_i \overset{\frown}{\underset{(n/d, n)}{\tilde{x}_{i+1}}}$$

we have the pairing matrix

$$O_{(x_i, x_{i+1})}^{(d)} := \begin{pmatrix} -a_{i+1} b_i S_{d-1} - a_i b_i S_d - a_{i+1} b_{i+1} S_d - a_i b_{i+1} S_{d+1} & S_d a_i^2 + \xi a_{i+1} S_d a_i + a_{i+1}^2 S_d \\ -\xi b_{i+1} S_d b_i - b_{i+1}^2 S_d - b_i^2 S_d & a_i b_{i+1} S_{d-1} + a_i b_i S_d + a_{i+1} b_{i+1} S_d + a_{i+1} b_i S_{d+1} \end{pmatrix},$$

where $S_d = \frac{2}{d} T'_n \left(\frac{\xi}{2} \right)$. The Chebyshev polynomials are denoted by T_n and $\xi = 2 \cos \frac{\pi}{n}$.

(iii) For a free pairing

$$x_i \underbrace{\quad}_{a} x_{i+1} \quad \dots \quad x_j \underbrace{\quad}_{a} x_{j+1}$$

we have the pairing matrix

$$F_{(x_i, x_{i+1}, x_j, x_{j+1})} := \begin{pmatrix} a_j b_i + a_{j+1} b_{i+1} & -a_i a_j - a_{i+1} a_{j+1} \\ b_i b_j + b_{i+1} b_{j+1} & -a_i b_j - a_{i+1} b_{j+1} \end{pmatrix}.$$

Proof. For all three pairings, we use the technique described above: We first use the inverse standard map to map the geodesic from x_i to x_{i+1} to the line 0 to ∞ . Then, we apply the map we need for the pairing and map it back to the right interval, again using the standard map.

- (i) For the even pairing, we first apply (as explained) the inverse standard map. Then, we use the map S to exchange 0 and ∞ . Then, we map back with the standard map

$$\Lambda_{(x_i, x_{i+1})} \cdot S \cdot \Lambda_{(x_i, x_{i+1})}^{-1}.$$

After some simplifications we obtain the result.

- (ii) The odd pairing works analog to the even pairing – except we use R_n in the middle.
 (iii) For the free pairing, we need to reverse the orientation of the hyperbolic arcs. We need to map x_i to x_{j+1} and vice versa. We achieve this by the following

$$\Lambda_{(x_j, x_{j+1})} \cdot S \cdot \Lambda_{(x_i, x_{i+1})}^{-1}.$$

□

We now derive the insertion operator which we already have introduced. From a geometric point of view its purpose is to “insert the right fractions”. If we have a part of a Farey sequence (x_i, x_{i+1}) , we see the corresponding hyperbolic arc as an edge of a special polygon. If we extend this special polygon, we need to introduce more cusps. These cusps are obtained as follows. The hyperbolic arc x_i, x_{i+1} has two adjacent triangles which fit into the corresponding tessellation. The standard map gives us the matrix which maps the fundamental domain to this triangle. We now rotate this triangle around the elliptic point ρ_n , using the matrix R_n . This gives us a hyperbolic n -gon whose vertices are exactly the points we need to insert into our original sequence. They are calculated by letting the calculated matrices operate on the point x_i

$$\begin{aligned} I_\mu(x_i, x_j) &= (\Lambda_{(x_i, x_j)} \cdot R_n^\mu \cdot \Lambda_{(x_i, x_j)}^{-1})(x_i) \\ &= (\Lambda_{(x_i, x_j)} \cdot R_n^\mu)(0). \end{aligned}$$

To show that the two definitions of the insertion operator are equal, we need the powers of R_n .

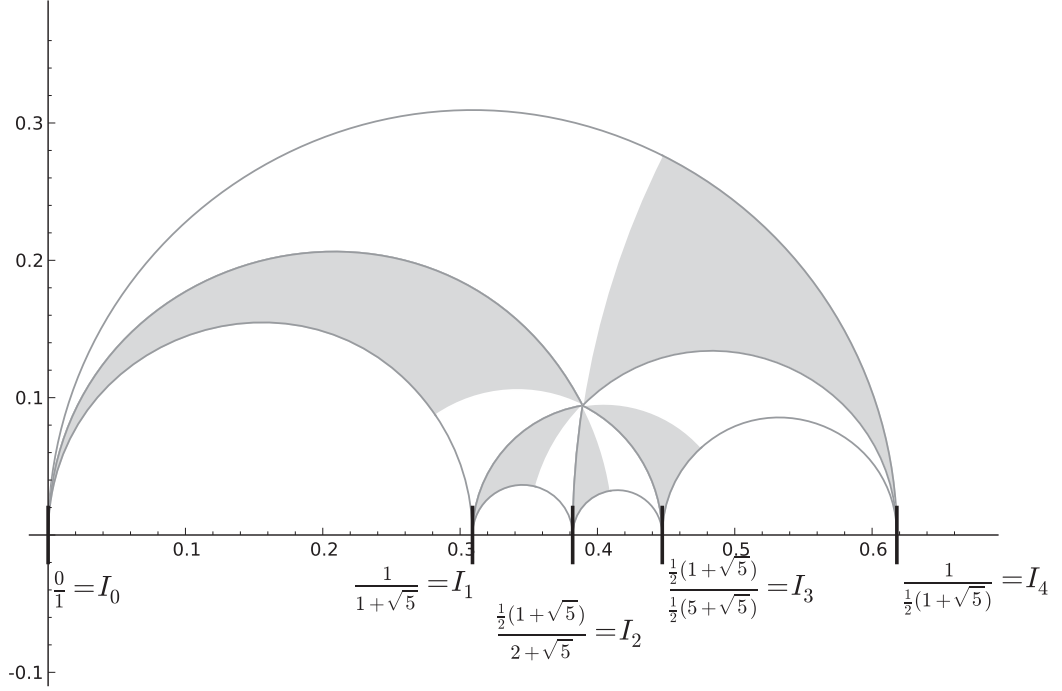


Figure 6.5.: Geometric interpretation of the insertion operators

6.6 Lemma. Let $R_n = R = \begin{pmatrix} 0 & -1 \\ 1 & -2\cos(\frac{\pi}{n}) \end{pmatrix}$. Then,

$$R^\mu = \begin{pmatrix} (-1)^{\mu+1} \csc\left(\frac{\pi}{n}\right) \sin\left((\mu-1)\frac{\pi}{n}\right) & (-1)^\mu \csc\left(\frac{\pi}{n}\right) \sin\left(\mu\frac{\pi}{n}\right) \\ (-1)^{\mu+1} \csc\left(\frac{\pi}{n}\right) \sin\left(\mu\frac{\pi}{n}\right) & (-1)^\mu \csc\left(\frac{\pi}{n}\right) \sin\left((\mu+1)\frac{\pi}{n}\right) \end{pmatrix}.$$

Proof. We prove this lemma with a calculation. In a first step, we diagonalize the matrix $R = A \cdot D \cdot A^{-1}$, where

$$A = \begin{pmatrix} e^{-i\frac{\pi}{n}} & e^{i\frac{\pi}{n}} \\ 1 & 1 \end{pmatrix}, \quad D = \begin{pmatrix} -e^{i\frac{\pi}{n}} & 0 \\ 0 & -e^{-i\frac{\pi}{n}} \end{pmatrix}.$$

Then, we have

$$\begin{aligned} R^\mu &= (A \cdot D \cdot A^{-1})^\mu \\ &= A \cdot D^\mu \cdot A^{-1} \\ &= A \cdot \begin{pmatrix} (-1)^\mu e^{i\frac{\pi}{n}} & 0 \\ 0 & (-1)^\mu e^{-i\frac{\pi}{n}} \end{pmatrix} \cdot A^{-1} \\ &= \begin{pmatrix} e^{i\pi\mu} \csc\left(\frac{\pi}{n}\right) \sin\left(\frac{\pi}{n} - \mu\frac{\pi}{n}\right) & e^{i\pi\mu} \csc\left(\frac{\pi}{n}\right) \sin\left(\mu\frac{\pi}{n}\right) \\ -e^{i\pi\mu} \csc\left(\frac{\pi}{n}\right) \sin\left(\mu\frac{\pi}{n}\right) & e^{i\pi\mu} \csc\left(\frac{\pi}{n}\right) \sin\left((\mu+1)\frac{\pi}{n}\right) \end{pmatrix}. \end{aligned}$$

□

This lemma is used to construct the insertion operators as follows. We first use the powers of the matrix R and map it then, to an interval $x_i = \frac{a_i}{b_i}$, $x_j = \frac{a_j}{b_j}$, using again the standard map. The images of 0 under the different powers of R , give the point of the insertion operators

$$\begin{aligned}
I_\mu\left(\frac{a_i}{b_i}, \frac{a_j}{b_j}\right) &= \left(\Lambda_{(x_i, x_j)} \cdot R^\mu\right)(0) \\
&= \left(\begin{array}{c} e^{i\pi\mu} \csc\left(\frac{\pi}{n}\right) \left(a_j \sin\left(\frac{\pi-\pi\mu}{n}\right) - a_i \sin\left(\frac{\pi\mu}{n}\right) \right) \\ e^{i\pi\mu} \csc\left(\frac{\pi}{n}\right) \left(a_j \sin\left(\frac{\pi\mu}{n}\right) + a_i \sin\left(\frac{\pi(\mu+1)}{n}\right) \right) \\ e^{i\pi\mu} \csc\left(\frac{\pi}{n}\right) \left(b_j \sin\left(\frac{\pi-\pi\mu}{n}\right) - b_i \sin\left(\frac{\pi\mu}{n}\right) \right) \\ e^{i\pi\mu} \csc\left(\frac{\pi}{n}\right) \left(b_j \sin\left(\frac{\pi\mu}{n}\right) + b_i \sin\left(\frac{\pi(\mu+1)}{n}\right) \right) \end{array} \right) (0) \\
&= \frac{e^{i\pi\mu} \csc\left(\frac{\pi}{n}\right) \left(a_j \sin\left(\frac{\pi\mu}{n}\right) + a_i \sin\left(\frac{\pi(\mu+1)}{n}\right) \right)}{e^{i\pi\mu} \csc\left(\frac{\pi}{n}\right) \left(b_j \sin\left(\frac{\pi\mu}{n}\right) + b_i \sin\left(\frac{\pi(\mu+1)}{n}\right) \right)}.
\end{aligned}$$

In this formula we cancel the term $e^{i\pi\mu} = \pm 1$, since this is only a sign. This sign corresponds in terms of matrices to the negative of the identity which is irrelevant since we are working in $\text{PSL}_2(\mathbb{R})$.

Construction of a generalized Farey symbol

In this subsection, we construct a Farey symbol from a given subgroup of a Hecke group Δ_n . We start with a certain (unfinished) Farey symbol, check whether we can pair anything and if we cannot, we add more fractions, using the insertion operators.

Let $\Gamma \subseteq \Delta_n$ be a subgroup of finite index. Then, the following algorithm produces a generalized Farey symbol.

Algorithm 3. (i) Start with the unfinished Farey symbol

$$\frac{-1}{0} \quad \underbrace{\hspace{1.5cm}} \quad \frac{0}{1} \quad \underbrace{\hspace{1.5cm}} \quad \frac{1}{0}.$$

(ii) For each unpaired side x_i, x_{i+1} check if

- the even pairing matrix $E_{(x_i, x_{i+1})}$,
- or any free pairing matrix $F_{(x_i, x_{i+1}, x_j, x_{j+1})}$ for any other side x_j, x_{j+1} ,

is in the subgroup Γ . If this holds, assign that pairing.

(iii) For each unpaired side x_i, x_{i+1} check if any n/d -odd pairing matrix $O_{(x_i, x_{i+1})}^{(d)}$, is in the subgroup. If this holds, insert $n/d - 1$ points (on the left) and assign that

From the class numbers we easily find a set of representative of the cusp-classes. Just choose for each number an arbitrary fraction.

Furthermore, we calculate the cusp widths of the cusps. To each fraction we associate an individual width. This is the number of cosets which have this fraction as an edge – divided by two. Hence, this number needs not to be an integer. To get the actual cusp widths, need to sum all cusp widths in a given class. This number of cosets is calculated as follows. Let

$$\cdots x_{i-1} \underbrace{\quad}_{p_{i-1}} x_i \underbrace{\quad}_{p_i} x_{i+1} \cdots$$

be a part of a $(2, n)$ -Farey symbol. Then, we define

$$w_i := \begin{cases} \frac{g(x_{i-1}, x_{i+1})}{2 \cos\left(\frac{\pi}{n}\right)} & \text{if } p_{i-1} \text{ and } p_i \text{ are both free or even} \\ \frac{g(x_{i-1}, x_{i+1})}{2 \cos\left(\frac{\pi}{n}\right)} - \frac{1}{2} & \text{if } p_{i-1} \text{ or } p_i \text{ is odd} \\ \frac{g(x_{i-1}, x_{i+1})}{2 \cos\left(\frac{\pi}{n}\right)} - 1 & \text{if } p_{i-1} \text{ and } p_i \text{ are both odd.} \end{cases}$$

Added up these numbers w_i over all fractions c_i in the cusp class gives the width.

Genus and index

For the genus and the index there are helpful formulas. First of all, we compute the rank of $\pi_1(\Gamma \backslash \mathbb{H})$ which is the rank of the (un-compactified) modular curve. This rank is equal to the number of free pairings which is determined by counting the number of pairings greater than zero and dividing by two. Alternatively it is the largest pairing number. This rank is also calculated as $r = 2g + t - 1$, where t is the number of cusps. Hence, we have a formula for the genus

$$g = \frac{r - t + 1}{2}.$$

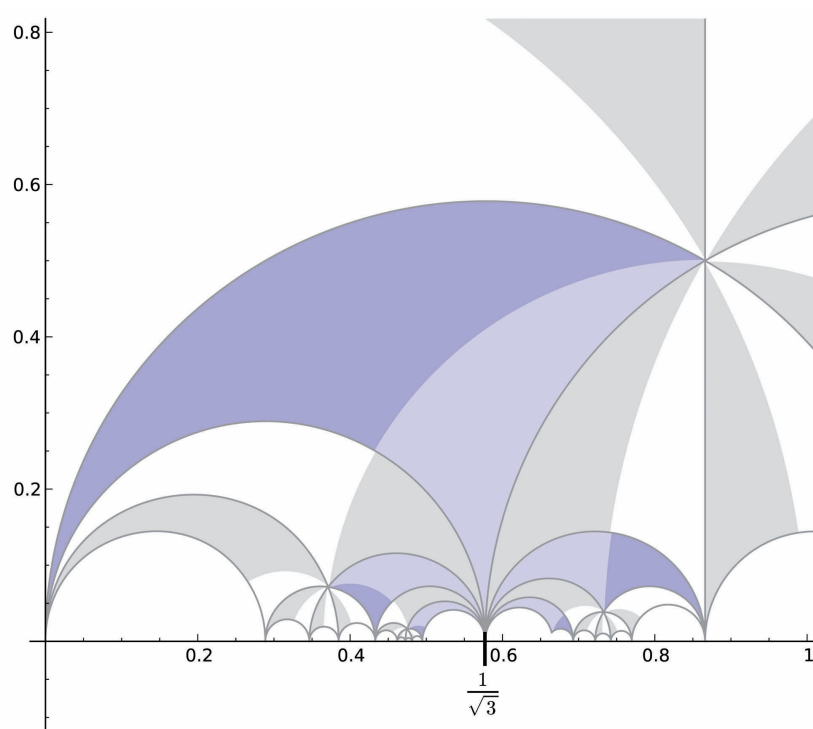
The index of the subgroup is calculated with the help of the formula for Hurwitz.

Coset representatives and a fundamental domain

The idea of calculating coset representatives works as follows. For each fraction we want to “fan out” images of \mathcal{F} . Here, \mathcal{F} is the fundamental domain of the Hecke group Δ_n , see figure 6.6.

The endpoints of this fan are the neighbor fractions. From this, we find number of parts the fan needs. We define for a fraction in a Farey symbol

$$\cdots x_{i-1} \underbrace{\quad}_{p_{i-1}} x_i \underbrace{\quad}_{p_i} x_{i+1} \cdots$$


 Figure 6.6.: Fan out at $\frac{1}{\sqrt{3}}$

the “fan width” as follows

$$\omega_i := \begin{cases} \frac{g(x_{i-1}, x_{i+1})}{2 \cos\left(\frac{\pi}{n}\right)} & \text{if } p_{i-1} \text{ and } p_i \text{ are both free or even} \\ \frac{g(x_{i-1}, x_{i+1})}{2 \cos\left(\frac{\pi}{n}\right)} - 1 & \text{if } p_i \text{ is odd} \\ \frac{g(x_{i-1}, x_{i+1})}{2 \cos\left(\frac{\pi}{n}\right)} - 2 & \text{if } p_{i-1} \text{ and } p_i \text{ are both odd.} \end{cases}$$

The rest is similar to our standard techniques. As we know how to fan out at infinity, using the matrix $T = \begin{pmatrix} 1 & 1 \\ 0 & 1 \end{pmatrix}$, we map this to the fraction in question. Hence, the coset representatives are given via the following formulas

$$\mathcal{R} = \bigcup_{i=0}^n \left\{ S \cdot T^j \cdot \Lambda_{(x_{i-1}, x_i)}, 0 \leq j < \omega_i \right\}. \quad (6.7)$$

An example of a $(2, 4)$ -Farey symbol – discussed in detail

We finish this chapter with a detailed example of a generalized Farey symbol. The triangle group we are looking at is the group $\Delta(2, 4)$. The subgroup Γ we choose, is

given by the monodromy of the alternating group of length 6. It is a group of order 360 and it is generated by the following two elements

$$\begin{aligned}\sigma_2 &= (1, 2)(3, 4) \in \mathfrak{S}_6, \\ \sigma_4 &= (1, 6, 4, 2)(3, 5) \in \mathfrak{S}_6.\end{aligned}$$

In chapter 4 we presented an algorithm to check the membership of a group in Δ_n to be in a subgroup defined by permutations. To check, whether a matrix is in this subgroup, we used algorithm 1 described in chapter 4.

The first part is to construct the Farey symbol. According to algorithm 3, we start with

$$\frac{-1}{0} \frown \frac{0}{1} \frown \frac{1}{0}.$$

The possible pairing matrices are

$$\begin{aligned}E_{\left(\frac{0}{1}, \frac{1}{0}\right)} &= \begin{pmatrix} 0 & -1 \\ 1 & 0 \end{pmatrix} && \notin \Gamma, \\ O_{\left(\frac{0}{1}, \frac{1}{0}\right)}^{(1)} &= \begin{pmatrix} \sqrt{2} & -1 \\ 1 & 0 \end{pmatrix} && \notin \Gamma, \\ O_{\left(\frac{0}{1}, \frac{1}{0}\right)}^{(2)} &= \begin{pmatrix} -1 & \sqrt{2} \\ -\sqrt{2} & 1 \end{pmatrix} && \notin \Gamma.\end{aligned}$$

No pairing is possible, so we have to introduce new fractions. For this, we use the insertion operator $I_1\left(\frac{0}{1}, \frac{1}{0}\right) = \frac{1}{\sqrt{2}}$ and $I_2\left(\frac{0}{1}, \frac{1}{0}\right) = \frac{\sqrt{2}}{1}$, resulting in the new symbol

$$\frac{-1}{0} \frown \frac{0}{1} \frown \frac{1}{\sqrt{2}} \frown \frac{\sqrt{2}}{1} \frown \frac{1}{0}.$$

Now, we find sides which can be paired

$$\begin{aligned}E_{\left(\frac{1}{0}, \frac{1}{\sqrt{2}}\right)} &= \begin{pmatrix} \sqrt{2} & -1 \\ 3 & -\sqrt{2} \end{pmatrix} && \in \Gamma, \\ F_{\left(\frac{-1}{0}, \frac{0}{1}, \frac{\sqrt{2}}{1}, \frac{1}{0}\right)} &= \begin{pmatrix} 1 & \sqrt{2} \\ 0 & 1 \end{pmatrix} && \in \Gamma, \\ O_{\left(\frac{1}{\sqrt{2}}, \frac{\sqrt{2}}{1}\right)}^{(2)} &= \begin{pmatrix} -7 & 5\sqrt{2} \\ -5\sqrt{2} & 7 \end{pmatrix} && \in \Gamma.\end{aligned}$$

For the $4/2$ -pairing we need to insert another fraction $I_1\left(\frac{1}{\sqrt{2}}, \frac{\sqrt{2}}{1}\right) = \frac{2\sqrt{2}}{3}$. We obtain the following unfinished Farey symbol

$$\frac{-1}{0} \frown \frac{0}{1} \frown \frac{1}{\sqrt{2}} \frown \frac{2\sqrt{2}}{3} \frown \frac{\sqrt{2}}{1} \frown \frac{1}{0}.$$

1 o (2, 4) 1

The last unpaired edge of the symbol is identified to be an even pairing

$$E\left(\frac{1}{\sqrt{2}}, \frac{\sqrt{2}}{1}\right) = \begin{pmatrix} 7\sqrt{2} & -9 \\ 11 & -7\sqrt{2} \end{pmatrix} \in \Gamma.$$

This results in the Farey symbol

$$\frac{-1}{0} \underset{1}{\frown} \frac{0}{1} \underset{\circ}{\frown} \frac{1}{\sqrt{2}} \underset{\circ}{\frown} \frac{2\sqrt{2}}{3} \underset{(2,4)}{\frown} \frac{\sqrt{2}}{1} \underset{1}{\frown} \frac{1}{0}.$$

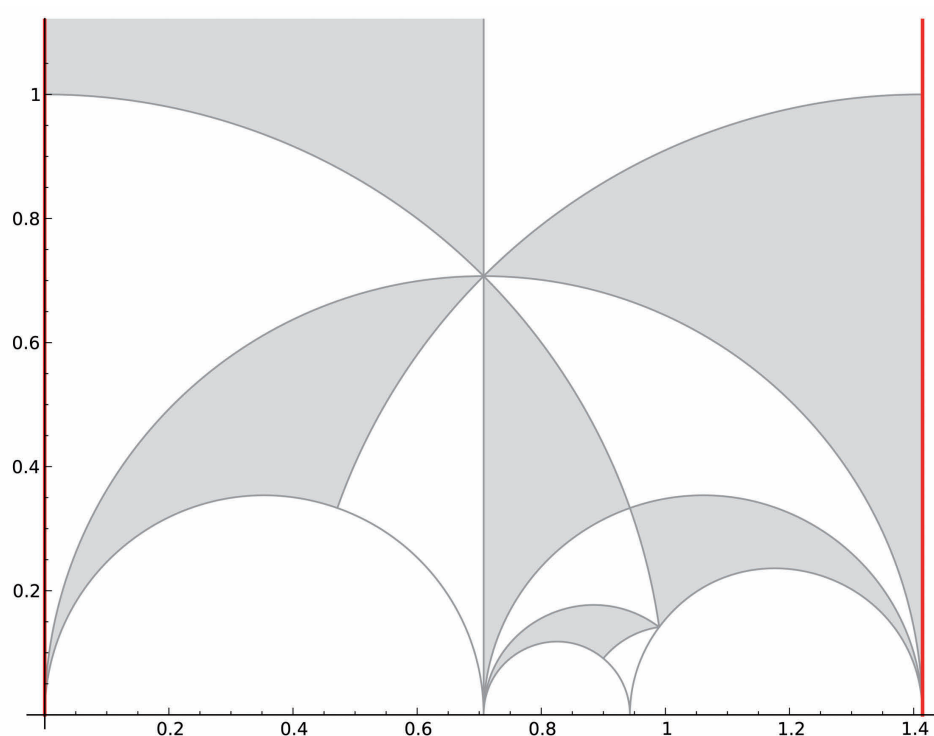


Figure 6.7.: The special polygon for this example

By looking at the pairing matrices, we find a minimal set of generators for our subgroup - the pairing matrices

$$\Gamma = \left\langle \begin{pmatrix} \sqrt{2} & -1 \\ 3 & -\sqrt{2} \end{pmatrix}, \begin{pmatrix} 1 & \sqrt{2} \\ 0 & 1 \end{pmatrix}, \begin{pmatrix} -7 & 5\sqrt{2} \\ -5\sqrt{2} & 7 \end{pmatrix}, \begin{pmatrix} 7\sqrt{2} & -9 \\ 11 & -7\sqrt{2} \end{pmatrix} \right\rangle.$$

The widths of the fractions are calculated with the formulas we presented.

| x_i | w_i | Cusp class |
|-----------------------------|------------------------------------------------------------------------------------------------------|------------|
| $x_{-1} = \frac{1}{0}$ | $\frac{g\left(\frac{0}{1}, \frac{\sqrt{2}}{1}\right)}{\sqrt{2}} = 1$ | 1 |
| $x_0 = \frac{0}{1}$ | $\frac{g\left(\frac{1}{0}, \frac{1}{\sqrt{2}}\right)}{\sqrt{2}} = 1$ | 2 |
| $x_1 = \frac{1}{\sqrt{2}}$ | $\frac{g\left(\frac{0}{1}, \frac{2\sqrt{2}}{3}\right)}{\sqrt{2}} = 2$ | 2 |
| $x_2 = \frac{2\sqrt{2}}{3}$ | $\frac{g\left(\frac{1}{\sqrt{2}}, \frac{3}{2\sqrt{2}}\right)}{\sqrt{2}} - \frac{1}{2} = \frac{1}{2}$ | 2 |
| $x_3 = \frac{\sqrt{2}}{1}$ | $\frac{g\left(\frac{3}{2\sqrt{2}}, \frac{1}{0}\right)}{\sqrt{2}} - \frac{1}{2} = \frac{3}{2}$ | 2 |

The last row of the table was found using the algorithm to construct the cusp classes. From this table, we see that our group has two inequivalent cusps. This first cusp is ∞ and has width 1 and the second one is represented by 0 and has width $1 + 2 + \frac{1}{2} + \frac{3}{2} = 5$.

Genus and index are calculated in the usual way. We have one free pairing which is also the rank of $\pi_1(\Gamma \backslash \mathbb{H})$ and two cusps - which gives a genus of zero. The index is calculated to be six.

We end the example by calculating the coset representatives. Following the algorithm, we first need to find fan-widths for all fractions and then calculate the cosets using formula (6.7).

| x_i | ω_i | Coset representatives |
|-----------------------------|------------------------------------------------------------------------------|----------------------------------------------------------------------------------------------------------------------------------------------------------------------------------------------------------------------------------------------------------------------------------------------|
| $x_{-1} = \frac{1}{0}$ | $\frac{g\left(\frac{0}{1}, \frac{\sqrt{2}}{1}\right)}{\sqrt{2}} = 1$ | $S \cdot T^0 \cdot \Lambda_{\left(\frac{0}{1}, \frac{\sqrt{2}}{1}\right)}^{-1} = \begin{pmatrix} 0 & -1 \\ 1 & -\sqrt{2} \end{pmatrix}$ |
| $x_0 = \frac{0}{1}$ | $\frac{g\left(\frac{1}{0}, \frac{1}{\sqrt{2}}\right)}{\sqrt{2}} = 1$ | $S \cdot T^0 \cdot \Lambda_{\left(\frac{-1}{0}, \frac{0}{1}\right)}^{-1} = \begin{pmatrix} 1 & 0 \\ 0 & 1 \end{pmatrix}$ |
| $x_1 = \frac{1}{\sqrt{2}}$ | $\frac{g\left(\frac{0}{1}, \frac{2\sqrt{2}}{3}\right)}{\sqrt{2}} = 2$ | $S \cdot T^0 \cdot \Lambda_{\left(\frac{0}{1}, \frac{1}{\sqrt{2}}\right)}^{-1} = \begin{pmatrix} \sqrt{2} & -1 \\ 1 & 0 \end{pmatrix}$ $S \cdot T^1 \cdot \Lambda_{\left(\frac{0}{1}, \frac{1}{\sqrt{2}}\right)}^{-1} = \begin{pmatrix} \sqrt{2} & -1 \\ -1 & \sqrt{2} \end{pmatrix}$ |
| $x_2 = \frac{2\sqrt{2}}{3}$ | $\frac{g\left(\frac{1}{\sqrt{2}}, \frac{3}{2\sqrt{2}}\right)}{\sqrt{2}} = 1$ | $S \cdot T^0 \cdot \Lambda_{\left(\frac{1}{\sqrt{2}}, \frac{2\sqrt{2}}{3}\right)}^{-1} = \begin{pmatrix} 3 & -2\sqrt{2} \\ -2\sqrt{2} & 3 \end{pmatrix}$ |
| $x_3 = \frac{\sqrt{2}}{1}$ | $\frac{g\left(\frac{3}{2\sqrt{2}}, \frac{1}{0}\right)}{\sqrt{2}} - 1 = 1$ | $S \cdot T^0 \cdot \Lambda_{\left(\frac{3}{2\sqrt{2}}, \frac{\sqrt{2}}{1}\right)}^{-1} = \begin{pmatrix} 1 & -\sqrt{2} \\ \sqrt{2} & -1 \end{pmatrix}$ |

Chapter 7.

The Schwarzian derivative

You have the ring and I see your Schwarzian is as big as mine. Now let's see how well you handle it!

(Dark Helmet in Space Balls)

In this chapter we calculate the Hauptmodul for triangle groups. To do this, we map the fundamental domain of these groups to the complex plane, respectively to the upper half plane. Since we do this conformally, we need the theory of conformal mappings. Especially we will use the Schwarzian derivative. Furthermore, we will explain how to obtain the Picard-Fuchs equations for subgroups of a triangle group.

Introduction to the Schwarzian derivative

Definition. We define the Schwarzian derivative

$$\mathcal{S}(f)(z) = \left(\frac{f''(z)}{f'(z)} \right)' - \frac{1}{2} \left(\frac{f''(z)}{f'(z)} \right)^2 = \frac{f'''(z)}{f'(z)} - \frac{3}{2} \left(\frac{f''(z)}{f'(z)} \right)^2.$$

Since we will do some calculations with this derivative, we collect some rules how to handle it.

7.1 Lemma. For smooth functions $f, g: \mathbb{C} \rightarrow \mathbb{C}$ the following holds.

- (i) Chain rule: $\mathcal{S}(f \circ g) = (\mathcal{S}(f) \circ g) (g')^2 + \mathcal{S}(g)$.
- (ii) Derivative of the inverse: $\mathcal{S}(f^{-1}) = -\frac{\mathcal{S}(f) \circ f^{-1}}{(f'(f^{-1}))^2}$, if f^{-1} exists and is smooth.
- (iii) Derivative of the reciprocal: $\mathcal{S}\left(\frac{1}{f}\right) = \mathcal{S}(f)$.
- (iv) Invariant under Möbius transformations: Let $\begin{pmatrix} a & b \\ c & d \end{pmatrix} \in \text{PSL}_2(\mathbb{R})$ be a matrix and $F = A.f$. Then $\mathcal{S}(f)(z) = \mathcal{S}(F)(z)$.
- (v) The Schwarzian differential equation for the inverse function: If the inverse f^{-1} of the function f satisfies a Schwarzian DGL $\mathcal{S}(f^{-1})(t) - 2Q(t) = 0$, then the function f satisfies

$$\mathcal{S}(f)(t) + 2Q(f) \cdot (f)'(t)^2 = 0.$$

Proof. We prove this lemma by direct computations.

(i) *Chain rule:*

$$(f \circ g)' = (f' \circ g) \cdot g'$$

$$\begin{aligned} (f \circ g)'' &= (f' \circ g)' \cdot g' + (f' \circ g) \cdot g'' \\ &= (f'' \circ g) \cdot g'^2 + (f' \circ g) \cdot g'' \end{aligned}$$

$$\frac{(f \circ g)''}{(f \circ g)'} = \frac{f''(g)g''}{f'(g)} + \frac{g''}{g'}$$

$$\begin{aligned} \mathcal{S}(f \circ g)(t) &= \left(\frac{f(g)''}{f(g)'} \right)' - \frac{1}{2} \left(\frac{f(g)''}{f(g)'} \right)^2 \\ &= \left(\frac{f''(g)g'}{f'(g)} + \frac{g''}{g'} \right)' - \frac{1}{2} \left(\frac{f''(g)g'}{f'(g)} + \frac{g''}{g'} \right)^2 \\ &= \left(\frac{f''(g)g'}{f'(g)} \right)' + \underbrace{\left(\frac{g''}{g'} \right)'}_{\rightarrow \mathcal{S}(g)(t)} - \frac{1}{2} \left(\frac{f''(g)g'}{f'(g)} \right)^2 - \frac{f''(g)g''}{f'(g)} - \underbrace{\frac{1}{2} \left(\frac{g''}{g'} \right)^2}_{\rightarrow \mathcal{S}(g)(t)} \\ &= \underbrace{\frac{f''(g)}{f'(g)} \cdot g''}_{\textcircled{1}} + \left(\frac{f''(g)}{f'(g)} \right)' g'^2 - \underbrace{\frac{f''(g)}{f'(g)} g''}_{\textcircled{1}} - \frac{1}{2} \left(\frac{f''(g)}{f'(g)} \right)^2 g'^2 + \mathcal{S}(g)(t) \\ &= \mathcal{S}(f)(g) \cdot g'^2 + \mathcal{S}(g)(t). \end{aligned}$$

(ii) The *derivative of the inverse* follows from the first point. Let f be a smooth function and f^{-1} its inverse, $f \circ f^{-1} = \text{id}$ and $f^{-1} \circ f = \text{id}$. Since $\mathcal{S}(x)(x) = 0$, we have

$$\begin{aligned} 0 &= \mathcal{S}(f^{-1} \circ f)(t) = \mathcal{S}(f^{-1})(f) \cdot f'^2 + \mathcal{S}(f)(t), \\ \Rightarrow \mathcal{S}(f^{-1})(f(t)) &= -\frac{\mathcal{S}(f)(t)}{(f'(t))^2}. \end{aligned}$$

Choosing $t = f^{-1}(z)$ yields the result.

(iii) We define $r(x) = \frac{1}{x}$ and use again the first point.

$$\begin{aligned} \mathcal{S}\left(\frac{1}{f}\right)(x) &= \mathcal{S}(r \circ f)(x) \\ &= \underbrace{(\mathcal{S}(r)(x) \circ f)}_{=0} \cdot f'^2 + \mathcal{S}(f)(x). \end{aligned}$$

It is also possible to derive this as special case of the next part.

(iv) We define $F = \frac{af+b}{cf+d}$ for constants a, b, c , and d , with the constraint $ad - cb \neq 0$. The condition that the determinant is equal to one is not necessary. We have the derivative of F

$$F' = \frac{ad - bd}{(cf + d)^2} f'$$

and for the logarithmic derivative of this

$$\frac{F''}{F'} = \frac{f''}{f'} - \frac{2cf'}{cf + d}.$$

Hence,

$$\begin{aligned} \left(\frac{F''}{F'}\right)' &= \left(\frac{f''}{f'}\right)' + \frac{2c^2 f'^2}{(cf + d)^2} - \frac{2cf''}{cf + d}, \\ \left(\frac{F''}{F'}\right)^2 &= \left(\frac{f''}{f'}\right)^2 + \frac{4c^2 f'^2}{(cf + d)^2} = \frac{2cf''}{cf + d}. \end{aligned}$$

Therefore, we obtain for the Schwarzian derivative

$$\mathcal{S}(F)(z) = \mathcal{S}(f)(z).$$

(v) This follows directly from the second part. □

Conformal mappings

A conformal mapping is a map that preserves the angle between two differentiable arcs. These maps are used for example to solve a partial differential equation in unusual domains. We map the domain in question to the complex plane or a disc and solve the partial differential equation there. Then we pull the solution back in the original domain and obtain the solution. A good overview of this technique is the book of Driscoll and Trefethen [DT02].

We follow in rough lines the book of Nehari [Neh52]. We work with the fundamental domains of the triangle groups, as we described them in chapter 4. Since they are bounded by geodesics in the hyperbolic geometry of the upper half plane, they fall in the category of *domains bounded by circular arcs*. [Neh52, Chapter V, Section 7]

We start with a closed subset of the complex plane bounded by circular arcs. We denote the edges of the polygon with z_i and the angle by $\pi\alpha_i$. Our goal is to construct a map f which maps a given polygon to the upper half plane. The boundary of the polygon should map to the real axis. We denote the images of the edges by $a_i = f(z_i) \in \mathbb{R}$. This will result in a differential equations of the form

$$\mathcal{S}(f)(z) = Q(z).$$

The geometry of the polygon determines the rational function $Q(z)$. We give a rough sketch how to construct this differential equation. The book of Nehari [Neh52] does this construction in full detail.

Using the symmetry principle [Neh52, Chapter V, Section 5], we see that this map is everywhere regular, except of the points a_1, \dots, a_n . Hence, the derivative does not vanish. By a suitable linear transformation, any one of the circular arcs bounding the polygon, can be mapped onto a part of the real axis. If $w \rightarrow W$ is this linear transformation, we see that it does not change the Schwarzian derivative, by 7.1. Furthermore, it can be shown that the Schwarzian derivative of the map we are looking for is real at all point of the real axis, except a_1, \dots, a_n . At these points the function will have singularities. We look at the vertex a_ν with the angle $\pi\alpha_\nu$ and perform a linear transformation which transforms this singularity into the origin and transforms the two arcs into straight lines with the angle $\pi\alpha_\nu$. The Schwarzian derivative was not effected by this transformation. Since the mapping is conformal, the angle of these two lines will still be $\pi\alpha_\nu$. The singularity of the function at $z = a_\nu$ is obtained from the assumption that the function maps a piece of the real axis containing $z = a_\nu$ onto two linear segments meeting at the origin with the angle $\pi\alpha_\nu$. Such a function $f(z)$ is of the form

$$f(z) = (z - a_\nu)^{\alpha_\nu} f_1(z)$$

where $f_1(z)$ is regular at $z = a_\nu$ and $f_1(a_\nu) \neq 0$. Furthermore, $f_1(z)$ is real, if z is real. We obtain

$$\mathcal{S}(f)(z) = \frac{1}{2} \frac{1 - \alpha_\nu^2}{(z - a_\nu)^2} + \frac{\beta_\nu}{z - a_\nu} + f_2(z)$$

where $f_2(z)$ is a regular function at a_ν and $\beta_\nu = \frac{1 - \alpha_\nu^2}{\alpha_\nu} \frac{f_1'(a_\nu)}{f_1(a_\nu)}$ is a real constant. These are called the *accessory parameters*. By applying the same argument to all the points a_ν , we obtain that the expression

$$\mathcal{S}(f)(z) - \sum_{\nu=1}^n \frac{1}{2} \frac{1 - \alpha_\nu^2}{(z - a_\nu)^2} - \frac{\beta_\nu}{z - a_\nu}$$

is regular at all points a_1, \dots, a_n and therefore at all points at the real axis. Hence, we have a function which is regular in the closure on the domain and real on the boundary - this implies the function to be a constant which we denote by γ .

The function $f(z)$, mapping the upper half plane \mathbb{H} onto a curvilinear polygon, satisfies the differential equation

$$\mathcal{S}(f)(z) = \sum_{\nu=1}^n \frac{1}{2} \frac{1 - \alpha_\nu^2}{(z - a_\nu)^2} + \frac{\beta_\nu}{z - a_\nu} + \gamma.$$

Here, β_1, \dots, β_n , and γ are constants which have to be calculated. There are not independent of each other. If none of the points a_1, \dots, a_n coincide with the point at infinity, the function $f(z)$ must be regular at $z = \infty$. The expansion at infinity has the form

$$f(z) = c_0 + \frac{c_1}{z} + \frac{c_2}{z^2} + \dots$$

If we compute the Schwarzian derivative of this expansion, we see that the first term is $\frac{1}{z^4}$. On the other hand, the first terms of the differential equation is

$$\begin{aligned} & \gamma + \frac{1}{z} \sum_{\nu=1}^n \beta_{\nu} \\ & + \frac{1}{z^2} \sum_{\nu=1}^n \left(a_{\nu} \beta_{\nu} + \frac{1}{2} (1 - \alpha_{\nu})^2 \right) \\ & + \frac{1}{z^3} \sum_{\nu=1}^n \left(\beta_{\nu} a_{\nu}^2 + a_{\nu} (1 - \alpha_{\nu}^2) \right) + \mathcal{O} \left(\frac{1}{z^4} \right). \end{aligned}$$

From this, we obtain four conditions for the constants

$$\begin{aligned} 0 &= \gamma, \\ 0 &= \sum_{\nu=1}^n \beta_{\nu}, \\ 0 &= \sum_{\nu=1}^n \left(2a_{\nu} \beta_{\nu} + (1 - \alpha_{\nu})^2 \right), \\ 0 &= \sum_{\nu=1}^n \left(\beta_{\nu} a_{\nu}^2 + a_{\nu} (1 - \alpha_{\nu}^2) \right). \end{aligned}$$

A curvilinear triangle

In this section, we calculate the mapping f from above for a curvilinear triangle. This is needed for mapping the fundamental domain of an extended triangle group to the upper half plane. In the end, this will result in the calculation of the hauptmodul for triangle groups. This method was also used in the article [DGMS13].

After the discussion in the end of the last paragraph, we are now able to fully calculate the case of an arbitrary curvilinear triangle. We will end with the task of solving a Schwarzian differential equation. To solve this equation, we explain a helpful relation to a second order differential equation. In our case, this is a hypergeometric differential equation – which is well understood.

Again, the source is the book of Nehari, but now we will change the calculations. To get rid of the indices, we first rename the angles of the triangle; $\alpha_1 = \alpha$, $\alpha_2 = \beta$, and $\alpha_3 = \gamma$ and the points $a_1 = a$, $a_2 = b$, and $a_3 = c$. We have seen that the following Schwarzian differential equation describes a map from a curvilinear triangle to the complex plane.

$$\mathcal{S}(f)(z) = \sum_{\nu=1}^3 \frac{1}{2} \frac{1 - \alpha_{\nu}^2}{(z - \alpha_{\nu})^2} + \frac{\beta_{\nu}}{z - \alpha_{\nu}}.$$

According to the last section, we have the following restrictions on the accessory parameters β_{ν} .

$$\begin{aligned} 0 &= \beta_1 + \beta_2 + \beta_3, \\ \alpha^2 + \beta^2 + \gamma^2 - 3 &= 2a\beta_1 + 2b\beta_2 + 2c\beta_3, \\ a(\alpha^2 - 1) + b(\beta^2 - 1) + c(\gamma^2 - 1) &= a^2\beta_1 + b^2\beta_2 + c^2\beta_3. \end{aligned}$$

Solving for the unknown β_ν , we obtain

$$\begin{aligned}\beta_1 &= -\frac{b(\alpha^2 - \beta^2 + \gamma^2 - 1) + c(\alpha^2 + \beta^2 - \gamma^2 - 1) - 2a(\alpha^2 - 1)}{2(a-b)(a-c)}, \\ \beta_2 &= \frac{a(-\alpha^2 + \beta^2 + \gamma^2 - 1) + c(\alpha^2 + \beta^2 - \gamma^2 - 1) - 2b(\beta^2 - 1)}{2(a-b)(b-c)}, \\ \beta_3 &= \frac{a(-\alpha^2 + \beta^2 + \gamma^2 - 1) + b(\alpha^2 - \beta^2 + \gamma^2 - 1) - 2c(\gamma^2 - 1)}{2(c-a)(b-c)}.\end{aligned}$$

We plug these into the Schwarzian differential equation and simplify the right-hand side to

$$\mathcal{S}(f)(z) = \frac{1}{(z-a)(z-b)(z-c)} \left(\frac{(1-\alpha^2)(a-b)(a-c)}{2(z-a)} + \frac{(1-\beta^2)(b-a)(b-c)}{2(z-b)} + \frac{(1-\gamma^2)(c-a)(c-b)}{2(z-c)} \right).$$

Now, we choose special points for the points a , b , and c . The point b is moved to infinity and the point a is set to zero. The choice for the point c is more complicated. For $\alpha = \frac{\pi}{2}$, which corresponds to the Hecke groups, we choose

$$c = \eta := \exp\left(\pi \sec \frac{\pi}{n} + 2\Psi(1) - \Psi\left(1 - \frac{1}{2}\left(\frac{1}{n} + \frac{1}{2}\right)\right) - \Psi\left(1 + \frac{1}{2}\left(\frac{1}{n} - \frac{1}{2}\right)\right)\right). \quad (7.2)$$

Here, $\Psi(z) = \frac{\Gamma'(z)}{\Gamma(z)}$ is the logarithmic derivative of the Γ -function. The Γ -function is for complex numbers with positive real part defined as $\Gamma(z) = \int_0^\infty x^{z-1} e^{-x} dx$. With this choice of c , we obtain a map which maps exactly the fundamental domain of the triangle groups we constructed in chapter 4 to the upper half plane. For the calculation of this value, we refer to the work of Raleigh [Ral62, formula I], Carathéodory [Car54, §394], the thesis by Leo [Leo08], or by Jermann [Jer13].

We obtain for the Schwarzian derivative

$$\mathcal{S}(f)(z) = \frac{1}{2z(z-\eta)} \left(\frac{\eta(\alpha^2 - 1)}{z} + (1 - \beta^2) + \frac{\eta(1 - \gamma^2)}{z - \eta} \right). \quad (7.3)$$

The next task is to solve this equation. One way to obtain the solution is by using hypergeometric functions.

7.4 Lemma. *Let $u_1(x)$ and $u_2(x)$ be two linear independent solutions of the linear differential equation*

$$u''(z) + p(z)u(z) = 0.$$

Then, the function

$$w(z) = \frac{u_1(z)}{u_2(z)}$$

is a solution of the Schwarzian differential equation

$$\mathcal{S}(w)(z) = 2p(z).$$

Proof. The proof of this lemma is a calculation – the same as in the book of Nehari.

We have $u_2 = wu_1$ and plug it into the second order differential equation

$$\begin{aligned}
0 &= u_1'' + pu_1 \\
&= (wu_2)'' + pwu_2 \\
&= w''u_2 + w'u_2' + wu_2'' + pwu_2 \\
&= w''u_2 + w'u_2' + w \underbrace{(u_2'' + pu_2)}_{=0} \\
&= w''u_2 + w'u_2' \\
\Rightarrow \frac{w''}{w'} &= -2 \frac{u_2'}{u_2}.
\end{aligned}$$

Thus,

$$\begin{aligned}
\mathcal{S}(w)(z) &= \left(\frac{w''}{w'}\right)' - \frac{1}{2} \left(\frac{w''}{w'}\right)^2 \\
&= -2 \left(\frac{u_2'}{u_2}\right)' - 2 (u_2' u_2)^2 \\
&= -2 \frac{u_2''}{u_2} = -2 \frac{-pu_2}{u_2} = 2p.
\end{aligned}$$

□

This lemma allows us to translate the Schwarzian differential equation into a second order differential equation with three singularities. Such a differential equation is a hypergeometric differential equation and it has hypergeometric functions as solutions.

We are more interested in finding the solution in the form of a q -series. In the next section we construct such a solution.

The calculation of the hauptmodul for triangle groups

In this section we calculate the hauptmodul of the triangle groups, using the theory developed before. When we introduced the triangle groups and their operation on the upper half plane, we also defined the extended triangle groups. Using these, we split the fundamental domain of the triangle groups into two parts, each part is a possible fundamental domain for the extended groups. We will assume that the hauptmodul maps one of these fundamental domains to the upper half plane. This put us in the position of finding a function which maps a curvilinear polygon to the upper half plane \mathbb{H} . We have discussed this problem in the last subsection in detail and is now used to obtain the q -series of the hauptmodul of the triangle groups.

Previously we ended with a differential equation – the Schwarzian differential equation. We now solve this equation in term of a q -series.

Finding the hauptmodul $j_{a,b}(\tau)$

We start with the triangle group $\Delta(a, b)$. The fundamental domain is a triangle with angles $\frac{\pi}{a}$, $\frac{\pi}{b}$, and $\frac{\pi}{\infty} = 0$ – we choose this triangle to have the edges i , $\rho_{a,b}$, and $\cot \frac{\pi}{a}$, as we did in chapter 4. The inverse hauptmodul $\tau(j)$ should map this triangle to the upper half plane. According to the last section, the inverse hauptmodul satisfies a Schwarzian

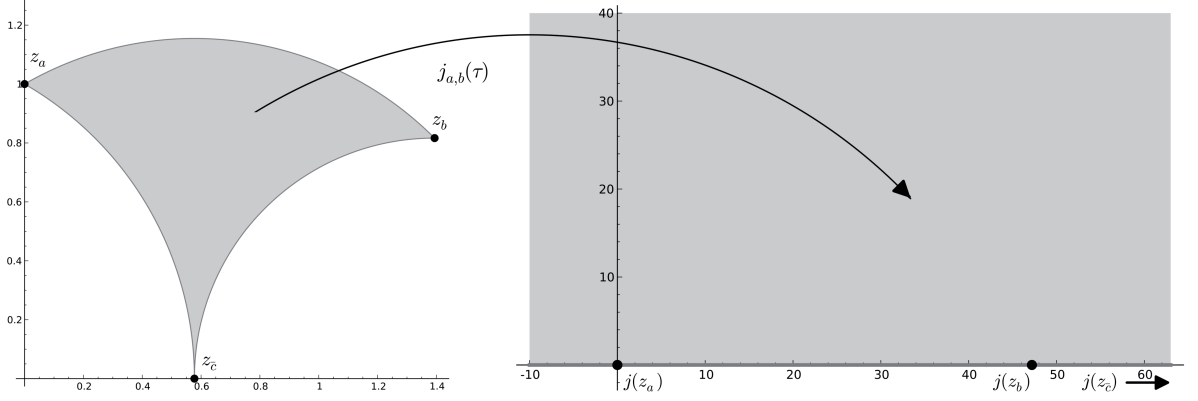


Figure 7.1.: Mapping property of the hauptmodul

differential equation

$$\mathcal{S}(\tau)(j) = 2Q(j),$$

with $Q(z) = \frac{1}{4z(z-\eta)} \left(\frac{\eta(\alpha^2-1)}{z} + (1-\beta^2) + \frac{\eta(1-\gamma^2)}{z-\eta} \right)$ as in the last section, formula (7.3). From lemma 7.1, point we obtain an equation for the hauptmodul itself

$$\mathcal{S}(j)(\tau) + 2Q(j)(j')^2 = 0. \quad (7.5)$$

Now, we make a general ansatz for the hauptmodul. We know that it behaves like $\frac{1}{q}$ as $\tau \rightarrow \infty$. The parameter $q = \exp(2\pi i\tau/w)$ was introduced in chapter 3, formula (3.4). Hence, we write j as a Fourier expansion with unknown coefficients

$$j(\tau) = \frac{1}{q} + \sum_{i=0}^{\infty} c_i q^i = \frac{1}{q} + c_0 + c_1 q + c_2 q^2 + c_3 q^3 + O(q^4)$$

and apply (7.5)

$$\begin{aligned} 0 &= \mathcal{S}(j)(\tau) + 2Q(j)(j')^2 \\ &= \left(\frac{\eta}{2} \left(1 - \frac{1}{a^2} - \frac{1}{b^2} \right) - c_0 \right) q \\ &+ \left(\frac{1}{2} \left(3c_0^2 + 3c_0\eta \left(\frac{1}{a^2} - \frac{1}{b^2} - 1 \right) + \eta^2 \left(-\frac{2}{a^2} + \frac{1}{b^2} + 2 \right) \right) - 8c_1 \right) q^2 \\ &+ O(q^3). \end{aligned}$$

These equations must vanish for each power of q . We obtain a system of equations. Although they are not linear equations, the highest Fourier coefficient appearing in the n th equation is c_{n-1} . This coefficient appears only linear. Hence, we solve this system by solving the n th equation for c_{n-1} and use a backward substitution. The first coefficients are following.

$$\begin{aligned}
c_0 &= \frac{\eta(a^2b^2 + a^2 - b^2)}{2a^2b^2}, \\
c_1 &= \frac{\eta^2(5a^4b^4 - 2a^4b^2 - 3a^4 - 2a^2b^4 + 6a^2b^2 - 3b^4)}{64a^4b^4}, \\
c_2 &= -\frac{\eta^3(2a^6b^4 - a^6b^2 - a^6 - 2a^4b^6 + 3a^4b^2 + a^2b^6 - 3a^2b^4 + b^6)}{54a^6b^6}, \\
c_3 &= -\frac{\eta^4}{32768a^8b^8} \left(31a^8b^8 - 76a^8b^6 - 662a^8b^4 + 404a^8b^2 + 303a^8 - 76a^6b^8 \right. \\
&\quad \left. + 1436a^6b^6 - 404a^6b^4 - 1212a^6b^2 - 662a^4b^8 \right. \\
&\quad \left. - 404a^4b^6 + 1818a^4b^4 + 404a^2b^8 - 1212a^2b^6 + 303b^8 \right).
\end{aligned}$$

This gives us the q -expansion for the triangle groups. As similar result can be found in [DGMS13].

The Picard-Fuchs equation

Once we calculated the hauptmodul for a finite index subgroup $\Gamma \subseteq \Delta$, we can also calculate the *Picard-Fuchs equation*. In the next chapter, we explain how one finds such a hauptmodul for a subgroups of a triangle group. We know that the hauptmodul should satisfy an equation of the following type

$$\begin{aligned}
&\mathcal{S}(j)(z) + 2Q(j) \cdot (j'(z))^2 = 0 \\
\Rightarrow Q(j) &= \frac{\mathcal{S}(j)(z)}{(j'(z))^2}
\end{aligned} \tag{7.6}$$

where, $Q(z)$ is a rational function. We call (7.6) the *Picard-Fuchs equation* for the subgroups Γ . If we assume, we calculated the q -series of the hauptmodul j , we use this equation to find the rational function $Q(z)$. We calculated the right-hand side by plugging in the given q -series and obtain $Q(j(\tau))$. Then, we plug in this result the inverse series of $1/j$. This result in a series for $Q(1/t)$. We construct the exact function $Q(1/t)$ by using a Padé approximant.

(Not) finding the hauptmodul using conformal mappings

We constructed the hauptmodul of triangle groups by using the theory of conformal mappings. The fundamental domain was mapped to the complex plane. One idea is to calculate the Picard-Fuchs equation in the same way for subgroup of triangle groups.

This idea does not work and we will give an example where it fails. In the theory we presented, we do not map the complete triangle to the complete complex plane, but “half” of the fundamental domain to the upper half plane. So we have to find a way to cut the fundamental domain into two halves. In some examples, this subdivision looks natural – for example for $\Gamma_0(2)$, see figure 7.2. In general, this division line need not

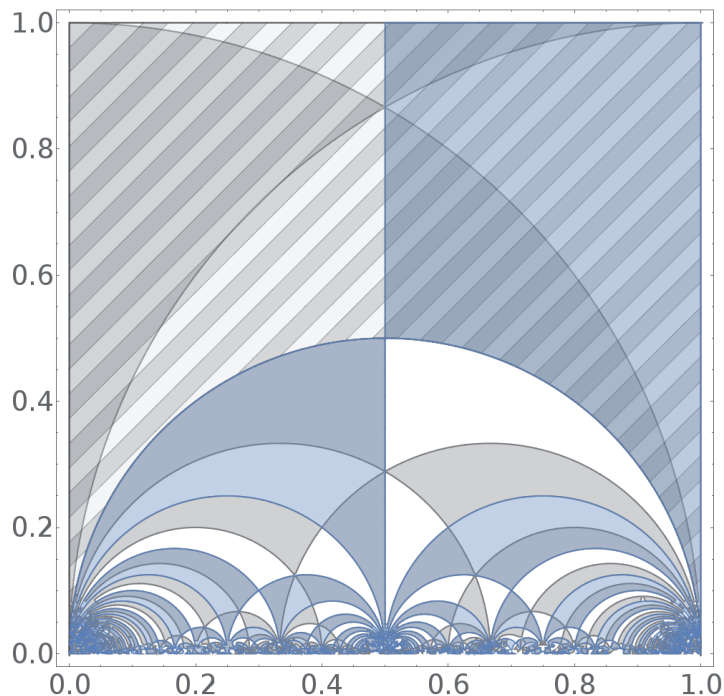


Figure 7.2.: The striped area is the fundamental domain and the blue area is where the imaginary part of the hauptmodul take positive values.

to be a geodesic. Let us take a look at an example, where this happens. We define the group with the monodromy representation.

$$S_2 = (1, 4)(2, 6)(5, 7),$$

$$S_3 = (1, 6, 4)(2, 5, 3).$$

These two permutations define a subgroup of the modular group. Its fundamental domain is figure 7.3 and the corresponding dessin d’enfants is figure 7.4 Using the methods from chapter 5 or the next chapter, is it possible to extract the rational covering

$$R_\Gamma(z) = \frac{1}{256923577521058878088611477224235621321607z \cdot \left(3456(249\sqrt{-3} + 1763)z + 823543 \right) \cdot \left(678223072849 - 51230962944(5\sqrt{-3} - 3272)z - 644972544(72061\sqrt{-3} - 2850105)z^2 \right)^3}.$$

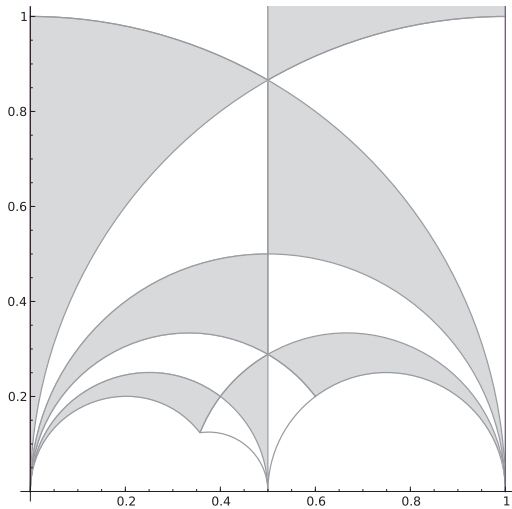


Figure 7.3.: The fundamental domain

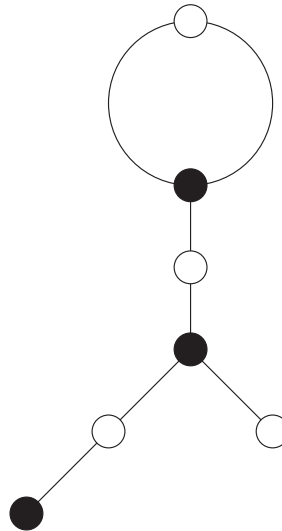


Figure 7.4.: The corresponding dessin

Plugging this into the equation $J = R_\Gamma(j_\Gamma)$, we obtain the q -series of the hauptmodul for this group. Then, we plot the area, where the imaginary part of this function is greater than zero – figure 7.5. From this picture one sees that the partition of the fundamental domain into a part which maps into the upper half plane and a part which maps into the lower half plane need not to coincide with the Dedekind tessellation. It is not even bounded by geodesics. To be sure that we do not see an artifact in plotting, we also calculated an approximation for the point on the line with imaginary part 0.185, where the hauptmodul has vanishing imaginary part. For this, we used a bisection method. We found that at the point $z_0 = 0.466989452 + 0.185i$ the value of the hauptmodul is $8.019477450 + 7.9 \cdot 10^{-10}$. Furthermore, the exact point where the imaginary part vanishes is within a range of 10^{-10} of z_0 . Especially, we see that this vanishing point does not have real part 0.5.

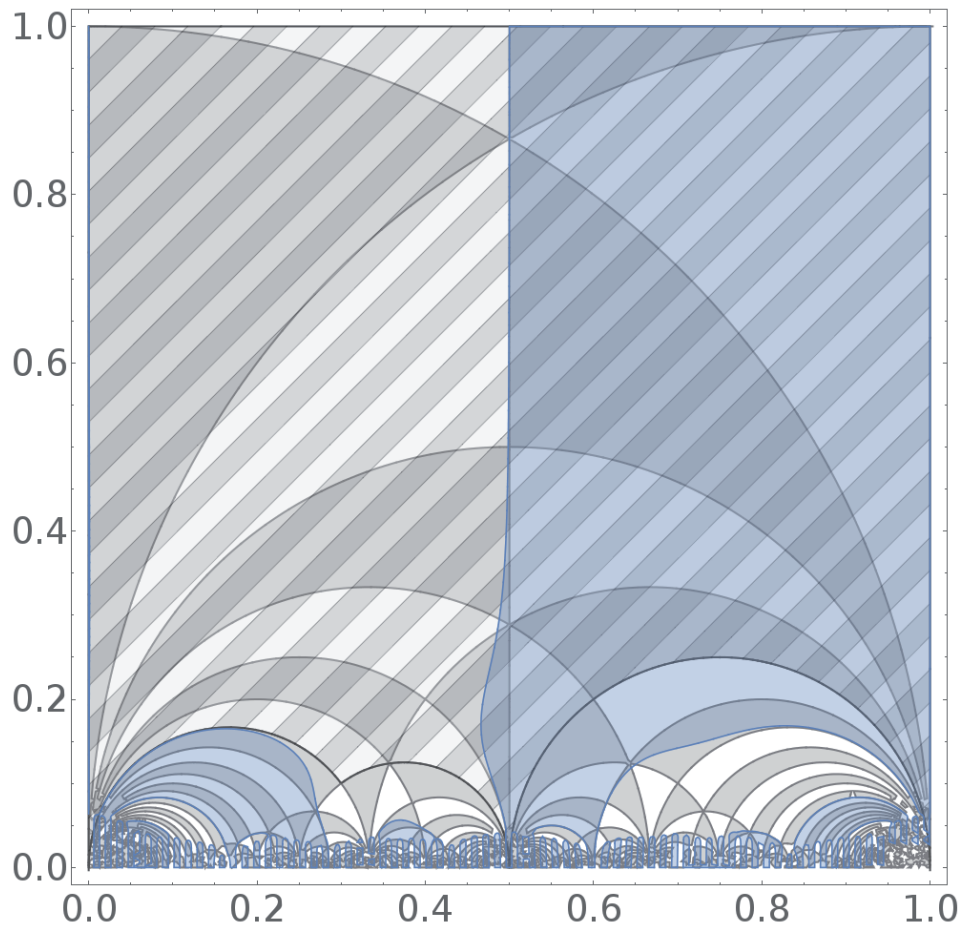


Figure 7.5.: The striped area is the fundamental domain and the blue area is where the imaginary part of the hauptmodul take positive values. In addition, we plotted the Dedekind tessellation.

Chapter 8.

Numerics

Any fool can write code that a computer can understand.
Good programmers write code that humans can understand.

(Martin Fowler)

In this chapter we present the numerical methods we used to calculate Hauptmoduls for finite index subgroups of triangle groups. The first method uses series expansion of modular forms. It goes back to Hejhal [Hej99]. He used it to calculate Maass wave forms. The second method is new and based on the idea of Monien that every holomorphic function must obey a partial differential equation.

Series expansions

In this approach, we restrict ourselves to the calculation of the Fourier expansion of modular forms and functions for finite index subgroups of the modular group. Nevertheless, it is also possible to use this method for general triangle groups as Hejhal did it [Hej99], [Hej04], and Wang [Wan94]. Selander and Strömbergson [SS02], Strömberg [Str02], Klug et. al [KMSV14], and Sijssling and Voight [SV14] also applied this method successfully.

The Fourier coefficients of the modular forms we compute are determined by an integral along a line. This integral is discretized and shifted into the complex plane. Now, we pull back each individual point into the fundamental domain, giving pull back maps in the subgroup. From the transformation property, we derive a system of linear equations which an approximation of the coefficients must obey. Solving this system, gives us the approximation we are looking for.

The main issue is the question: How much one should lift the line we are integrating along into the complex plane? On the one hand, we need to pull it down to catch enough different pull backs and on the other hand, one needs to pull it up to increase the absolute value of q and therefore, improve the numerical stability.

To improve the precision of these calculations, one takes the other cusps into account. This also improves the numerical stability. Selander and Strömbergson [SS02] as well as Strömberg [Str02] did this. Here, the question of how much one should lift the line of integration into the complex plane becomes a major problem. For each cusp, we obtain a different expansion parameter with different areas of convergence.

If we want to find modular functions, essentially the same procedure works. In addition, we need to control their behavior at infinity.

Modular forms

For the numerical calculation of cusp forms we follow the approach of Hejhal [Hej92] in the version of Strömbergson and Selander [SS02]. First, we introduce some notations. Let $\Gamma \subseteq \mathrm{SL}_2(\mathbb{Z})$ a subgroup of finite index. We denote the representatives of the cusp classes of this group by P_1, \dots, P_t . Furthermore, we fix a connected fundamental domain \mathfrak{F} for Γ . For each cusp $P \in \mathbb{H}^*$, there is a map $E_P \in \Gamma$, mapping P to a representative P_j . We call this the *reduction to an elementary cusp*. Furthermore, we divide the fundamental domain into sections, such that the points in each section are as close as possible to a cusp in the fundamental domain. A point $z \in \mathfrak{F} \subseteq \mathbb{H}$ is in the section corresponding to the cusp $P \in \mathfrak{F}$, if and only if P minimizes $\mathrm{dist}(P, z)$ among all possible fractions P . Then, we define for each point in the upper half plane the maps U_z and $J(z)$ in the following ways.

If z is the section corresponding to the cusp P , we define $U_z := E_P$. Furthermore, if E_P maps P to the elementary cusp P_i and we set $J(z) = i$.

Now, we describe the algorithm to calculate modular forms. Let $F(z) \in S_k(\Gamma)$ be a cusp form for Γ . We prefer to work with an automorphy factor of modulus one to make the calculations more stable. Hence, we define $f(z) := y^{\frac{k}{2}} F(z)$, with $y = \mathrm{Im}(z)$. Now, we have the transformation property

$$[f|_k \begin{pmatrix} a & b \\ c & d \end{pmatrix}](z) := \frac{|cz + d|^k}{(cz + d)^k} f\left(\frac{az + b}{cz + d}\right) = f(z)$$

for all $\begin{pmatrix} a & b \\ c & d \end{pmatrix} \in \Gamma$. For each cusp P_j , we define the *normalizer* of the cusp as a map $N_j \in \mathrm{PSL}_2(\mathbb{R})$, such that it maps the cusp to infinity $N_j.c_j = \infty$ and the stabilizer of the cusp is $N_j^{-1} \cdot \begin{pmatrix} 1 & 1 \\ 0 & 1 \end{pmatrix} \cdot N_j$. We use this normalizer to pull back a cusp P_j to infinity and calculate a Fourier expansion at infinity. This results in an expansion at the cusp P_j

$$[f|_k N_j^{-1}](z) = y^{\frac{k}{2}} \sum_{n \geq 1} a_n^{(j)} e^{2\pi i n z}.$$

Now, we calculate the Fourier coefficients $a_n^{(j)}$ using a Fourier integral. This integral will be discretized using the points $z_m := x_m + iy := \frac{1}{2Q}(m - \frac{1}{2}) + iy$, with a fixed $y \in \mathbb{R}$ and a $2Q$ the number of discretization points.

$$\begin{aligned} y^{\frac{k}{2}} a_n^{(j)} &= \int_0^1 [f|_k N_j^{-1}](z) e^{-2\pi i n z} \, dz \\ &\approx \frac{1}{2Q} \sum_{m=1}^{2Q} [f|_k N_j^{-1}](z_m) e^{-2\pi i n x_m} e^{2\pi n y}. \end{aligned}$$

The matrix $T_{mj} \in \Gamma$ denotes the pullback of the point $N_j^{-1} z_m$ to the fundamental domain, $T_{mj} N_j^{-1} z_m = \widehat{z_{mj}} \in \mathfrak{F}$. Now, we deduce the system of linear equations which will allow

us to compute the cusp forms.

$$\begin{aligned}
[f|_k N_j^{-1}](z_m) &= \left[[f|_k U_{\widehat{z_{m_j}}} T_{m_j}] |_k N_j^{-1} \right](z_m) \\
&= \left[[f|_k N_{J(\widehat{z_{m_j}})}^{-1}] |_k \underbrace{N_{J(\widehat{z_{m_j}})} U_{\widehat{z_{m_j}}} T_{m_j} N_j^{-1}}_{:= \begin{pmatrix} * & * \\ c_{mj} & d_{mj} \end{pmatrix}} \right](z_m) \\
&= \frac{|c_{mj} z_m + d_{mj}|^k}{(c_{mj} z_m + d_{mj})^k} \left[f|_k N_{J(\widehat{z_{m_j}})}^{-1} \right](z_{mj}^*) \\
&\approx \frac{|c_{mj} z_m + d_{mj}|^k}{(c_{mj} z_m + d_{mj})^k} \left((y_{mj}^*)^{\frac{k}{2}} \sum_{l=1}^{M_0} a_l^{(J(\widehat{z_{m_j}}))} e^{2\pi i l z_{mj}^*} \right).
\end{aligned}$$

Hence, we obtain the following system of equations

$$a_n^{(j)} y^{\frac{k}{2}} e^{-2\pi n y} = \sum_{j'=1}^t \sum_{l=1}^{M_0} a_l^{(j')} V_{nl}^{(jj')}.$$

The entries of the matrix V are as follows.

$$V_{nl}^{(jj')} := \frac{1}{2Q} \sum_{m=1}^{2Q} \frac{|c_{mj} z_m + d_{mj}|^k}{(c_{mj} z_m + d_{mj})^k} (y_{mj}^*)^{\frac{k}{2}} e^{2\pi i l z_{mj}^*} e^{-2\pi i n x_m}.$$

Now, we solve these equations for example with a LU-decomposition [PTVF02, chapter 2.3]. There are also some techniques to further improve the accuracy for the higher Fourier coefficients, see [Wan94].

With the help of this method, we were able to calculate cusp forms of weight 4 for Hsu's example of index 10. In chapter 9 we present the result of this calculation.

Modular functions

For calculating the hauptmodul, we use essentially the same approach as for cusp forms. Here, we make the additional assumption that the group $\Gamma \subseteq \mathrm{PSL}_2(\mathbb{Z})$ has genus zero.

We start with the Fourier series for the hauptmodul.

$$\begin{aligned}
j_\Gamma(\tau) &= \frac{1}{q} + \sum_{n \geq 1} a_n q^n \\
&= e^{2\pi y} e^{-2\pi i x} + \sum a_n e^{-2\pi n y} e^{2\pi i x n}.
\end{aligned}$$

Similar to the calculations for the modular forms, we write down the Fourier integral and discretize it with the help of the points $z_j = x_j + iy$, where y is fixed and $x_j = \frac{j}{2Q}$,

for $j = 0, \dots, 2Q$. We define $z_j^* := P(N_\infty^{-1}z_j)$.

$$\begin{aligned}
 a_n e^{-2\pi n y} &= \int_0^1 j_\Gamma(z) e^{-2\pi i n x} dz \\
 &\approx \frac{1}{2Q} \sum_{j=1}^{2Q} j(z_j) e^{-2\pi i n x_j} \\
 &= \frac{1}{2Q} \sum_{j=1}^{2Q} j(z_j^*) e^{-2\pi i n x_j} \\
 &= \frac{1}{2Q} \sum_{j=1}^{2Q} \left(e^{-2\pi i l z_j^*} + \sum_{l \geq 1} a_l e^{2\pi i l z_j^*} \right) e^{-2\pi i n x_j} \\
 \Rightarrow \underbrace{\frac{-1}{2Q} \sum_{j=1}^{2Q} e^{-2\pi i z_j^*} e^{-2\pi i n x_j}}_{=: b_n} &= \sum_{l \geq 1} a_l \underbrace{\left(\frac{1}{2Q} \sum_{j=1}^{2Q} e^{2\pi i l z_j^*} e^{-2\pi i n x_j} + \delta_{n,l} e^{-2\pi l y} \right)}_{=: V_{n,l}}.
 \end{aligned}$$

This is again a system of linear equations, but this time with a different left-hand side. The solution is an approximation for the coefficients of the hauptmodul.

The FEM-method for the calculation of a hauptmodul

In this section we describe a new method to efficiently calculate the hauptmodul of a subgroup of a triangle group.

Let $\Gamma \subseteq \Delta_n$ be a genus zero subgroup of finite index. We denote with J the hauptmodul of the triangle group and the hauptmodul of a subgroup with j_Γ . Take the rational function as in chapter 3, denoted by R_Γ . As we have seen, it has the property $J = R_\Gamma(j_\Gamma)$. The main goal is to find the rational function R_Γ . We start with the following observation. The values of the J function at the elliptic points are $J(i) = \eta$ and $J(\rho) = 0$. If we plug this into the definition of the rational function, we obtain

$$\begin{aligned}
 0 &= J(\rho) = R_\Gamma(j_\Gamma(\rho)), \\
 0 &= \eta - J(i) = \eta - R_\Gamma(j_\Gamma(i)), \\
 0 &= \frac{1}{J(0)} = \frac{1}{R_\Gamma(j_\Gamma(0))}.
 \end{aligned}$$

From these calculations we see that the values of the hauptmodul j_Γ at the elliptic points of order n , respectively of order 2 are the zeros of the function R_Γ respectively $\eta - R_\Gamma$. Furthermore, the values at the cusps are the singularities of the function R_Γ .

Hence, we would like to calculate the value of the hauptmodul at certain points in the fundamental domain. The hauptmodul is a holomorphic function on a Riemann surface.

A holomorphic function has a harmonic real and imaginary part [HC64, Drittes Kapitel, §7]. There are numerical methods to calculate harmonic functions. Hence, we find an approximation for the real and the imaginary part by solving two partial differential equations.

Let $\mathfrak{F}_\Gamma = \mathfrak{F}$ be the fundamental domain of the subgroup Γ . If a cusp in this domain is equivalent to the cusp infinity, we cut it at a certain height h with a geodesic: For the cusp infinity itself, we remove the part of the fundamental domain where the imaginary part is larger than h . For the other cusps, we map the cusp to infinity – using the pairings – and remove the area, where imaginary part of the image of this map is larger than h . We triangulate the resulting subset. Then, we run a finite element solver on this domain with the boundary conditions

- (i) the pairings as periodic boundary conditions,
- (ii) since $j_\Gamma = \frac{1}{q} + \mathcal{O}(q)$, we define on the cutting line the function $\frac{1}{q}$ as Dirichlet boundary condition.

With these boundary conditions we solve the Laplace equation. After the solution, we evaluate the result at the elliptic points respectively the cusps and obtain an approximation for the zeros respectively the singularities of the function R_Γ .

The complete algorithm

Let $\Gamma \subseteq \Delta = \Delta(2, n)$, with $n \geq 3$ be a finite index subgroup and $\mathcal{F} = \mathcal{F}_\Gamma$ the corresponding Farey symbol. The hyperbolic triangle with the vertices $0, i$, and $\rho = \rho_{2,n} = e^{\frac{i\pi}{n}}$ is denoted by \mathcal{T}_0 and the hyperbolic triangle with vertices $i\infty, i$ and ρ is denoted by \mathcal{T}_∞ . In chapter 4 we introduced the map $\tau_c: \mathbb{H} \rightarrow \mathbb{H}, z \mapsto (\bar{z})^{-1}$, see lemma 4.3 which maps \mathcal{T}_0 to \mathcal{T}_∞ and vice versa. It has the property that it fixes the points on the circle with norm equal to one which is a border of both triangles.

Note that the union of \mathcal{T}_0 and \mathcal{T}_∞ , denoted by $\mathcal{T} = \mathcal{T}_0 \cup \mathcal{T}_\infty$, is the closure of a fundamental domain of Δ .

If we remove the points with imaginary part greater than h , for some $h > 1$, from the triangle \mathcal{T}_∞ , we obtain a hyperbolic quadrilateral \mathcal{T}_h with the vertices $i, \rho, \cos\left(\frac{\pi}{n}\right) + ih$, and ih , see figure 8.2.

We fix a height h and calculate a triangulation of the polygons \mathcal{T}_0 and \mathcal{T}_h . Since the map τ_c fixes the arc from i to ρ , we choose the triangulation in such a way that the border points on this arc of both triangles are the same. This choice allows us to glue the two triangulations together. In chapter 6 we calculated a set of coset representatives $\{c_1, \dots, c_r\}$, such that the set

$$\mathfrak{F} = \{c_1^{-1} \mathcal{T}, \dots, c_r^{-1} \mathcal{T}\} = \{c_1^{-1} \mathcal{T}_0, \dots, c_r^{-1} \mathcal{T}_0, c_1^{-1} \mathcal{T}_\infty, \dots, c_r^{-1} \mathcal{T}_\infty\}$$

is a connected fundamental domain of the operation of the group Γ on the extended upper half plane \mathbb{H}^* . Using this, we construct an approximation of the fundamental domain in the following way.

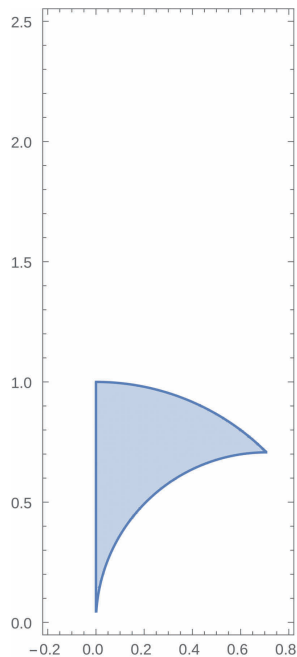


Figure 8.1.: The triangle \mathcal{T}_0

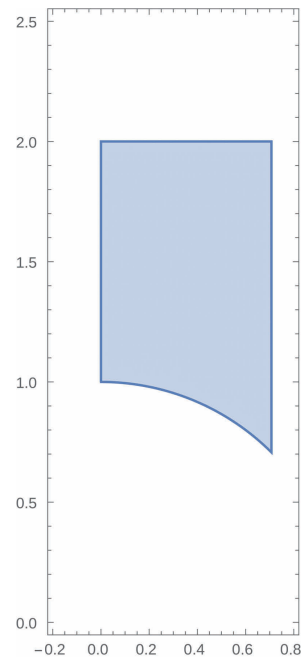


Figure 8.2.: The triangle \mathcal{T}_2

Algorithm 4.

- (i) Start with the empty set $F = \{\}$.
- (ii) For each coset $c_i^{-1} = \begin{pmatrix} a & b \\ c & d \end{pmatrix}$ do the following.
 - a) Check, if c_i^{-1} maps the cusp ∞ to a cusp which is equivalent to ∞ .
 - i. If it does, add $c_i^{-1}\mathcal{T}_h$ to F .
 - ii. If it does not, add $(c_i^{-1} \circ \tau_c)\mathcal{T}_0$ to F .
 - b) Check, if c_i^{-1} maps the cusp 0 to a cusp which is equivalent to ∞ .
 - i. If it does, add $(c_i^{-1} \circ \tau_c)\mathcal{T}_h$ to F .
 - ii. If it does not, add $c_i^{-1}\mathcal{T}_0$ to F .

8.1 Lemma. *The resulting domain F from algorithm 4 has the following properties.*

- (i) *It is a connected subset of \mathbb{H} .*
- (ii) *Any triangulation of the triangles \mathcal{T}_0 and \mathcal{T}_h which coincides on the hyperbolic arc from i to ρ , induces a triangulation of F .*
- (iii) *Any triangulation obtained from (ii) is compatible with the pairings. If a pairing maps one side of F to another side, it also maps the border points of the triangulation to each other.*

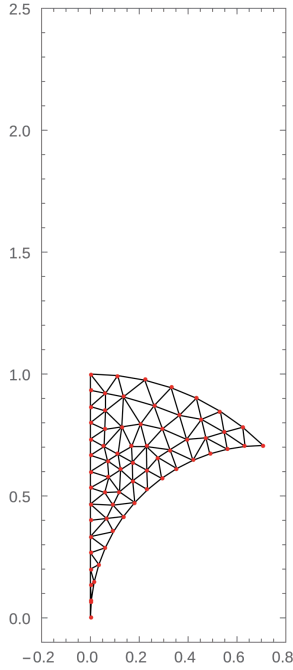


Figure 8.3.: A triangulation of \mathcal{T}_0

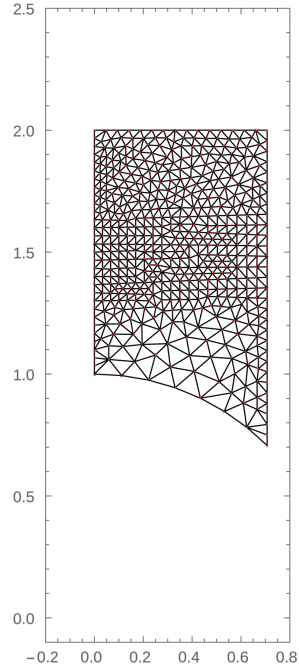


Figure 8.4.: A triangulation of \mathcal{T}_2

Example. As an example, we will look at the subgroup of $\Delta(2, 4)$ which has the monodromy representation $S_2 = (1, 2)(3, 4)(5, 6)$ and $S_4 = (1, 2, 3, 5)$. It has the Farey symbol

$$-\infty \underset{1}{\frown} \frac{0}{1} \underset{1}{\frown} \frac{1}{\sqrt{2}} \underset{(1,4)}{\frown} \frac{\sqrt{2}}{1} \underset{(1,4)}{\frown} \infty.$$

and the generators are the matrices

$$\left\{ \begin{pmatrix} 1 & 0 \\ \sqrt{2} & 1 \end{pmatrix}, \begin{pmatrix} 3\sqrt{2} & -5 \\ 5 & -4\sqrt{2} \end{pmatrix}, \begin{pmatrix} \sqrt{2} & -5 \\ 1 & -2\sqrt{2} \end{pmatrix} \right\}.$$

The index of this subgroup in $\Delta(2, 4)$ is six and the coset representatives we will be using are

$$\left\{ \begin{pmatrix} 1 & 0 \\ 0 & 1 \end{pmatrix}, \begin{pmatrix} 1 & \sqrt{2} \\ 0 & 1 \end{pmatrix}, \begin{pmatrix} 0 & -1 \\ 1 & -\sqrt{2} \end{pmatrix}, \begin{pmatrix} 1 & -\sqrt{2} \\ \sqrt{2} & -1 \end{pmatrix}, \begin{pmatrix} \sqrt{2} & 1 \\ 1 & \sqrt{2} \end{pmatrix}, \begin{pmatrix} \sqrt{2} & -1 \\ 1 & 0 \end{pmatrix} \right\}.$$

From this, we find a fundamental domain. Using algorithm 4 above, we obtain a triangulation of an approximation of the fundamental domain. We use the triangulations of \mathcal{T}_0 and \mathcal{T}_2 in figure 8.3 and 8.4. From the generalized Farey symbol we read of the cusps which are ∞ and 0. The other fractions $\frac{1}{\sqrt{2}}$ and $\frac{\sqrt{2}}{1}$ are identified with ∞ . We see the different behavior in the triangulation at the fractions. While the point 0 is a part of the domain, the fractions $\frac{1}{\sqrt{2}}$ and $\frac{\sqrt{2}}{1}$ are spared out. In figure 8.7 you see this detail. \square

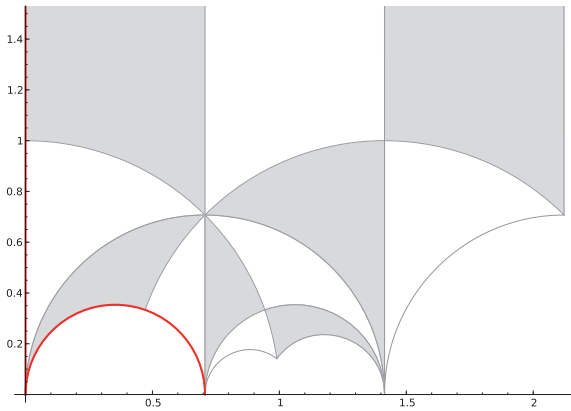


Figure 8.5.: A fundamental domain

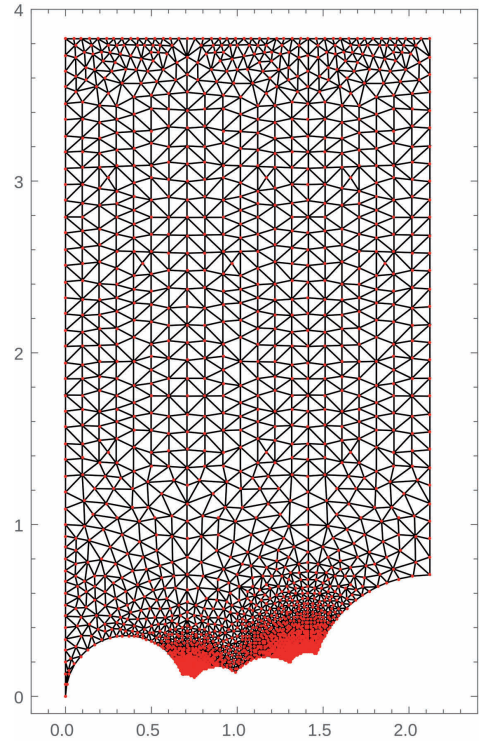


Figure 8.6.: The corresponding triangulation

According to chapter 3 the hauptmodul j_Γ of the subgroup has the following properties. It is a holomorphic function on the Riemann surface $X(\Gamma)$ and has the asymptotic behavior $j_\Gamma(\tau) = \frac{1}{q} + \mathcal{O}(q)$ for $\tau \rightarrow i\infty$. As usual, we define $q := e^{2\pi i\tau/w}$ where w is the cusp width of infinity in Δ . Being a holomorphic function on the Riemann surface contains actually two conditions. On the one hand it is a *holomorphic* function and on the other hand it is a function *on the Riemann surface*. From standard arguments – using the Cauchy-Riemann-Equations, see for example [Ah153, chapter 1.2] – we know that the real and the imaginary part are harmonic functions. Hence, we want to solve the Laplace equation numerically.

The second part is that the function lives on a Riemann surface. This surface is well known to us. A model for this surface is the fundamental domain, together with the side identifications. We already constructed a triangulation of the fundamental domain which respects the pairings – see lemma 8.1. This means that we need to solve the Laplace equation on the fundamental domain with periodic boundary conditions where the periodicity is given via the pairing matrices.

Up to now, a constant function solves this equation. We have the second condition that $j_\Gamma(\tau) = \frac{1}{q} + \mathcal{O}(q)$ and a boundary where we have not apply any condition yet. This boundary is the upper edge of the triangle \mathcal{T}_h and its images from algorithm 4. As we have seen, this upper edge is going to $i\infty$ as h goes to ∞ . Hence, the hauptmodul should behave like $\frac{1}{q}$ on this upper edge and its images from algorithm 4. A short calculation

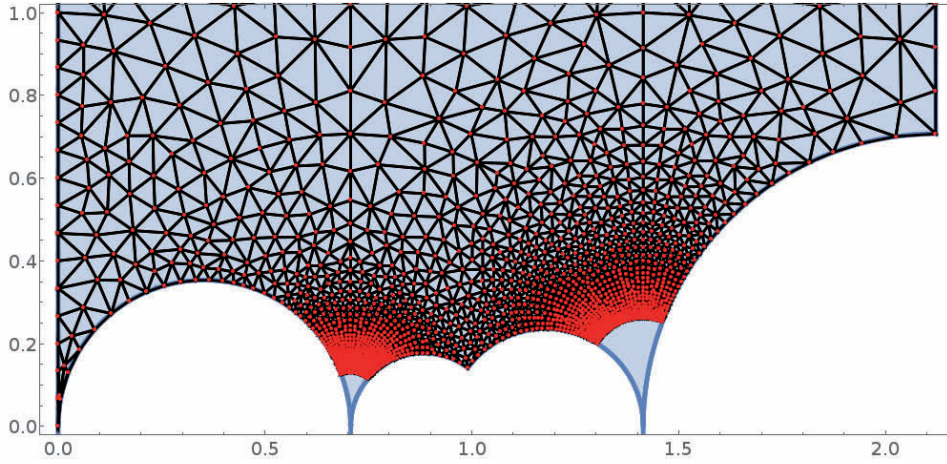


Figure 8.7.: Detail of the fundamental domain and the triangulation

gives us

$$\begin{aligned} \frac{1}{q} &= e^{-2\pi iz/w} \\ &= e^{-2\pi i(x+iy)/w} \\ &= \cos(2\pi x/w) \cdot e^{2\pi y/w} - i \sin(2\pi x/w) \cdot e^{2\pi y/w}. \end{aligned}$$

Here, w denotes the cusp width of infinity of Γ . This gives us our second boundary condition for the line from ih to $ih + \cos\left(\frac{\pi}{n}\right)$ and its images. On the line connecting $i \cdot h$ and $i \cdot h + \cos\left(\frac{\pi}{n}\right)$ we apply the conditions

$$\begin{aligned} g_r(x) &= \cos(2\pi x/w) \cdot e^{2\pi h/w} && \text{for the real part,} \\ g_i(x) &= -\sin(2\pi x/w) \cdot e^{2\pi h/w} && \text{for the imaginary part.} \end{aligned}$$

For the images of this line, we map these functions using the inverse cosets.

With these two boundary conditions, we let a finite element solver solve this problem numerically. Then, we evaluate the result at the elliptic points and the cusps and get approximations for the zeros and the singularities of the rational covering. From these approximations we will need to reconstruct the exact values. We improve the accuracy by Newton's method. Before we explain how this works we will give some technical remarks on our implementation.

Example. We continue with our example we started above. The subgroup Γ of $\Delta(2, 4)$ which is given by the monodromy representation

$$\begin{aligned} S_2 &= (1, 2)(3, 4)(5, 6), \\ S_4 &= (1, 2, 3, 5). \end{aligned}$$

Applying the boundary conditions on the mesh we constructed above and solving numerically the Laplace equation results in the following figures: 8.8 for the real part and

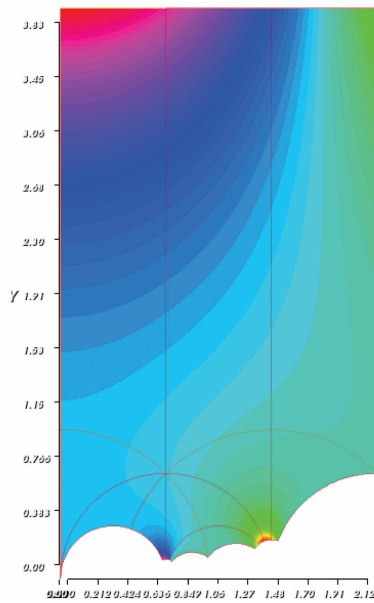


Figure 8.8.: The real part of the solution

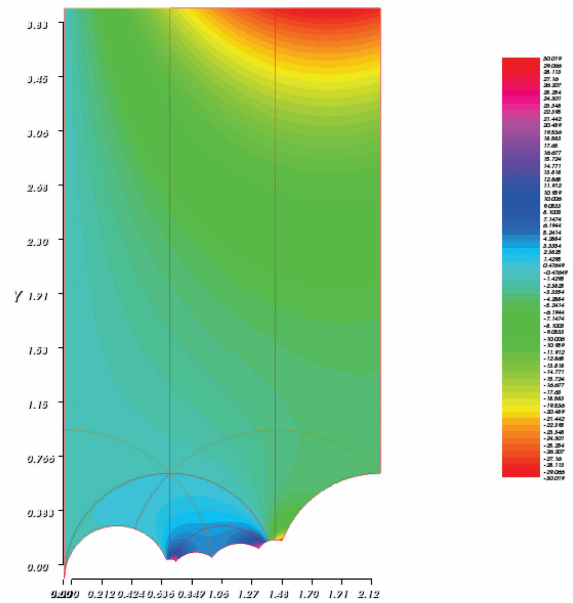


Figure 8.9.: The imaginary part of the solution

8.9 for the imaginary part. One sees the Dirichlet boundary conditions at all cusps which are equivalent to infinity.

The values at the points elliptic and parabolic points are in table 8.1. In this table we used the abbreviation $E_{(2)}$ for an elliptic point of order 2, $E_{(4)}$ for an elliptic point of order 4 in the interior and $E_{(4)}^b$ for an elliptic point of order 4 on the boundary. A cusp is denoted by C .

Remarks on the implementation

We implemented these algorithms mainly in Sage. Of course, we used the already mentioned generalized Farey symbols. The choice of the finite element solver was a difficult task, since most of the solvers we looked at were not able to handle this kind of periodic boundary conditions. We decided to use FreeFem++ [Hec12]. Then, we wrote a Sage script which takes the subgroup in the monodromy representation as input. It generates, using the algorithms above, a FreeFem++ script and executes it. This FreeFem++ script generates the mesh by glueing the coset tessellation together and solves on this mesh the Laplace equation with the boundary conditions as described above. We evaluate the solution at the elliptic points and the cusps. FreeFem++ writes the results to a file which is then read by Sage.

Newton's method to improve accuracy

In the last section we ended with an approximation for the values of the hauptmodul at the elliptic points and the cusps. We have seen that the values at the elliptic points

| Point z | Kind of point | values from FEM | value from exact result | error |
|-----------------------------------------------|---------------|---------------------|-------------------------|-------|
| i | $E_{(2)}$ | $2.3097 - 0.0012i$ | $2.3013 + 0.0000i$ | 0.37% |
| $\sqrt{2} + i$ | $E_{(2)}$ | $-0.6520 - 3.0844i$ | $-0.6506 - 3.0937i$ | 0.28% |
| $\frac{2}{3}\sqrt{2} + \frac{i}{3}$ | $E_{(2)}$ | $-0.6524 + 3.0832i$ | $-0.6506 + 3.0937i$ | 0.31% |
| $\frac{\sqrt{2}}{2} + \frac{\sqrt{2}}{2}i$ | $E_{(4)}$ | $1.0040 - 0.0008i$ | $1.0000 + 0.0000i$ | 0.40% |
| $\frac{3\sqrt{2}}{2} + \frac{\sqrt{2}i}{2}$ | $E_{(4)}^b$ | $-1.0022 - 3.9880i$ | $-1.0000 - 4.0000i$ | 0.27% |
| $\frac{7\sqrt{2}}{10} + \frac{\sqrt{2}}{10}i$ | $E_{(4)}^b$ | $-1.0032 + 3.9869i$ | $-1.0000 + 4.0000i$ | 0.29% |
| 0 | C | $2.0075 - 0.0010i$ | $2.0000 + 0.0000i$ | 0.37% |

Table 8.1.: Values at special points

of order n resp. of order 2 are the zeros of the rational function $R_\Gamma(z)$, respectively $\eta + R_\Gamma(z)$. The values at the cusps are points, where $R_\Gamma(z)$ has singularities. From the chapter about dessin d'enfants we know even more. To each group corresponds a unique dessin d'enfant and from this, we deduce the form of the rational function. Furthermore, we have explained how to obtain a system of algebraic equations which the coefficients of our rational function need to satisfy. Let $\Gamma \subset \Delta(2, n, \infty)$ be a subgroup of finite index. The system of algebraic equations which needs to be satisfied is $\underline{G}(\underline{c}) = 0$. It comes from the theory of dessins d'enfants 5.2 in chapter 5. In this step, we use this function \underline{G} for Newton's method, an iterative algorithm to find a zero of a function.

Let c_0 be a starting value. In general it is difficult to find a reasonable value for c_0 . But in our case we calculate a starting value using the approximation from the last step. Then, we perform the following iteration.

$$x_{n+1} = x_n - (\mathcal{J}(\underline{G})(x_n))^{-1} \underline{G}(x_n)$$

The matrix $\mathcal{J}(\underline{G})$ is the Jacobian matrix of \underline{G} . In practice, solve the linear equation

$$\mathcal{J}(\underline{G})(x_n) \delta_n = -\underline{G}(x_n)$$

and find the next step via

$$x_{n+1} = x_n + \delta_n.$$

If our starting value is close enough to the exact value, we use this iteration to improve our approximation to arbitrary precision. Since we want to find the exact values, we reconstruct them from the approximation.

Reconstruction of algebraic numbers from an approximation

Given an approximation of an algebraic number $z \in \mathbb{C}$, we find the exact values using the LLL algorithm - see [Coh93, 2.7.2]. This algorithm gives a polynomial $p(x) =$

$a_0 + \cdots + a_n x^n \in \mathbb{Z}[x]$ such that $|p(z)|$ is minimal. The degree n of the polynomial is fixed before. After calculating this polynomial, we solve the equation $p(x) = 0$ and choose the root, which is closest to the approximation.

In the setting of calculating the rational covering, we do this for every coefficient and obtain a rational function in $\overline{\mathbb{Q}}(x)$. To check, if we calculated the right algebraic number, we just need to check, whether the equations coming from the dessin d'enfants hold.

Example. We finish this chapter by finishing the example, we have been looking at. In the last section, we gave the results of the finite element solver. We used Newton's method to improve the accuracy and identified the number as we just described. The resulting rational covering is

$$R_\Gamma(z) = \frac{(z+1)^4(z^2+6z+25)}{z}.$$

Using this, we calculate the first terms of the q -series of the hauptmodul

$$j_\Gamma(\tau) = \frac{1}{q} - 2 - 3q + 6q^2 + 2q^3 + 2q^4 - 5q^5 - 16q^6 + 12q^7 + \mathcal{O}(q^8).$$

Since the cusp width of ∞ is $5\sqrt{2}$, we define $q = \exp\left(\frac{2\pi i\tau}{5\sqrt{2}}\right)$. Further numerical experiments suggest that this series is actually be written as a product.

Conjecture.

$$j_\Gamma(\tau) = \frac{(\tilde{\eta}(q)\tilde{\eta}(q^2))^2}{(\tilde{\eta}(q^5)\tilde{\eta}(q^{10}))^2},$$

where $\tilde{\eta}(q) = q^{1/24} \prod_{n=1}^{\infty} (1 - q^n)$.

Furthermore, if we choose $\tilde{\eta}$ as the Dedekind eta function $\eta(\tau) = \tilde{q}^{1/24} \prod_{n=1}^{\infty} (1 - \tilde{q}^n)$ with $\tilde{q} = \exp(2\pi i\tau)$, this series corresponds to the McKay-Thompson series for the class $10C$ of the monster [FMN94].

Chapter 9.

Results

In theory there is no difference between theory and practice. In practice there is.

(Yogi Berra)

In this chapter we present some examples we calculated using the methods described in the previous chapters. We start with examples of finite index subgroups of the modular group. One calls a subgroup Γ of the modular group a *congruence subgroup* if there is a $N \in \mathbb{N}$, such that

$$\Gamma(N) := \left\{ \begin{pmatrix} a & b \\ c & d \end{pmatrix} \in \mathrm{PSL}_2(\mathbb{Z}) \mid \begin{pmatrix} a & b \\ c & d \end{pmatrix} \equiv \begin{pmatrix} 1 & 0 \\ 0 & 1 \end{pmatrix} \pmod{N} \right\} \subseteq \Gamma.$$

These congruence subgroups are handled very well, by using the theory of the Hecke operators. But for non-congruence subgroups, not much is known. Hence, our examples are non-congruence subgroups of the modular group.

Non-congruence subgroups of the modular group

Hsu's example of index 10

In the article of Hsu [Hsu96], the author presents a non-congruence subgroup of index 10 and level 30^a. He describes it by the monodromy representation

$$\begin{aligned} S_2 &= (1\ 2)(3\ 4)(5\ 6)(7\ 8)(9\ 10), \\ S_3 &= (1\ 8\ 3)(2\ 4\ 6)(5\ 7\ 6). \end{aligned}$$

It is a non-congruence subgroup of genus 0, generated by

$$\left\{ \begin{pmatrix} 1 & 2 \\ 0 & 1 \end{pmatrix}, \begin{pmatrix} -2 & 1 \\ -7 & 3 \end{pmatrix}, \begin{pmatrix} 4 & -3 \\ 3 & -2 \end{pmatrix} \right\}.$$

It has the cusps

$$\{0, 1, \infty\}.$$

^aHsu defined the level to be the order of the matrix $\begin{pmatrix} 1 & 1 \\ 0 & 1 \end{pmatrix}$ in the subgroup

The coset representatives calculated by the Farey symbols are

$$\left\{ \begin{pmatrix} 1 & 0 \\ 0 & 1 \end{pmatrix} \begin{pmatrix} 1 & -1 \\ 0 & 1 \end{pmatrix}, \begin{pmatrix} 2 & -1 \\ 1 & 0 \end{pmatrix}, \begin{pmatrix} 1 & -1 \\ 1 & 0 \end{pmatrix}, \begin{pmatrix} 1 & -1 \\ 2 & -1 \end{pmatrix}, \begin{pmatrix} -1 & 0 \\ 2 & -1 \end{pmatrix}, \right. \\ \left. \begin{pmatrix} 1 & -2 \\ 1 & -1 \end{pmatrix}, \begin{pmatrix} 0 & -1 \\ 1 & -1 \end{pmatrix}, \begin{pmatrix} -1 & 0 \\ 1 & -1 \end{pmatrix}, \begin{pmatrix} 0 & -1 \\ 1 & -2 \end{pmatrix} \right\}.$$

From the cosets is it possible to construct a fundamental domain of the subgroup, as we described it in chapter 2. We draw the result for this example with the help of Sage in figure 9.1.

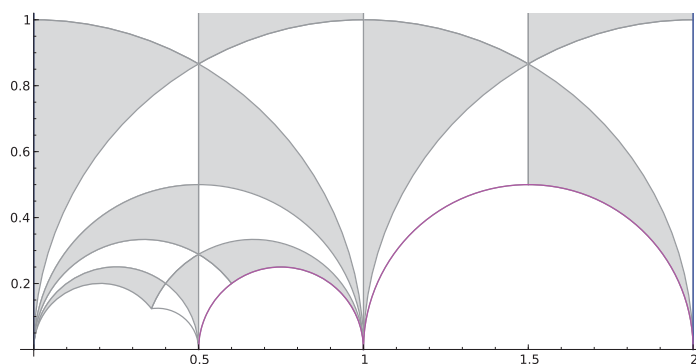


Figure 9.1.: A fundamental domain of Hsu's Example of index 10

In chapter 3, diagram 3.7, we introduced a covering $R_\Gamma: \mathbb{P}^1(\mathbb{C}) \rightarrow \mathbb{P}^1(\mathbb{C})$. We calculated this covering using the methods described in the previous chapters and obtained the following rational function

$$R_\Gamma(z) = \frac{(16z + 5\sqrt{5}) (1048576z^3 + 163840\sqrt{5}z^2 + 16000z + 625\sqrt{5})^3}{78125\sqrt{5}z^2 (512z + 25\sqrt{5})^3}.$$

To obtain this result, our Sage program took about 4 seconds of CPU-time on a standard desktop computer.

As we have seen, from the knowledge of the rational covering, we calculate the q -series of the hauptmodul. Since the cusp ∞ as width 2, we choose $q := \exp(2\pi i\tau/2)$ and obtain for the first coefficients of the Fourier expansion of the hauptmodul

$$\frac{1}{q} + \frac{3796}{625}q - \frac{131072}{15625\sqrt{5}}q^2 - \frac{5076598}{1953125}q^3 \\ + \frac{6649020416}{244140625\sqrt{5}}q^4 - \frac{51910860648}{6103515625}q^5 - \frac{4489710403584}{152587890625\sqrt{5}}q^6 + O(q^7).$$

It was also possible to obtain the Picard-Fuchs equation. As we have seen, this equation

is of the form $\mathcal{S}(\tau)(j_\Gamma) = Q_\Gamma(j_\Gamma)$, where $Q_\Gamma(z)$ is the following

$$Q_\Gamma(z) = \frac{1}{2z^2} + \frac{18625\sqrt{5}}{7776(25z + 16\sqrt{5})} + \frac{2500}{9(25z + 16\sqrt{5})^2} + \frac{484375\sqrt{5}}{124416(125z + 512\sqrt{5})} \\ + \frac{15625}{2(125z + 512\sqrt{5})^2} - \frac{65\sqrt{5}}{512z}.$$

Furthermore, we were also able to find the first coefficients of the cusp form of weight 4. Note that for this group the space of cusp forms of weight 4 is one dimensional. Hence, all cusp forms of this weight are linear dependent on the given one.

$$f(\tau) = q + \frac{1}{2^{3/5}}q^2 - \frac{41}{82^{1/5}}q^3 + \frac{33}{4 \cdot 2^{4/5}}q^4 - \frac{625}{64 \cdot 2^{2/5}}q^5 - \frac{2269}{640}q^6 + \frac{953}{2560 \cdot 2^{3/5}}q^7 + \mathcal{O}(q^8).$$

Some notes on the uniqueness

The rational covering, the hauptmodul, and the Picard-Fuchs equation need not to be unique. For example the rational function R_Γ is only unique up to a Möbius transformation. To calculate the hauptmodul from this rational function, we need the function to have a singularity at $t = 0$. Since there are three singularities, we have three different choices. Each of these corresponds to an expansion at a different cusp. In this example, we transform the covering via $x \mapsto x - \frac{125}{512\sqrt{5}}$ and obtain

$$\tilde{R}_\Gamma(z) = R_\Gamma\left(z - \frac{125}{512\sqrt{5}}\right) = \\ \frac{(512\sqrt{5}z + 675) \left(134217728\sqrt{5}z^3 + 6553600z^2 - 3392000\sqrt{5}z + 75937\right)^3}{6710886400000000\sqrt{5} \left(25\sqrt{5} - 512z\right)^2 z^3}.$$

This results in a different expansion, with $q = \exp(2\pi i\tau/3)$

$$\frac{1}{q^1} + \frac{33 \cdot 2^{1/3}}{5 \cdot 5^{2/3}} + \frac{2619}{200 \cdot 10^{1/3}}q^1 + \frac{74323}{20000}q^2 - \frac{18080901}{1600000 \cdot 10^{2/3}}q^3 \\ - \frac{10933939251}{400000000 \cdot 10^{1/3}}q^4 + \mathcal{O}(q^5),$$

and in a different Picard-Fuchs equation

$$\frac{1}{2t^2} - \frac{5\sqrt{5}}{64t} + \frac{2318625\sqrt{5}}{32768(675t + 512\sqrt{5})} + \frac{202500}{(675t + 512\sqrt{5})^2} \\ - \frac{109375}{32768(25\sqrt{5}t - 512)} + \frac{3125}{2(25\sqrt{5}t - 512)^2}.$$

Hsu's example of index 18

In the same article [Hsu96], he also presents a second non-congruence subgroup which is of index 18 and level 24.

$$S_2 = (1\ 5)(2\ 11)(3\ 10)(4\ 15)(6\ 18)(7\ 12)(8\ 14)(9\ 16)(13\ 17),$$

$$S_3 = (1\ 7\ 11)(2\ 18\ 5)(3\ 9\ 15)(4\ 14\ 10)(6\ 17\ 12)(8\ 13\ 16).$$

It is again a non-congruence subgroup of genus 0, generated by

$$\left\{ \begin{pmatrix} 1 & 2 \\ 0 & 1 \end{pmatrix}, \begin{pmatrix} 5 & -2 \\ 3 & -1 \end{pmatrix}, \begin{pmatrix} 11 & -6 \\ 13 & -7 \end{pmatrix}, \begin{pmatrix} 25 & -18 \\ 32 & -23 \end{pmatrix}, \begin{pmatrix} -1 & 0 \\ 0 & -1 \end{pmatrix} \right\}.$$

It has the cusps

$$\left\{ 0, \frac{1}{2}, \frac{2}{3}, \frac{3}{4}, \infty \right\}.$$

The coset representatives are

$$\left\{ \begin{pmatrix} 1 & 0 \\ 0 & 1 \end{pmatrix}, \begin{pmatrix} 1 & -1 \\ 0 & 1 \end{pmatrix}, \begin{pmatrix} 2 & -1 \\ 1 & 0 \end{pmatrix}, \begin{pmatrix} 1 & -1 \\ 1 & 0 \end{pmatrix}, \begin{pmatrix} 3 & -2 \\ 2 & -1 \end{pmatrix}, \begin{pmatrix} 1 & -1 \\ 2 & -1 \end{pmatrix}, \right.$$

$$\begin{pmatrix} 4 & -3 \\ 3 & -2 \end{pmatrix}, \begin{pmatrix} 1 & -1 \\ 3 & -2 \end{pmatrix}, \begin{pmatrix} 5 & -4 \\ 4 & -3 \end{pmatrix}, \begin{pmatrix} 1 & -1 \\ 4 & -3 \end{pmatrix}, \begin{pmatrix} 1 & -1 \\ 5 & -4 \end{pmatrix}, \begin{pmatrix} 1 & -2 \\ 1 & -1 \end{pmatrix},$$

$$\left. \begin{pmatrix} 0 & -1 \\ 1 & -1 \end{pmatrix}, \begin{pmatrix} -1 & 0 \\ 1 & -1 \end{pmatrix}, \begin{pmatrix} -2 & 1 \\ 1 & -1 \end{pmatrix}, \begin{pmatrix} -3 & 2 \\ 1 & -1 \end{pmatrix}, \begin{pmatrix} -4 & 3 \\ 1 & -1 \end{pmatrix}, \begin{pmatrix} 0 & -1 \\ 1 & -2 \end{pmatrix} \right\}.$$

The fundamental domain constructed from the cosets is figure 9.2.

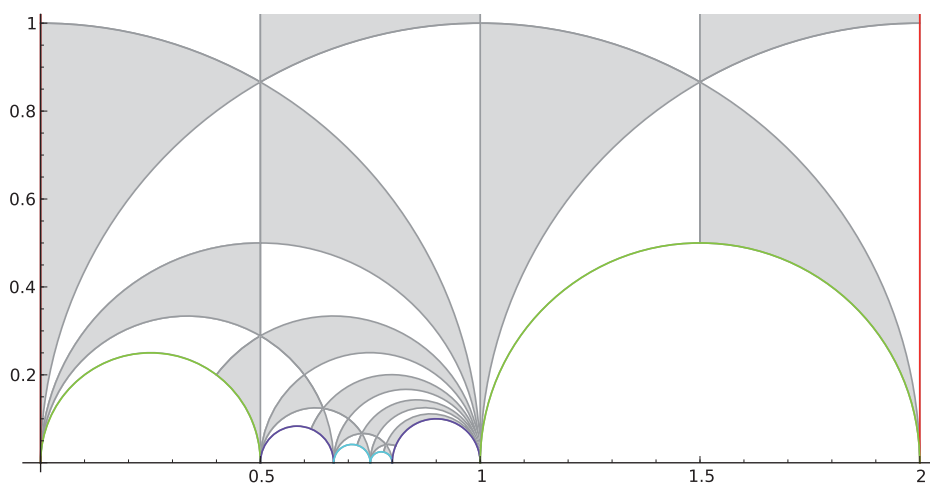


Figure 9.2.: A fundamental domain of Hsu's Example of index 18

Analog Hsu's example of index 10, we calculate the rational covering. This calculation needed around 40 seconds of CPU-time on our desktop computer.

$$R_{\Gamma}(z) = \left(729(4782969z^6 + 51018336z^5 + 1243335744z^4 + 11448262656z^3 + 42672697344z^2 + 67278864384z + 35071459328)^3 \right) / \left(((729z^2 - 1296z - 11712)^3(27z + 104)^8(27z + 88)^2) \right).$$

The first coefficients of the expansion of the hauptmodul are as follows.

$$j_{\Gamma}(\tau) = \frac{1}{\sqrt{q}} + \frac{104}{27} + \frac{4340}{729}q^{1/2} + \frac{81920}{19683}q - \frac{1746014}{531441}q^{3/2} + O(q^2).$$

Again, we defined $q := \exp(2\pi i\tau)$.

The Q -term of the Picard-Fuchs equation is

$$Q(z) = \frac{1}{2z^2} + \frac{27}{32z} + \frac{729}{2(27z - 16)^2} + \frac{8019}{32(27z - 16)} + \frac{17915904}{(729z^2 - 6912z + 4096)^2} - \frac{6561(9z - 80)}{8(729z^2 - 6912z + 4096)}.$$

Sporadic groups

The next groups are examples suggested by Monien.

The sporadic group M_{12}

$$S_2 = (1\ 2)(3\ 9)(4\ 5)(6\ 7)(8\ 12)(10\ 11),$$

$$S_3 = (1\ 10\ 2)(3\ 8\ 11)(4\ 9\ 6).$$

The group generated by S_2 and S_3 is the Mathieu group M_{12} [WWT⁺]. This group is a sporadic group of order 95040. For a discussion for which sporadic group this construction is possible see the article by Magaard [Mag93].

The Mathieu groups have lately drawn attention to themselves since the discovery of the *Mathieu or umbral moonshine* ([EOT11], [CDH12], [DGO15]). Similar to the "classical" monstrous moonshine ([CN79], [Bor92]) there is a connection between certain (mock) modular forms and representations of the Mathieu group (or in the classical case, the monster group).

If we use M_{12} as monodromy, obtain a non-congruence subgroup of index 12 of $\mathrm{PSL}_2(\mathbb{Z})$. Its level is 11 and its genus zero. The generators are

$$\left\{ \begin{pmatrix} 1 & 1 \\ 0 & 1 \end{pmatrix}, \begin{pmatrix} -3 & 1 \\ -13 & 4 \end{pmatrix}, \begin{pmatrix} -7 & 3 \\ -19 & 8 \end{pmatrix}, \begin{pmatrix} -4 & 3 \\ -7 & 5 \end{pmatrix} \right\},$$

it has the cusps

$$\{0, \infty\}$$

and a set of coset representatives is

$$\left\{ \begin{pmatrix} 1 & 0 \\ 0 & 1 \end{pmatrix}, \begin{pmatrix} 3 & -1 \\ 1 & 0 \end{pmatrix}, \begin{pmatrix} 2 & -1 \\ 1 & 0 \end{pmatrix}, \begin{pmatrix} 1 & -1 \\ 1 & 0 \end{pmatrix}, \begin{pmatrix} 2 & -1 \\ 3 & -1 \end{pmatrix}, \begin{pmatrix} -1 & 0 \\ 3 & -1 \end{pmatrix}, \begin{pmatrix} 1 & -1 \\ 2 & -1 \end{pmatrix}, \right. \\ \left. \begin{pmatrix} -1 & 0 \\ 2 & -1 \end{pmatrix}, \begin{pmatrix} -3 & 1 \\ 2 & -1 \end{pmatrix}, \begin{pmatrix} 0 & -1 \\ 1 & -1 \end{pmatrix}, \begin{pmatrix} -1 & 0 \\ 1 & -1 \end{pmatrix}, \begin{pmatrix} -2 & 1 \\ 1 & -1 \end{pmatrix} \right\}.$$

The fundamental domain is figure 9.3. Using the methods we described in this thesis,

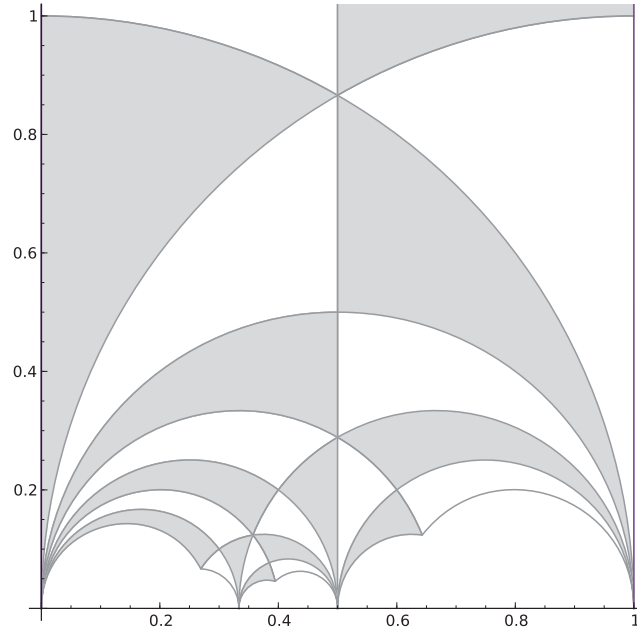


Figure 9.3.: A fundamental domain for M_{12}

we calculate the rational covering in about 6 seconds of CPU-time. We abbreviate $\omega = \sqrt{-11}$.

$$R_{\Gamma}(z) = \frac{1}{55788550416} \cdot \left(15251194969974z^3 - 2324522934(-1210\omega - 17651)z^2 \right. \\ \left. - 118098(-369427399\omega - 1131975836)z + 50817103760819\omega - 108237990465161 \right) \\ \left(15251194969974z^3 - 2324522934(-3146\omega - 1557547)z^2 \right. \\ \left. - 354294(-4936057181\omega - 66065392948)z \right. \\ \left. + 12153453472899035\omega + 15941668103377087 \right)^3 \\ \left/ \left(6561z + 968\omega - 17372 \right)^{11} \right.$$

The sporadic group M_{11}

To give an example which is not a subgroup of the modular group, we choose the group generated by the following two permutations.

$$\begin{aligned} S_2 &= (1\ 9)(3\ 10)(4\ 11)(5\ 6), \\ S_4 &= (1\ 8\ 10\ 7)(2\ 9\ 6\ 11). \end{aligned}$$

This results in the Mathieu group M_{11} . The Fuchsian group defined by these permutations is a subgroup of the triangle group $\Delta(2, 4)$. It has index 11 and genus zero. The generators are

$$\left\{ \begin{pmatrix} -2\sqrt{2} & -5 \\ 1 & \sqrt{2} \end{pmatrix}, \begin{pmatrix} -4\sqrt{2} & -5 \\ 5 & 3\sqrt{2} \end{pmatrix}, \begin{pmatrix} -\sqrt{2} & -1 \\ 3 & \sqrt{2} \end{pmatrix}, \right. \\ \left. \begin{pmatrix} \sqrt{2} & -1 \\ 3 & -\sqrt{2} \end{pmatrix}, \begin{pmatrix} 3\sqrt{2} & -5 \\ 5 & -4\sqrt{2} \end{pmatrix}, \begin{pmatrix} \sqrt{2} & -3 \\ 1 & -\sqrt{2} \end{pmatrix} \right\}$$

and a set of coset representatives is

$$\left\{ \begin{pmatrix} 1 & 0 \\ 0 & 1 \end{pmatrix}, \begin{pmatrix} 1 & -\sqrt{2} \\ 0 & 1 \end{pmatrix}, \begin{pmatrix} -\sqrt{2} & -1 \\ 1 & 0 \end{pmatrix}, \begin{pmatrix} -\sqrt{2} & 1 \\ 1 & -\sqrt{2} \end{pmatrix}, \begin{pmatrix} -1 & -\sqrt{2} \\ \sqrt{2} & 1 \end{pmatrix}, \begin{pmatrix} -1 & 0 \\ \sqrt{2} & -1 \end{pmatrix}, \right. \\ \left. \begin{pmatrix} 0 & -1 \\ 1 & 0 \end{pmatrix}, \begin{pmatrix} 0 & -1 \\ 1 & -\sqrt{2} \end{pmatrix}, \begin{pmatrix} 1 & -\sqrt{2} \\ \sqrt{2} & -1 \end{pmatrix}, \begin{pmatrix} \sqrt{2} & 1 \\ 1 & \sqrt{2} \end{pmatrix}, \begin{pmatrix} \sqrt{2} & -1 \\ 1 & 0 \end{pmatrix} \right\}$$

A fundamental domain is figure 9.4. We also calculated the rational function.

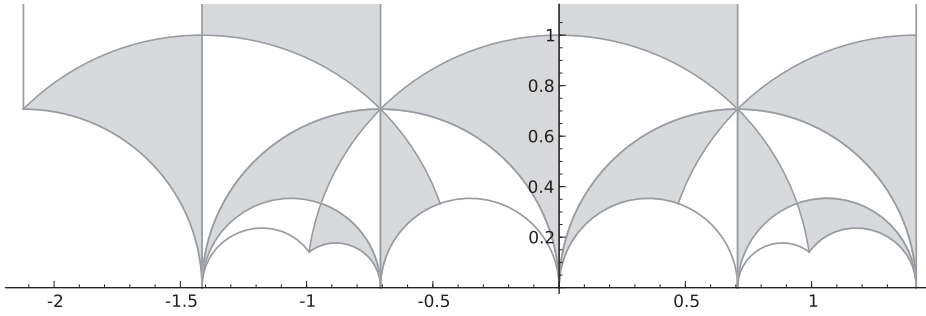


Figure 9.4.: A fundamental domain for M_{11}

$$\begin{aligned} R_{\Gamma}(z) &= (z^2 + a_1z + a_2)^4 \cdot (z^3 + a_3z^2 + a_4z + a_5) \\ &\cong (z^2 - (0.3113 + 0.2519i)z + (-1.828 - 0.922i))^4 \cdot \\ &\quad (z^3 + (1.245 + 1.008i)z^2 - (5.113 + 3.146i)z + (-4.165 - 11.867i)). \end{aligned}$$

The coefficients a_1, \dots, a_5 are given as follows:

$$\begin{aligned}
 a_1 &= (-1)^{3/11} \sqrt[11]{-\frac{51109}{3321506250} - \frac{39677\sqrt{-11}}{3321506250}}, \\
 a_2 &= -\frac{\sqrt[22]{-1} \left(-51109 - 39677\sqrt{-11}\right)^{2/11} (3\sqrt{11} + 8i)}{9 \cdot 5^{10/11} \cdot 6^{2/11}}, \\
 a_3 &= -4 \cdot a_1, \\
 a_4 &= \frac{1}{978} (2857 + 73\sqrt{-11}) \cdot a_2, \\
 a_5 &= -\frac{2(-1)^{5/11} \sqrt[11]{-1348402095065702 - 632453541676781\sqrt{-11}}}{3^{8/11} \cdot 5^{4/11}}.
 \end{aligned}$$

The roots are chosen according to the numerical values.

Chapter 10.

Perspectives

Nos mathematici sumus isti veri poetae sed quod fingimus nos et probare decet.

(We as mathematicians are the true poets, except we have to prove what our fantasy creates.)

(*Leopold Kronecker*)

Based on the idea of Monien, we presented a new technique to calculate *hauptmoduls* of finite index subgroups of the modular groups and of triangle groups. This method was used to calculate rational coverings given by a *dessin d'enfants*. We calculated numerically an approximation of the *hauptmodul*, by solving the Laplace equation on a certain Riemann surface. We represented this surface as a subset of the extended upper half plane together with the identification of the boundary. These identifications of the boundaries were interpreted as periodic boundary conditions. Together with the condition that the function behaves like $\frac{1}{q}$ for a suitable q , we obtained a partial differential equation which was solved using the finite element method. Combining this with the theory of *dessin d'enfants* and Newton's algorithm it was possible to improve the accuracy up to an arbitrary level. Using the LLL algorithm we identified from this approximation the exact numbers and verified their correctness using again the theory of the *dessins*.

To properly handle the subgroups of the triangle groups, we generalized the theory of Farey symbols to general Hecke groups. The main differences to the classical Farey symbols was the possible existence of *holes* in the sequence. These holes corresponded to certain elliptic points for the Hecke groups which can only occur if the parameter n of the Hecke group Δ_n is not a prime number.

Possible improvements

One of the first possible improvements is a proper implementation of the notion of triangle groups and generalized Farey symbols in Sage. A guiding example of such an implementation should be the existing classical Farey symbols. For reasons of performance one should implement the Farey symbols in *C++* with an interface to Sage. Here, a technical issue appears. In the classical setting, the relevant matrices are *integer* matrices and there are good implementations of these like GMP [GMP]. For general

triangle groups, we need number fields and up to now there is no suitable and fast implementation of these.

If we are working with groups of large index, like the Janko group J_2 of index 100, we can calculate the Farey symbol (figure 10.1) and an approximation of the hauptmodul. But the precision of this approximation is not enough that Newton's method

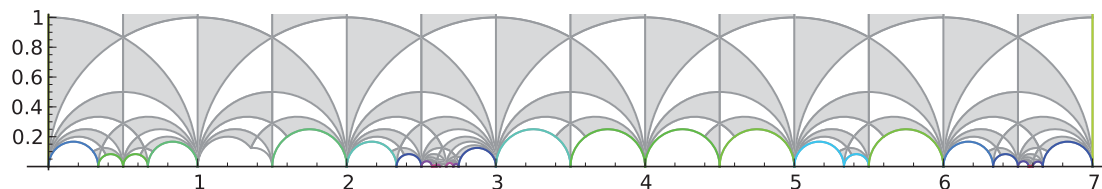


Figure 10.1.: Fundamental domain for the Janko group J_2

is converging. Hence, we need to have a finite element solver which works with higher precision.

Modular forms

Since we are now able to find modular functions for finite index subgroups of genus zero of Hecke groups, the next step is to find modular forms. In the article *Automorphic forms for triangle groups* [DGMS13] the authors claim that it is possible to calculate all automorphic forms for a genus zero Fuchsian group from the hauptmodul. This can be used to develop a program to calculate all automorphic forms for a given finite index subgroup of a Hecke group of genus zero. From this point, we have a gigantic pool of examples to look at. For example we can collect data for the Atkin-Swinnerton-Dyer conjecture [ASD71]. This is a conjecture about congruence relations on the Fourier coefficients of modular forms. Although there is some numerical data, cf. [LLY05b], [Lon08] etc., we can use this program for a more systematic search.

Further perspectives

Generalized Farey symbols

In this thesis we presented a generalization of the Farey symbols as a tool to handle the Hecke groups. Further developments are still possible. As a perspective, we show some approaches.

- (i) There are many well known algorithms for the classical Farey symbols. For example, there is an algorithm using the Farey symbols to decide whether a given matrix is in a subgroup ([LLT95a], [LLT95b]). These algorithms should be generalized such that they can be applied on the n -Farey symbols.
- (ii) Furthermore, it should be possible to generalize the notion of the Farey symbols to subgroups of general non-compact triangle groups. As we have seen, for the Hecke

groups $\Delta(2, n)$ we needed $n - 2$ insertion operators. In the general context of a triangle group $\Delta(a, b)$, we need two “types” of insertion operators $I^{(a)}$ and $I^{(b)}$ which are applied alternating. Similar to the Hecke groups, there are $a - 2$ operators of type $I^{(a)}$ and $b - 2$ operators of type $I^{(b)}$. Looking at the special case of $a = 2$, we see that there are no operators of type $I^{(a)}$.

- (iii) For the classical Farey sequences, we know a lot. Which theorems do generalize to n -Farey sequences or even (a, b) -Farey sequences? Although it should not be too hard to prove, we state the following conjecture as an example.

Conjecture. Let $F_\nu = \left\{ \frac{a_1}{b_1}, \dots, \frac{a_{m_\nu}}{b_{m_\nu}} \right\}$ be a complete n -Farey sequence. Then,

$$\sum_{i=1}^{m_\nu} \frac{1}{a_i b_i} = \nu.$$

First numerical evidence suggests that this conjecture holds.

Another fascinating fact about classical Farey sequences is the following. Let $F_n = \{x_{0,n}, \dots, x_{m_n,n}\}$ be the n^{th} -Farey sequence and $E_n = \{y_{0,n}, \dots, y_{m_n,n}\}$ with $y_{i,n} = \frac{i}{m_n - 1}$ equidistantly distributed points on the interval $[0, 1]$. The difference between these two sequences is defined as $d_{k,n} = x_{k,n} - y_{k,n}$.

10.1 Theorem (Franel [Fra24] and Landau [Lan24]). *The following statements are equivalent:*

- a) $\sum_{k=1}^{m_n} d_{k,n} = \mathcal{O}(n^r) \quad \forall r > -1,$
- b) $\sum_{k=1}^{m_n} d_{k,n} = \mathcal{O}(n^r) \quad \forall r > \frac{1}{2},$
- c) *The Riemann hypothesis.*

Does this theorem generalize to n -Farey sequences?

The generalized Farey sequences seem to have fascinating properties and a deep arithmetic structure. Although it seems that they inherit most of the characteristics from the classical Farey sequences, they also could contain nice and new structures, which are worthwhile to discover.

Appendix A.

Selected Mathematica programs

In this chapter we present the source code of some selected Mathematica programs [WR14].

Finding the dessin for a given Belyĭ function

For a Belyĭ function f we like to know how the corresponding dessin looks like. For this purpose, we wrote a function which produces the dessin. It works as follows. Since the dessin is the pre-image of the interval $[0, c]$ for some $c \in \mathbb{R}$, we discretize this interval and solve the equation $f(t_i) = x_i$, for x_i the discrete points on the interval. Then, we plot all solutions t_i .

```
Dessin[f_, pts_:10, white_:False, black_:True, cut_:0.02, scale_:1728]:=
Block[{L, XL, R0, R1, g, g0, g1},
  L = Table[scale (n/pts)^2, {n, 0, pts}];
  XL = {Re[#], Im[#]}&/@ Flatten[x/.Table[NSolve[f[x]==L[[i]], x],
    {i, Length[L]}]];
  R0 = {Re[#], Im[#]}&/@ Flatten[x/.NSolve[f[x]==L[[1]], x]];
  R1 = {Re[#], Im[#]}&/@ Flatten[x/.NSolve[f[x]==L[[-1]], x]];
  g = ListPlot[XL,
    PlotRange->{{Min[XL\[Transpose][[1]]] - cut,
      Max[XL\[Transpose][[1]]] + cut},
      {Min[XL\[Transpose][[2]]] - cut,
      Max[XL\[Transpose][[2]]] + cut}}
  ];
  If[black,
    g0 = ListPlot[R0, PlotStyle->{Black, PointSize[Large]}],
    g0 = Graphics[]
  ];
  If[white,
    g1 = ListPlot[R1, PlotStyle->{Red, PointSize[Large]}],
    g1 = Graphics[]
  ];
  Show[g, g0, g1, AspectRatio->Automatic]
]
```

Sample output

As an example, we calculate the dessin for the tetrahedron, see chapter 5, figure 5.3. Note that we specified the Belyĭ function, such that it branches over 0, 1, and ∞ . Here, we use a modification such that it branches over 0, 1728, and ∞ . The function is now

$$f(z) = -1728 \frac{64z^3 (z^3 - 1)^3}{(8z^3 + 1)^3}.$$

```
f[z_] = -1728 (64 z^3 (z^3 - 1)^3) / (8 z^3 + 1)^3
```

```
Dessin[f, 25, True, True]
```

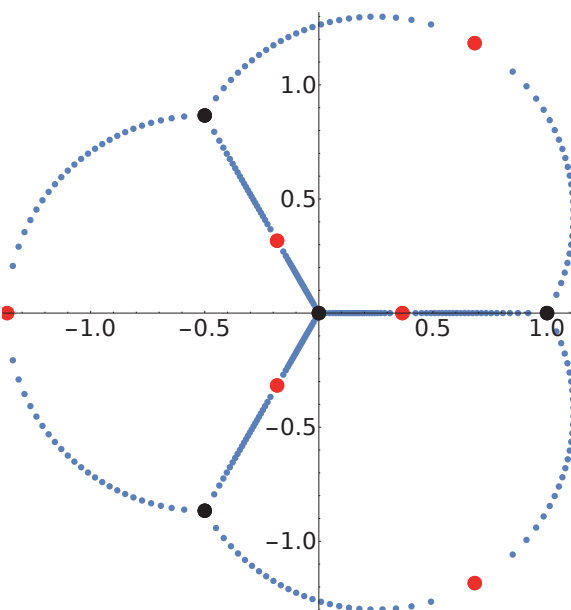


Figure A.1.: Sample output for a dessin in Mathematica

Calculating the hauptmodul from a rational covering and vice versa

Let $\Gamma \subseteq \Delta$ be a subgroup of finite index of a triangle group Δ . Furthermore, let J be the hauptmodul for Δ . In chapter 3, we explained how we calculate the hauptmodul for the subgroup, if we know the rational covering \tilde{R}_Γ . This covering has the property that $J = \tilde{R}_\Gamma(j_\Gamma)$. We actually prefer to work with a covering which has the property $J = R_\Gamma\left(\frac{1}{j_\Gamma}\right)$. In a first step, we will expand the function $R_\Gamma(x)$ in a series. $R_\Gamma(x) = \frac{a}{x^w} + \mathcal{O}(1)$, where $a \in \mathbb{R}$ is some constant and w the cusp width. As an element of the ring of Laurent

series, this element is not invertible. The reciprocal $\frac{1}{R_\Gamma}(x) = \frac{x^w}{a} + \mathcal{O}(x^{w+1})$ is actually invertible. Hence, we do the following short calculation

$$\begin{aligned} J &= R_\Gamma \left(\frac{1}{j_\Gamma} \right) \\ \Rightarrow \frac{1}{J} &= \frac{1}{R_\Gamma} \left(\frac{1}{j_\Gamma} \right) \\ \Rightarrow \left(\frac{1}{R_\Gamma} \right)^{-1} \left(\frac{1}{J} \right) &= \frac{1}{j_\Gamma} \\ \Rightarrow 1 / \left(\frac{1}{R_\Gamma} \right)^{-1} \left(\frac{1}{J} \right) &= j_\Gamma. \end{aligned}$$

We use this formula to calculate the q -expansion of the hauptmodul.

```
ToHauptmodul[f_, n_:32] :=
  1 / (Normal[InverseSeries[1/Series[f[q], {q, 0, n}]]]
    /. q -> 1/J[n]) + O[q]^n
```

The other direction works similar

$$\begin{aligned} J &= R_\Gamma \left(\frac{1}{j_\Gamma} \right) \\ \Rightarrow J \left(\left(\frac{1}{j_\Gamma} \right)^{-1} \right) &= R_\Gamma. \end{aligned}$$

This results in the series expansion for the covering R_Γ . From the general theory we know that this series is actually a rational function. To obtain the rational function, we calculate a Padé approximant.

```
ToRationalFunction[hauptmodul_, numdeg_:12, denomdeg_:8] :=
  Factor[
    PadéApproximant[
      (Normal[J] /. q -> InverseSeries[1/hauptmodul]),
      {q, 0, {numdeg, denomdeg}}
    ]
  ]
```


Appendix B.

FreeFem++

The reason why we decided to use FreeFem++ [Hec12], is the way boundary conditions are handled. The requirement was that we needed a solver for partial differential equations which is able to handle arbitrary boundary conditions. We will explain how this is done. This construction is based on an example which can be found in the wiki for the software FreeFem++: [FB]. We continue to use the notation from chapter 8. The example we look at in this chapter corresponds to the subgroup $\Gamma_0(2)$ of the modular group $\mathrm{PSL}_2(\mathbb{Z}) = \Delta(2,3)$.

First of all, we start to define the height h of the triangles and a discretization parameter n which controls the number of triangulation.

```
real h = 3.0000000000000000;  
int n = 25;
```

Then, we define the boundaries of the triangles and construct an area out of this.

```
border L1(t=1.0,0.0) {  
  x = 0.0;  
  y = t;  
  label = 1;  
}  
  
border bow(t=1.0,0.0) {  
  x = 1.0 + cos(pi/3.0*(t+2.0));  
  y = sin(pi/3.0*(t+2.0));  
  label = 2;  
}  
  
border topbow(t=2./3.,1.0) {  
  x = cos(pi/2.*t);  
  y = sin(pi/2.*t);  
  label = 3;  
}  
  
mesh Th1 = buildmesh(L1(n)+bow(n)+topbow(n/2), fixeborder=true);
```

This constructs the triangle which we called \mathcal{T}_0 . Analog to this, we define the triangle \mathcal{T}_h . Note that each boundary has an individual label. To convince ourselves that these triangles are correct we plot them, see figure B.1 and B.2.

```

plot(Th1);
plot(Th2);
    
```

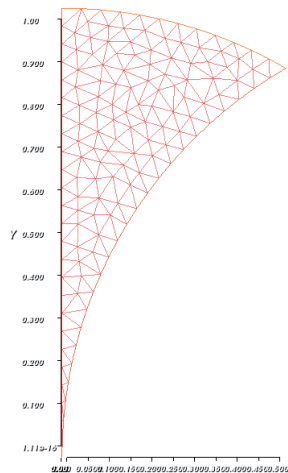


Figure B.1.: The plot of Th1

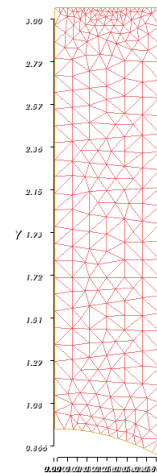


Figure B.2.: The plot of Th2

Following algorithm 4 from chapter 8, we now construct the fundamental domain due to certain condition on the cusps ∞ and 0. For each coset, we map one of the triangles and add it to the fundamental domain. As an example, we look at the coset for $c_1 = \begin{pmatrix} 1 & -1 \\ 1 & 0 \end{pmatrix}$. Then, we have

$$\begin{aligned}
 c_1^{-1}(x + iy) &= \frac{x + iy - 1}{x + iy} \\
 &= -\frac{x - 1}{x^2 + y^2 - 2x + 1} + i\frac{y}{x^2 + y^2 - 2x + 1}.
 \end{aligned}$$

Now, we map the triangle Th1 with this map to obtain a new triangle which will be added to the fundamental domain. In FreeFem++ we do it as follows.

```

mesh T1c1 = movemesh(Th1, [-(x - 1)/(x^2 + y^2 - 2*x + 1), y/(x^2 + y^2 - 2*x + 1)]);
    
```

This constructs a new mesh which is mapped in the right place. Running over all cosets using algorithm 4, we obtain a set of unrelated discretized triangles. Due to the construction, the boundaries of these triangles are compatible. The discretization points on boundary coincide, if the boundaries do. This allows us to define a new mesh.

```

mesh T = T1c0 + T2c0 + T1c1 + T2c1 + T1c2 + T2c2 ;
    
```

Next, we take care of the boundary conditions. Lemma 8.1 asserts that the mesh is compatible with the periodic boundary conditions which are the pairings. To handle the pairings, we use the labels of the boundary. To make them individually accessible, we rename them.

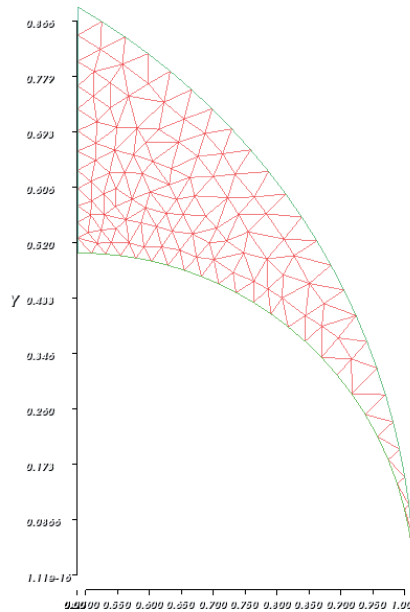


Figure B.3.: The plot of T1c1

```
r1 = [1, 11];
T1c1 = change(T1c1, label=r1);
```

These labels are now used to define the periodic boundary conditions.

```
func pairing = [[10, y], [13, y],
[11, x], [12, (2*x^2 + 2*y^2 - 3*x + 1)/(4*x^2 + 4*y^2 - 4*x + 1)]];
```

The rest is straight forward. We construct a space of finite elements with periodic boundary conditions, write down the Laplace equation in variational formulation, and the boundary condition for $z \rightarrow \infty$.

```
fespace Vh(T, P2, periodic=pairing);
Vh phi, psi, w;

solve LaplaceRe(phi, w, solver=LU) =
  int2d(T) (dx(phi)*dx(w) + dy(phi)*dy(w)) + on(7, phi= cos(2.*pi*x/1.0)*exp
(2.*pi*h/1.0000000000000000));
```

Then, the resulting function is evaluated at the elliptic points and the result is written in a file. The complete code for $\Gamma_0(2)$ looks a follows.

```
//File for Belyi(Congruence Subgroup Gamma0(2))

verbosity = 0;

real h = 3.0000000000000000;
```

```
int n = 25;

border L1(t=1.0,0.0) {
  x = 0.0;
  y = t;
  label = 1;
}

border bow(t=1.0,0.0) {
  x = 1.0 + cos(pi/3.0*(t+2.0));
  y = sin(pi/3.0*(t+2.0));
  label = 3;
}

border topbow(t=2./3.,1.0) {
  x = cos(pi/2.*t);
  y = sin(pi/2.*t);
  label = 2;
}

border L2(t=1.0,0.0) {
  x = 0.0;
  y = (h-1.)*t+1;
  label = 4;
}

border topbowinv(t=1.,2./3.) {
  x = cos(pi/2.*t);
  y = sin(pi/2.*t);
  label = 5;
}

border R(t=(sqrt(3.0)/2.0/h)^(1.0/1.0),1.0) {
  x = 0.5;
  y = h*t;
  label = 6;
}

border Top(t=0.5,0.0) {
  x = t;
  y = h;
  label = 7;
}

mesh Th1 = buildmesh(L1(n)+bow(n)+topbow(n/2), fixeborder=true);
mesh Th2 = buildmesh(L2(n)+topbowinv(n/2)+R(n)+Top(n), fixeborder=true);
int[int] r1;

mesh T1c0 = movemesh(Th1, [x, y]);
mesh T2c0 = movemesh(Th2, [x, y]);

r1 = [1,10];
```

```

T1c0 = change (T1c0, label=r1);
r1 =[4,10];
T2c0 = change (T2c0, label=r1);

mesh T1c1 = movemesh (Th1, [-(x - 1)/(x^2 + y^2 - 2*x + 1), y/(x^2 + y^2 -
2*x + 1)]);
mesh T2c1 = movemesh (Th1, [(x^2 + y^2 - x)/(x^2 + y^2 - 2*x + 1), y/(x^2 +
y^2 - 2*x + 1)]);

r1 =[1,11];
T1c1 = change (T1c1, label=r1);
r1 =[1,12];
T2c1 = change (T2c1, label=r1);

mesh T1c2 = movemesh (Th2, [-x + 1, y]);
mesh T2c2 = movemesh (Th1, [-x + 1, y]);

r1 =[4,13];
T1c2 = change (T1c2, label=r1);
r1 =[1,13];
T2c2 = change (T2c2, label=r1);

mesh T = T1c0 + T2c0 + T1c1 + T2c1 + T1c2 + T2c2 ;

func pairing = [[10,y], [13,y],
[11,x], [12, (2*x^2 + 2*y^2 - 3*x + 1)/(4*x^2 + 4*y^2 - 4*x + 1)]];

fespace Vh(T,P2,periodic=pairing);
Vh phi, psi, w;

solve LaplaceRe(phi,w, solver=LU) =
int2d(T) (dx(phi)*dx(w)+dy(phi)*dy(w)) +on(7, phi= cos(2.*pi*x/1.0)*exp
(2.*pi*h/1.0000000000000000));

solve LaplaceIm(psi,w, solver=LU) =
int2d(T) (dx(psi)*dx(w)+dy(psi)*dy(w)) +on(7, psi=-sin(2.*pi*x/1.0)*exp
(2.*pi*h/1.0000000000000000));

ofstream out ("fem_resultsNaB9GP.sage");
out << "w21 = [";
out << "CC(" << phi(0.5000000000000000,0.5000000000000000) << ", " << psi
(0.5000000000000000,0.5000000000000000) <<"), ";
out << "]" << endl;

out << "w22 = [";
out << "CC(" << phi(0.0000000000000000,1.0000000000000000) << ", " << psi
(0.0000000000000000,1.0000000000000000) <<"), ";
out << "]" << endl;

```

```
out << "w31 = [";  
out << "]" << endl;  
  
out << "w33 = [";  
out << "CC(" << phi(0.5000000000000000,0.866025403784439) << ", " << psi  
(0.5000000000000000,0.866025403784439)<<"), ";  
out << "]" << endl;  
  
out << "wc = [";  
out << "CC(" << phi(0.0000000000000000,0) << ", " << psi  
(0.0000000000000000,0)<<"), ";  
out << "]" << endl;
```

Appendix C.

The software system Sage

“Sage [SAG] is a free open-source mathematics software system licensed under the GPL. It builds on top of many existing open-source packages: NumPy, SciPy, matplotlib, Sympy, Maxima, GAP, FLINT, R and many more.”

Good introductions are on the home page of Sage. The founder of Sage, William Stein, also provides some good introductions – for example [Ste12] or [Ste07].

Our computer programs are mainly based on Sage. In this appendix we outline the way we used Sage to obtain our results.

For the modular group, Monien implemented the notion of the classical Farey symbols in *C++* and provided an interface to sage [Mon11]. As already mentioned in the outlook in chapter 10, a long term goal is to provide similar implementation for the generalized Farey symbols.

For the implementation of the Farey symbols, we first need a way to handle subgroups of triangle groups. For this we have implemented two classes which we called `triangle_group_2noo` and `subgroup_of_triangle_group`. The first class describes a triangle group $\Delta_n = \Delta(2, n, \infty)$ and the second one a subgroup of it.

The class `triangle_group_2noo`

This class is initialized with one integer parameter n which corresponds to the order of the second generator. Then, some characteristic values are calculated, like the points z_a, z_b , and the generators of the group δ_a , etc.

```
class triangle_group_2noo:
    def __init__(self, _n,):
        if( _n <= 2 ):
            print 'This is an Euclidian triple'
            print 'Not implemented'
        self.a = 2
        self.b = _n
        a = self.a
        b = self.b

        self.za = I.n()
        self.zb = (cot(pi/2)+csc(pi/2)*cos(pi/b)+I*csc(pi/2)*sin(pi/b)).n
        ()
```

```
self.zc = 2442.*I.n()
self.zcg= (1/tan(pi/2)).n()

V = MatrixSpace(SR,2,2)
self.da = V([cos(pi/2),-sin(pi/2),sin(pi/2),cos(pi/2)])
self.dai= (self.da)^-1
[ ... ]
self.S = self.da
self.T = self.dbi*self.da
[ ... ]

def __repr__(self):
    return 'TriangleGroup(2,%s,oo)' % self.b
```

To visualize the operation on the upper half plane we implement a function to plot the fundamental domain.

```
def fundamental_domain(self):
    g = Graphics()
    g += hyperbolic_triangle(self.za, self.zb, self.zc, \
                            fill=true, color='lightgrey')
    g += hyperbolic_triangle(self.za, self.zb, self.zcg, \
                            fill=true, color='white')
    g += hyperbolic_arc(self.za, self.zc, color='grey')
    g += hyperbolic_arc(self.zc, self.zb, color='grey')
    g += hyperbolic_arc(self.zb, self.zcg, color='grey')
    g += hyperbolic_arc(self.zcg, self.za, color='grey')
    d = g.get_minmax_data()
    g.set_axes_range(d['xmin'], d['xmax'], 0, 2)
    return g
```

A sample output of this function can be seen in the figure C.1. Furthermore, we implement the algorithm to solve the word problem which we described in chapter 4, algorithm 2.

```
def word_problem(self,A,readable=false):
    ergread=[]
    erg = []
    T=self.T
    S=self.S
    Ti=self.Ti
    counter = 0
    while A[1,0] !=0 and counter < 50:
        counter += 1
        while abs(A[0,0].n()) >= abs(A[1,0].n()):
            if sgn(A[0,0]) == sgn(A[1,0]):
                ergread.append("T")
                erg.append(1)
                A=Ti*A
            else:
                ergread.append("Ti")
```

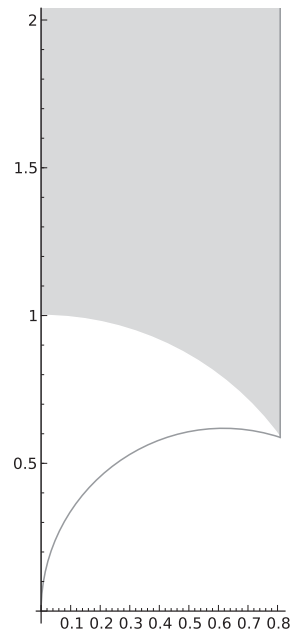


Figure C.1.: Fundamental domain for Δ_5

```

        erg.append(-1)
        A=T*A
        ergread.append("S")
        erg.append(0)
        A=S*A
    p = A[0,1]/A[0,0]/(self.T[0,1])
    if p < 0:
        for i in range(-p):
            ergread.append("Ti")
            erg.append(-1)
    else:
        for i in range(p):
            ergread.append("T")
            erg.append(1)
    if(readable):
        return ergread
    else:
        return erg

def expand_word(self, word):
    X = matrix(2,2,[1,0,0,1])
    for x in word:
        if x == 0 or x == 'S':
            X = X*self.S
        if x == 1 or x == 'T':
            X = X*self.T
        if x == -1 or x == 'Ti':
            X = X*self.Ti
    return X

```

The class `subgroup_of_triangle_group`

This class is initialized with two permutations σ_0 and σ_1 . To define a subgroup of the triangle group $\Delta(2, n, \infty)$, the order of σ_0 must be two and the order of σ_1 must equal n . Furthermore, the group $\langle \sigma_0, \sigma_1 \rangle$ generated by σ_0 and σ_1 must be transitive.

```
class subgroup_of_triangle_group:
    def __init__(self, _s0, _s1):
        if(not _s0 == _s0.inverse() ):
            print 'ERROR in __init__'
            print 'The first permutation (_s0 = %s) needs to be of order 2'
            print '\
              %_s0'
            raise AttributeError('s0 not of order 2')
            return None

        if(not PermutationGroup([_s0, _s1]).is_transitive() ):
            print 'ERROR in __init__'
            print 'The group generated by %s and %s is not a transitive'
            print 'group'\
              % (_s0, _s1)
            raise AttributeError('Group not transitive')
            return None

        self.s1 = PermutationGroupElement(_s1)
        self.s0 = PermutationGroupElement(_s0)
        self.sinf = (self.s1*self.s0).inverse()
        self.a = 2
        self.b = self.s1.order()
        self.c = self.sinf.order()
        self.T = triangle_group_2noo(self.b)
        self.d = max(self.s0.domain())
        if( max(self.s1.domain()) > self.d ):
            self.d = max(self.s1.domain())
```

The most important part is to be able to check, if a given matrix is a member of this subgroup. We use the algorithm 1 of chapter 4. We solve the word problem, map the letters to the corresponding permutations, and check if the resulting permutation leaves the 1 invariant.

```
def __contains__(self, M):
    word = self.T.word_problem(M)
    p = Permutation(range(1, 1+len(self.cosets)))
    pS = Permutation(self.s0)
    pT = (Permutation(self.s1).inverse())*pS
    pTi= pT.inverse()
    for l in word:
```

```

    if( l == 0 ):
        p = p*pS
    if( l == 1 ):
        p = p*pT
    if( l == -1 ):
        p = p*pTi
    return (p(1) == 1)

```

The class `gFareySymbol`

Now, we present a short overview of the implementation of the generalized Farey symbols. We store the actually Farey symbol in three different arrays. One is for the nominators of the fractions, one for the denominators, and one for the pairings. The free pairings are marked with increasing integer numbers. The even pairings with -1 and the n/d with $-d \cdot 10$. As we explained in the chapter about the generalized Farey symbols, we are not allowed canceling a common term of a fraction. Hence, it seems more reasonable to store numerator as well as the denominator separately.

We initialize the Farey symbol with a subgroup of a triangle group G . As explained in the chapter about Farey symbols, we start with the unfinished symbol

$$\frac{-1}{0} \frown \frac{0}{1} \frown \frac{1}{0}.$$

The actual construction is done in the function `init_pairings()`. After calculating the Farey symbol itself, we also calculate the properties we are interested in, like the coset representatives, the cusps, etc.

```

class gFareySymbol:
    def __init__(self,G):
        self.a = [SR(-1), SR(0), SR(1)]
        self.b = [SR( 0), SR(1), SR(0)]
        self.pairing = [0, 0]
        [ ... ]
        self.pairing_max = 0
        self.init_pairing()

        self.x = [self.a[i]/self.b[i] for i in range(1,len(self.a)-1)]
        [ ... ]
        self.cosets = self.init_cosets()
        self.cusp_classes = self.init_cusp_classes()
        self.cusps = self.init_cusps()
        [ ... ]
    def init_pairing(self):
        tmp = self.check_pair(1)
        if tmp == -1 or self.pairing[-1] == -10:
            self.add_term(1)
        i = self.find_max_unpaired()
        while i >= 0:

```

```

if self.check_pair(i) == -1:
    self.add_term(i)
i = self.find_max_unpaired()

```

The function `check_pair` checks, if it is possible to assign a pairing. If it is possible, it returns the possible pairing. In addition, if the pairing is a n/d -odd pairing, it also inserts the necessary points. The rest of this class is a straight foreword implementation of the algorithms described in chapter 6.

The class `Belyi`

Before we start with the explanation of the class `Belyi`, we present an auxiliary class which turns out to be useful.

```

class VariableGenerator(object):
    def __init__(self, prefix):
        self.__prefix = prefix
    @cached_method
    def __getitem__(self, key):
        return SR.var("%s%s"%(self.__prefix, key))

```

If we now define a variable using `x = VariableGenerator('x')`, we obtain a class which returns the variable `x3` if one calls `x[3]`. Since we sum over an a priori unknown number of variables, we use this class to generate the necessary variables. The idea comes from [Gro].

In the class `Belyi` we collect all the information about the Belyi function and the dessin. It is initialized using a (generalized) Farey symbol.

```

class Belyi(group):
    def __init__(self, group):
        self.group = group
        FareySymbol.__init__(self, group)
    def __repr__(self):
        if hasattr(self.group, "__repr__"):
            return "Belyi(%s)" % self.group.__repr__()
        elif hasattr(self.group, "__repr__"):
            return "Belyi(%s)" % self.group.__repr__()
        else:
            return "Belyi(?)"

```

We added functions to calculate the dessin from the permutations as well as the structure of the corresponding Belyi function.

```

def dessin(self):
    e2 = list(Set([w.real()+I*w.imag() for w in \
        [(SL2Z(1)/w).acton(I) for w in self.coset_reps()]])
    graph= Graph(multiedges=True);
    liste = []

```

```

for i in range(len(e2)):
    if( len(e2) == 0 ):
        break
    images = [p.acton(e2[0]) for p in self.pairing_matrices()]
    tmp = list(Set(images).intersection(Set(e2)))
    tmp.append(e2[0])
    tmp = list(Set(tmp))
    [e2.remove(r) for r in tmp]
    liste.append(tmp)
for c in self.coset_reps():
    p0=(SL2Z(1)/c).acton((1+I*sqrt(3))/2)
    p0=p0.real()+I*p0.imag()
    p1=(SL2Z(1)/c).acton(I)
    p1=p1.real()+I*p1.imag()
    i=0
    for x in liste:
        if( p1 in x ):
            break
        i=i+1
    graph.add_edge((p0,liste[i][0]))
return graph
def function(self):
    from sage.misc.flatten import flatten
    G=self.dessin()
    black = list(G.bipartite_sets()[1])
    white = list(G.bipartite_sets()[0])
    blackdegree = flatten([G.degree([x]) for x in black])
    whitedegree = flatten([G.degree([x]) for x in white])
    if( max(blackdegree) < 3 ):
        tmp = white
        white = black
        black=tmp
        tmp = whitedegree
        whitedegree = blackdegree
        blackdegree=tmp
    bd1 = blackdegree.count(1)
    bd3 = blackdegree.count(3)
    if( len(blackdegree) != bd1+bd3 ):
        print "Error in Belyi.function"
        return -1
    x = VariableGenerator('x')
    z = SR.var('z')
    cw=self.cusp_widths()
    term1 =[x[i]*z**i for i in range(bd3)]
    term1.append(z**bd3)
    term1 = sum(term1)**3
    term2 = [x[i]*z**(i-bd3) for i in range(bd3,bd3+bd1)]
    term2.append(z**bd1)
    term2 = sum(term2)
    term3 = [(z+x[i+bd3+bd1])**cw[i] for i in range(len(cw)-1)]
    tmp = 1
    for x in term3:

```

```
    tmp = tmp*x
    return term1*term2/tmp
```

Note that this method of finding the structure of the Belyi function is quite inefficient. There are better and faster methods by using directly the permutations. From the result for the method `function`, we extract the coefficients of the resulting rational function and obtain the algebraic equations we need.

The function `rational_function`

We end with the function `rational_function`. This function is called with a subgroup of finite index of a triangle group. It first constructs an instance of a class `Belyi`, calculates a starting value using the FEM method, and runs Newton's method. From the result we extract algebraic expressions.

```
def rational_function(group, steps=15, prec=256, verbose=0):
    # This calculates a numerical approximation for the rational function
    f = Belyi(group)
    if( verbose > 0 ):
        print 'Starting with FEM && Newton'

    # Use the starting vector from FEM with Newton
    coef = f.newton(get_start_vector(f), steps, prec, verbose)
    if( verbose > 0 ):
        print 'Newton Done!'
        print 'Starting algdep for %s coefficients' %ZZ(len(coef))

    z = SR.var('z')
    for c in range(len(coef)):
        if( verbose > 0 ):
            print 'Starting the %s th coefficient' %ZZ(c)
        try:
            coef[c] = algebraic_approximation(coef[c], prec=prec)
        except:
            print 'could not find an algebraic expression for %s\n' % coef
                [c]

    if new:
        bf = f.belyi_function()
        bf = bf[0]
    else:
        bf = f.function_with_coef()
    x = VariableGenerator('x')
    Dic = dict([x[i], coef[i]] for i in range(len(coef)))

    return bf.substitute(Dic)
```

The implementation of Newton's method is straight forward and well known. The function `special_values_of_hauptmodul`, which is the FEM part, is worth a closer look. This function generates the `FreeFem++` script, runs it, and evaluated the result.

We start with the *header* of the FreeFem++ file which is the construction of the triangle Th1 and Th2 from appendix B. All results are written into a file, whose name is dynamically generated by Sage.

```
def special_values_of_hauptmodul(f, n=25):
    # This function generates a file for FreeFem++ and evaluates it
    # The result is the values of the hauptmodul at the elliptic points of
    # the Farey-Symbol f - the first parameter. The second parameter
    # controls the number of triangles used in FreeFem++

    header = """
verbosity = 0;

real h = %s;
int n = %s;

border L1(t=1.0,0.0) {
    x = 0.0;
    y = t;
    label = 1;
}
[ ... ]
border Top(t=0.5,0.0) {
    x = t;
    y = h;
    label = 7;
}

mesh Th1 = buildmesh(L1(n)+bow(n)+topbow(n/2), fixeborder=true);
mesh Th2 = buildmesh(L2(n)+topbowinv(n/2)+R(n)+Top(n), fixeborder=true);
"""

    # The file 'fem_filename' will be given to FreeFem++
    try:
        fem_filename = tmp_filename('group', '.edp')
        print "generating FreeFem++ file ", fem_filename
        fem = open(fem_filename, 'w')
    except IOError:
        print 'Cannot create a file called "group.edp" here.'
        print 'Stopping now.'
        return

    # In the first line you read the name of the group
    fem.write('//File for ' + str(f).replace('\n', '\n//') + '\n')

    # real h is the height of the fundamental domain
    # It is chosen as 3*cusp_width(oo)
    # n it the number of points on the border of the standard triangle

    fem.write(header%(RR(f.cusp_widths() [-1]*3.), ZZ(n)))
```

In the next part, we run over the cosets and map them according to algorithm 4. In this loop, we also rename the edges of the triangles.

```

cc = 0 # cosetcounter
for c in f.coset_reps():
    # BEGIN: Build the mesh
    # Has the first triangle infty as a vertex?
    if( c.a() == 0 ):
        tmp = (SL2Z(1)/c).acton(1/conjugate(z))
        fem.write('mesh T1c%s = movemesh(Th2,%cc)
        fem.write(str([tmp.real().factor(),tmp.imag().factor()])+');\n
        ')
        lab1 = 4
    else:
        [ ... ]

```

Then, we generate the mesh, insert the pairing functions, and solve the Laplace equations for real and imaginary part.

```

# Generate the mesh for FEM
fem.write('\n\nmesh T =')
tmp = '';
for j in range(cc):
    tmp+=' T1c%s + T2c%s +'%(j, j)
fem.write(tmp[0:-1])
fem.write('; \n\n')
# fem.write('; \n\nplot(T); \n\n\n')

# BEGIN: Construct pairing for periodic boundary conditions
# Assumption: The left and the right border are identified.
pairtext = 'func pairing = [[10,y],[%s,y],\n['%(10+len(frac)+f.nu2()+f
.nu3())
i=1
ellpt = 0
# insert the pairing function
for p in pairs[1:-1]:
    if( -3 == p ): # odd pairing
        [ ... ]
    if( -2 == p ): # even pairing
        [ ... ]
    if ( 0 < p ): #free pairing
        if( i != pairs.index(p) ):
            pairtext += '%s,x],['%(10 + pairs.index(p)+ellpt)
            tmp = f.pairing_matrices()[i].acton(z)
            tmp = tmp.real().factor();
            pairtext += '%s,%s],\n['%(i+10+ellpt,tmp)
        i+=1
fem.write(pairtext[0:-3]+'']; \n\n\n')
# END: Construct pairing for periodic boundary conditions

# Generate FEM-Space

```

```

fem.write(' fespace Vh(T,P2,periodic=pairing);\nVh phi, psi, w;\n\n')

# Solve for the real part
fem.write(' solve LaplaceRe(phi,w, solver=LU) = \n')
fem.write('      int2d(T) (dx(phi)*dx(w)+dy(phi)*dy(w))+on(7,phi= cos(2.*
      pi*x/'))
fem.write(str(float(f.cusp_widths() [-1])))
fem.write(')*exp(2.*pi*h/%s));\n\n'%RR(f.cusp_widths() [-1]))
[ ... ]

```

Then, we tell FreeFem++ to evaluate the result at the elliptic points.

```

# SUBBEGIN: Find identifications of e2 => Result in 'liste'
[ ... ]
# SUBEND: Find identifications of e2

# all elliptic points of order 2
e2 = [w.real()+I*w.imag() for w in \
      [(SL2Z(1)/w).acton(I) for w in f.coset_reps()]]
# dict of the identifications
Dic=dict([x[0],x[1]] for x in liste if len(x) ==2)
tmp = [e.substitute(Dic) for e in e2]
# e21: elliptic points on the boundary appear only once.
e21 = [x for x in tmp if tmp.count(x) == 1]
# e22: elliptic point in the middle appear exacty twice.
e22 = [x for x in tmp if tmp.count(x) == 2]
e22 = list(Set(e22))
# all elliptic points of order 3
[ ... ]
fem_outfile = tmp_filename('fem_results', '.sage')
fem.write('ofstream out("%s");\n' % fem_outfile)

# ell pt of order 2 on border
fem.write(' out << "w21 = [";\n')
for e in e21:
    fem.write(' out << "CC(" << phi(%s,%s) << ", " << psi(%s,%s)<<"
    ,";\n'\
                %(RR(e.real()),RR(e.imag()),RR(e.real()),RR(e.imag())
                )))
fem.write(' out << "]" << endl;\n\n')
[ ... ]

```

Finally, we run FreeFem++ and get the values at the critical points

```

# Let FreeFem run and grab the result!
os.system('FreeFem++-cli -nw %s > /dev/null' % fem_filename)
load(fem_outfile)

return [[w33,w31],[w22,w21],[wc]]

```

With the help of this function, we are able to get good starting values for Newton's method. To obtain these, we calculate approximations of the coefficients of the polyno-

mial we are interested in from the zeros and singularizes. This is done in the following function.

```
def get_start_vector(f):
    # This function produces a starting vector for the Newton-Algorithm
    [[w33,w31],[w22,w21],[wc]] = special_values_of_hauptmodul(f)
    x = SR.var('x')

    # append w33
    tmp = prod([(x-w) for w in w33])
    result = [t[0] for t in tmp.coefficients(x)][0:-1]

    # append w31
    for w in w31:
        result.append(-w)

    # append w22
    tmp = prod([(x-w) for w in w22])
    tmp = [t[0] for t in tmp.coefficients(x)][0:-1]
    result.append(tmp)
    result = flatten(result)

    # append w21
    for w in w21:
        result.append(-w)

    # append wc
    for w in wc:
        result.append(-w)

    return result
```

Combining all of these, we are able to produce the results form chapter 9.

Bibliography

- [Ahl53] Lars V. Ahlfors. *Complex analysis*. McGraw-Hill book company, Inc., 1953.
- [Apo90] Tom M. Apostol. *Modular Functions and Dirichlet Series in Number Theory*. Graduate Texts in Mathematics. Springer-Verlag, 1990.
- [ASD71] Arthur O. L. Atkin and H. Peter F. Swinnerton-Dyer. Modular forms on non-congruence subgroups. In *Combinatorics*, pages 1 – 25, University of California Los Angeles California 1968, 1971. American Mathematical Society,. Providence, R.I.
- [Bea95] Alan F. Beardon. *The Geometry of Discrete Groups (Graduate Texts in Mathematics)*. Springer, 1st ed. 1983. corr., 2nd printing 1995 edition, 1995.
- [Bel79] Gennadii V. Belyi. On Galois Extensions of a Maximal Cyclotomic Field. *Izvestiya Akademii Nauk SSSR. Seriya Matematicheskaya*, 43(2):267 – 276, 1979.
- [Bel02] Gennadii V. Belyi. Another proof of the three points theorem . *Matematicheskii Sobornik*, 193(3):21 – 24, 2002.
- [Ber94] Gabriel Berger. Hecke operators on noncongruence subgroups. *Comptes Rendus de l Académie des Sciences - Series I*, 319:915 – 919, 1994.
- [Bor92] Richard E. Borcherds. Monstrous moonshine and monstrous Lie superalgebras. *Inventiones mathematicae*, 109(1):405 – 444, Dec 1992.
- [Bru07] Lieven Le Bruyn. Blog entry: The best rejected proposal ever. Neverendingbooks.org, March 2007. [Accessed: 20th March 2015].
- [Car54] Constantin Carathéodory. *Theory of functions of a complex variable*. Chelsea Publishing Company, 1954.
- [Car09] Constantin C. Caranica. *Algorithms related to subgroups of the modular group*. PhD thesis, Louisiana State University, August 2009.
- [CDH12] Miranda C. N. Cheng, John F. R. Duncan, and Jeffrey A. Harvey. Umbral moonshine. <http://arxiv.org/abs/1204.2779>, April 2012.
- [CN79] John H. Conway and Simon P. Norton. Monstrous Moonshine. *Bulletin of the London Mathematical Society*, 11(3):308 – 339, Oct 1979.

- [Coh93] Henri Cohen. *A Course in Computational Algebraic Number Theory*. Graduate Texts in Mathematics. Springer, 1993.
- [CY95] Imin Chen and Noriko Yui. Singular values of Thompson Series. In *Groups, difference sets, and the Monster*, 1995.
- [DGMS13] Charles F. Doran, Terry Gannon, Hossein Movasati, and Khosro M. Shokri. Automorphic forms for triangle groups. *Communications in Number Theory and Physics*, 7(4):689 – 737, 2013.
- [DGO15] John F. R. Duncan, Michael J. Griffin, and Ken Ono. Proof of the umbral moonshine conjecture. <http://arxiv.org/abs/1503.01472>, March 2015.
- [DT02] Tobin A. Driscoll and Lloyd N. Trefethen. *Schwarz-Christoffel Mapping (Cambridge Monographs on Applied and Computational Mathematics)*. Cambridge University Press, 2002.
- [EOT11] Tohru Eguchi, Hiroshi Ooguri, and Yuji Tachikawa. Notes on the K3 Surface and the Mathieu Group M 24. *Experimental Mathematics*, 20(1):91 – 96, Mar 2011.
- [Euc08] Euclid. *The thirteen books of Euclid's Elements*. Cambridge University Press, 1908. Translated by Thomas Heath.
- [FB] Diego Floor and Winfried Boxleitner. Freefem++ - curved periodic boundary conditions. <http://www.um.es/freefem/ff++/pmwiki.php?n=Main.CurvedPeriodicBoundaryConditions>.
- [FHL⁺10] Liqun Fang, J. William Hoffman, Benjamin Linowitz, Andrew Rupinski, and Helena Verrill. Modular Forms on noncongruence subgroups and Atkin-Swinnerton-Dyer relations. *Journal of Experimental Mathematics*, 19(1):1 – 27, 2010.
- [FK80] Hershel M. Farkas and Irwin Kra. *Riemann Surfaces (Graduate Texts in Mathematics, Vol. 71)*. Springer-Verlag, 1980.
- [FMN94] David Ford, John McKay, and Simon Norton. More on replicable functions. *Communications in Algebra*, 22(13):5175 – 5193, 1994.
- [For51] Lester R. Ford. *Automorphic Functions*. Chelsea, New York, 1951.
- [For77] Otto Forster. *Riemannsche Flächen (Heidelberger Taschenbücher) (German Edition)*. Springer, 1977.
- [Fra24] Jérôme Franel. Les suites de Farey et le théorème des nombres premiers. *Nachrichten von der Königlichen Gesellschaft der Wissenschaften und der Georg-Augusts-Universität zu Göttingen*, pages 198 – 201, 1924.

- [Gan66] David Gans. A new model of the hyperbolic plane. *American Mathematical Monthly*, 73, 1966.
- [GAP] Gap - groups, algorithms, programming - a system for computational discrete algebra. <http://www.gap-system.org/>. [Accessed: 20th March 2015].
- [GGD12] Ernesto Gironde and Gabino González-Diez. *Introduction to Compact Riemann Surfaces and Dessins d'Enfants (London Mathematical Society Student Texts)*. Cambridge University Press, 2012.
- [GMP] The GNU Multiple Precision Arithmetic Library. <https://gmplib.org/>. [Accessed: 20th March 2015].
- [Goi] Edray H. Goins. Dessins d'Enfants in the Plane. Wolfram Demonstrations Project: <http://demonstrations.wolfram.com/preview.html?draft/26744/000017/DessinsDEnfantsInThePlane>. [Accessed: 20th March 2015].
- [Gro] Jason Grout. Variable generator. Will be included in an future version of Sage: <http://trac.sagemath.org/ticket/11576>. [Accessed: 20th March 2015].
- [Gro97] Alexander Grothendieck. Esquisse d'un Programme. In *Geometric Galois Actions*, volume 242, 1997.
- [Ham56] William R. Hamilton. Letter to John T. Graves "On the Icosian". In *Mathematical papers, Vol. III, Algebra*, 1856.
- [Hat01] Allen Hatcher. *Algebraic Topology*. Cambridge University Press, 2001.
- [HC64] Adolf Hurwitz and R. Courant. *Allgemeine Funktionen und elliptische Funktionen*. Springer, 1964.
- [Hec36] Erich Hecke. Über die Bestimmung Dirichletscher Reihen durch ihre Funktionalgleichung. *Mathematische Annalen*, 112:664 – 699, 1936.
- [Hec37] Erich Hecke. Über Modulfunktionen und die Dirichlet Reihen mit Eulerscher Produktentwicklung. *Mathematische Annalen*, 114:316 – 351, 1937.
- [Hec12] Frédéric Hecht. New development in FreeFem++. *Journal of Numerical Mathematics*, 20(3 – 4):251 – 265, 2012.
- [Hej92] Dennis A. Hejhal. *Eigenvalues of the Laplacian for Hecke triangle groups*. Number Nr. 469 in Memoirs of the American Mathematical Society. American Mathematical Society, 1992.

- [Hej99] Dennis A. Hejhal. On the Eigenfunctions for Hecke triangle groups. In D. Hejhal, J. Friedman, M. Gutzwiller, and A. Odlyzko, editors, *Emerging Applications fo Number Theory*, number 109 in IMA Series, pages 291 – 315. Springer, 1999.
- [Hej04] Dennis A. Hejhal. On the Calculation of Maass Cusp Forms. In *Proceedings of the “International School on Mathematical Aspects of Quantum Chaos II”*, Lecture Notes in Physics. Springer-Verlag, 2004.
- [Hsu96] Tim Hsu. Identifying congruence subgroups of the modular group. *Proceedings of the American Mathematical Society*, 124(5):1351 – 1359, 1996.
- [Jer13] Jonas Jermann. *Modular functions and integrals for Hecke Triangle Groups*. PhD thesis, ETH Zürich, 2013.
- [Jos97] Jürgen Jost. *Compact Riemann Surfaces: An Introduction to Contemporary Mathematics (Universitext)*. Springer, 1997.
- [Kat92] Svetlana Katok. *Fuchsian Groups (Chicago Lectures in Mathematics)*. University Of Chicago Press, 1. edition, 1992.
- [Kil80] Wilhelm Killing. Die Rechnung in Nicht-Euclidischen Raumformen. *Journal für die reine und angewandte Mathematik*, 89:265 – 287, 1880.
- [KL08] Chris A. Kurth and Ling Long. Computations with finite index subgroups of $\mathrm{PSL}_2(\mathbb{Z})$ using Farey Symbols. In *Advances in algebra and combinatorics, Proceedings of the second International Congress in Algebra and Combinatorics, World Scientific*, pages 225 – 242, 2008.
- [Kle79] Felix Klein. Über die Transformation elfter Ordnung der elliptischen Functionen. *Mathematische Annalen*, 15(3 – 4):533 – 555, Sep 1879.
- [Kle84] Felix Klein. *Vorlesungen über das Ikosaeder und die Auflösung der Gleichungen vom 5ten Grade*. Teubner, 1884.
- [KMSV14] Michael Klug, Michael Musty, Sam Schiavone, and John Voight. Numerical calculation of three-point branched covers of the projective line. *LMS Journal of Computation and Mathematics*, 17:379 – 430, 1 2014.
- [Kol95] János Kollár. *Shafarevich maps and automorphic forms*. Princeton University Press, 1995.
- [Kul91] Ravi S. Kulkarni. An arithmetic geometric method in the study of the subgroups of the modular group. *American Journal of Mathematics*, 113(6):1053 – 1133, 1991.
- [Kur09] Chris A. Kurth. *Modular forms and modular symbols for noncongruence groups*. PhD thesis, Iowa State University, 2009.

- [KV03] David Kohel and Helena Verrill. Fundamental Domains for Shimura Curves. *Journal de Théorie des Nombres de Bordeaux*, 15:205 – 222, 2003.
- [Lan24] Edmund Landau. Bemerkungen zu der vorstehenden Abhandlung von Herrn Frel. *Nachrichten von der Königlichen Gesellschaft der Wissenschaften und der Georg-Augusts-Universität zu Göttingen*, pages 202 – 206, 1924.
- [Leo08] John Garrett Leo. *Fourier Coefficients of Triangle Functions*. PhD thesis, University of California, 2008.
- [LLT95a] Mong-Lung Lang, Chong-Hai Lim, and Ser-Peow Tan. An algorithm for determining if a subgroup of the modular group is congruence. *Journal of the London Mathematical Society*, 51 (3):491 – 502, 1995.
- [LLT95b] Mong-Lung Lang, Chong-Hai Lim, and Ser-Peow Tan. Independent generators for congruence subgroups of Hecke groups. *Mathematische Zeitschrift*, 220 (4):569 – 594, 1995.
- [LLY05a] Wen-Ching Winni Li, Ling Long, and Zifeng Yang. Modular forms for non-congruence subgroups. *Quarterly Journal of Pure and Applied Mathematics*, 1(1):205 – 221, 2005.
- [LLY05b] Wen-Ching Winni Li, Ling Long, and Zifeng Yang. On Atkin-Swinnerton-Dyer congruence relations. *Journal of Number Theory*, 113(1):117 – 148, 2005.
- [Lon08] Ling Long. On Atkin-Swinnerton-Dyer congruence relations 3. *Journal of Number Theory*, 128(8):2413 – 2429, 2008.
- [LZ04] Sergei K. Lando and Alexander K. Zvonkin. *Graphs on surfaces and Their Applications*. Springer, 2004.
- [MAG] Magma computational algebra system. <http://magma.maths.usyd.edu.au/>. [Accessed: 20th March 2015].
- [Mag74] Wilhelm Magnus. *Noneuclidean Tessellations and Their Groups (Pure and Applied Mathematics, Volume 61)*. Academic Press, 1974.
- [Mag93] Kay Magaard. Monodromy and sporadic groups. *Communications in Algebra*, 21(12):4271 – 4297, Jan 1993.
- [Mai09] Robert S. Maier. On rationally parametrized modular equations. *Journal of the Ramanujan Mathematical Society*, 24:1 – 73, 2009.
- [Mas04] Bernard Maskit. *Kleinian Groups (Grundlehren der mathematischen Wissenschaften) (v. 287)*. Springer, 1988 edition, 3 2004.
- [Mil69a] M. H. Millington. On Cycloidal subgroups of the modular group. *Proceedings of the London Mathematical Society*, 19(3):164 – 176, 1969.

- [Mil69b] M. H. Millington. Subgroups of the classical modular group. *Journal of the London Mathematical Society*, 1(2):351 – 357, 1969.
- [Miy06] Toshitsune Miyake. *Modular Forms (Springer Monographs in Mathematics)*. Springer, 2006.
- [Mon11] Hartmut Monien. Farey symbol for arithmetic subgroups. sagemath.org, 2011. [Accessed: 20th March 2015].
- [MZ00] Nicolas Magot and Alexander Zvonkin. Belyi functions for Archimedean Solids. *Discrete Mathematics*, 217:249 – 271, 2000.
- [Neh52] Zeev Nehari. *Conformal mapping*. McGraw-Hill Book Company, Inc., 1952.
- [PTVF02] William H. Press, Saul A. Teukolsky, William T. Vetterling, and Brian P. Flannery. *Numerical Recipes in C++: The Art of Scientific Computing*. Cambridge University Press, February 2002.
- [Ral62] J. Raleigh. On the Fourier coefficients of triangle functions. *Acta Arithmetica*, 8(1):107 – 111, 1962.
- [Rat05] John G. Ratcliffe. *Foundations of Hyperbolic Manifolds*. Springer, 2005.
- [SAG] Sage. <http://www.sagemath.org/>. [Accessed: 20th March 2015].
- [Sch94] Leila Schneps. Dessins d’enfants on the Riemann sphere. In Cambridge University Press, editor, *The Grothendieck Theory of Dessins d’Enfants*. London Mathematical Society Lecture Notes 200, 1994.
- [Shi71] Goro Shimura. *Introduction to the Arithmetic Theory of Automorphic Functions*. Princeton University Press, 1971.
- [Spr57] George Springer. *Introduction to Riemann surfaces*. Addison-Wesley Publishing Company, Inc., 1957.
- [SS02] Björn Selander and Andreas Strömbergsson. Sextic coverings of genus two which are branched at three points. <http://www2.math.uu.se/research/pub/Selander1.pdf> [Accessed: 20th March 2015], 2002.
- [Ste07] W. Stein. *Modular forms, a computational approach*. Graduate studies in mathematics. American Mathematical Society, 2007.
- [Ste12] William Stein. Sage for Power Users. <http://wstein.org/books/sagebook/sagebook.pdf>, February 2012. [Accessed: 20th March 2015].
- [Str02] Fredrik Strömberg. *Computational Aspects of Maass waveforms*. PhD thesis, Department of Mathematics, Uppsala University., 2002.

- [SV14] Jeroen Sijsling and John Voight. On computing Belyi maps. *Publications Mathématiques de Besançon*, 1:73 – 131, November 2014. accepted to Publ. Math. Besançon.
- [SZ94] George Shabat and Alexander Zvonkin. Plane trees and algebraic numbers. *Contemporary Mathematics*, 178:233 – 275, 1994.
- [Ver] Helena Verrill. Fundamental domain drawer. <https://www.math.lsu.edu/~verrill/fundomain/>. [Accessed: 20th March 2015].
- [vHV12] Mark van Hoeij and Raimundas Vidunas. Belyi functions for hyperbolic hypergeometric-to-Heun transformations. *Physical Review Letters*, 111:107802, December 2012.
- [Wan94] James Z. Wang. Analytic number theory, complex variable, and supercomputers. Master’s thesis, University of Minnesota, August 1994.
- [Wol01] Jürgen Wolfart. Kinderzeichnungen und Uniformisierungstheorie. www.math.uni-frankfurt.de/~wolfart/Artikel/kizei.pdf, March 2001. [Accessed: 20th March 2015].
- [Wol06] Jürgen Wolfart. ABC for polynomials, dessins d’enfants, and uniformization - a survey. *Proceedings der ELAZ-Konferenz 2004*, pages 313 – 345, 2006.
- [WR14] Inc. Wolfram Research. Mathematica, version 10.0, 2014.
- [WWT⁺] Robert Wilson, Peter Walsh, Jonathan Tripp, Ibrahim Suleiman, Richard Parker, Simon Norton, Simon Nickerson, Steve Linton, John Bray, and Rachel Abbott. Atlas of finite group representations. <http://brauer.maths.qmul.ac.uk/Atlas/v3/>. [Accessed: 20th March 2015].
- [Zag08] Don Zagier. Elliptic modular forms and their applications. In *The 1-2-3 of Modular Forms: Lectures at a Summer School in Nordfjordeid, Norway*. Springer, 2008.
- [Zvo08] Alexander Zvonkin. Belyi functions: examples, properties, and applications. *Applications of Group Theory to Combinatorics*, pages 161 – 180, 2008.

List of Figures

| | | |
|-------|-------------------------------------------------------------------|----|
| 2.1. | “Parallel” lines in hyperbolic geometry | 6 |
| 2.2. | A hyperbolic 6-sided polygon | 8 |
| 2.3. | A hyperbolic triangle | 9 |
| 2.4. | Fundamental domain of a D_4 | 14 |
| 2.5. | Tessellation of the square | 14 |
| 2.6. | The Dedekind tessellation | 14 |
| 4.1. | Reflection of a hyperbolic triangle | 30 |
| 4.2. | Rotation of a hyperbolic triangle | 31 |
| 4.3. | The Euclidian triangle group $\Delta(2, 2)$ | 32 |
| 4.4. | The Euclidian triangle group $\Delta(2, 3, 6)$ | 32 |
| 4.5. | The Euclidian triangle group $\Delta(2, 4, 4)$ | 32 |
| 4.6. | The Euclidian triangle group $\Delta(3, 3, 3)$ | 32 |
| 4.7. | The spherical triangle group $\Delta(2, 2, 6)$ | 32 |
| 4.8. | The spherical triangle group $\Delta(2, 3, 4)$ | 32 |
| 4.9. | Hyperbolic triangle with given angles | 33 |
| 5.1. | Dessin d’enfant for z^7 | 45 |
| 5.2. | Dessin d’enfant for a Chebyshev polynomial | 45 |
| 5.3. | Dessin d’enfant of the tetrahedron | 45 |
| 5.4. | Dessin d’enfant of the cube | 45 |
| 5.5. | Dessin d’enfant for the dodecahedron | 45 |
| 5.6. | Dessin d’enfant with label | 46 |
| 5.7. | A fundamental domain for $\Gamma_0(6)$ | 50 |
| 5.8. | A fundamental domain with marked points | 50 |
| 5.9. | The dessin without identification | 50 |
| 5.10. | The dessin for the Belyĭ function of $\Gamma_0(6)$ | 50 |
| 6.1. | Examples of even and odd vertices | 54 |
| 6.2. | Examples of even, odd, and f edges | 54 |
| 6.3. | Example of a 4-special polygon. | 55 |
| 6.4. | A 2-odd pairing | 60 |
| 6.5. | Geometric interpretation of the insertion operators | 64 |
| 6.6. | Example of fanning out | 68 |
| 6.7. | The special polygon for the example discussed in detail | 70 |
| 7.1. | Mapping property of the hauptmodul | 80 |

| | | |
|-------|----------------------------------------------------------------------------|-----|
| 7.2. | Fundamental domain and image of the hauptmodul for $\Gamma_0(2)$ | 82 |
| 7.3. | The fundamental domain | 83 |
| 7.4. | The corresponding dessin | 83 |
| 7.5. | Fundamental domain and image of the hauptmodul for an index 7 subgroup | 84 |
| 8.1. | The triangle \mathcal{T}_0 | 90 |
| 8.2. | The triangle \mathcal{T}_2 | 90 |
| 8.3. | A triangulation of \mathcal{T}_0 | 91 |
| 8.4. | A triangulation of \mathcal{T}_2 | 91 |
| 8.5. | A fundamental domain | 92 |
| 8.6. | The corresponding triangulation | 92 |
| 8.7. | Detail of the fundamental domain and the triangulation | 93 |
| 8.8. | The real part of the solution | 94 |
| 8.9. | The imaginary part of the solution | 94 |
| 9.1. | A fundamental domain of Hsu's Example of index 10 | 98 |
| 9.2. | A fundamental domain of Hsu's Example of index 18 | 100 |
| 9.3. | A fundamental domain for M_{12} | 102 |
| 9.4. | A fundamental domain for M_{11} | 103 |
| 10.1. | Fundamental domain for the Janko group J_2 | 106 |
| A.1. | Sample output for a dessin in Mathematica | 110 |
| B.1. | FreeFem++ plot of triangle Th1 | 114 |
| B.2. | FreeFem++ plot of triangle Th2 | 114 |
| B.3. | FreeFem++ plot of a mapped triangle | 115 |
| C.1. | Fundamental domain for Δ_5 | 121 |

List of Symbols

| | |
|------------------------------|----------------------------------------------------------------------------------|
| \bar{A} | The closure of the topological space A , page 4 |
| \mathring{A} | The interior of the topological space A , page 4 |
| ∂A | The boundary of the topological space A , page 4 |
| $A(\Delta)$ | The set of all meromorphic, automorphic forms, page 23 |
| $A_k(\Delta)$ | The set of meromorphic, automorphic forms of a Fuchsian group Δ , page 22 |
| $\beta_{\underline{\sigma}}$ | A G -pairing of the permutation tuple $\underline{\sigma}$, page 38 |
| \mathbb{C} | The complex numbers, page 3 |
| δ_a | The rotation δ_a , page 36 |
| δ_b | The rotation δ_b , page 36 |
| δ_c | The rotation δ_c , page 36 |
| Δ | A generic Fuchsian group, page 11 |
| $\Delta(a, b)$ | The triangle group $\Delta(a, b, \infty)$, page 29 |
| $\Delta(a, b, c)$ | The triangle group of order a, b , and c , page 29 |
| Δ_n | The Hecke group $\Delta_n = \Delta(2, n, \infty)$, page 29 |
| Δ_p | The stabiliser of a point $p \in \overline{\mathbb{H}}$ in Δ , page 24 |
| $\Delta^*(a, b)$ | The extended triangle group, page 30 |
| $\Delta^*(a, b, c)$ | The extended triangle group, page 30 |
| Δ_n^* | The extended Hecke group $\Delta_n^* = \Delta^*(2, n, \infty)$, page 30 |
| $\det(A)$ | The determinate of the matrix A , page 3 |
| $E_{(x_i, x_j)}$ | The even pairing matrix, page 62 |
| $E_k(z)$ | The Eisenstein series of weight k , page 25 |
| $\mathbb{E}_k(z)$ | Eisenstein series of weight k , page 25 |

| | |
|--------------------------------------|-------------------------------------------------------------------------------------------------------------------------------------------------|
| η | The branching point for the Hecke groups, page 78 |
| η | The value of the hauptmodul of a triangle group at the elliptic point i , page 78 |
| $F_{(x_i, x_{i+1}, x_j, x_{j+1})}$ | Free pairing matrix, page 63 |
| $f _k \gamma$ | The slash operator, page 22 |
| \mathfrak{F} | The fundamental domain of a group operation, page 13 |
| $G(\Delta)$ | The set of all automorphic forms, page 23 |
| $G_k(\Delta)$ | The set of automorphic forms of weight k of a Fuchsian group Δ , page 22 |
| $GL_n(R)$ | The general linear group - the group of all invertible $n \times n$ - matrices, page 3 |
| $GL_2^+(\mathbb{R})$ | The group of invertible matrices over \mathbb{R} with positive determinant, page 22 |
| $g(x_i, x_j)$ | The function $g(x_i, x_j) = g\left(\frac{a_i}{b_i}, \frac{a_j}{b_j}\right) := a_i b_j - a_j b_i $, page 56 |
| \mathbb{H} | The upper half plane, page 6 |
| $\bar{\mathbb{H}}$ | The closed upper half plane, page 6 |
| $\mathbb{H}_\Delta^* = \mathbb{H}^*$ | The extended upper half plane for a Fuchsian group Δ with cusps P_Δ $\mathbb{H}_\Delta^* = \mathbb{H} \cup P_\Delta$, page 16 |
| $j_\Delta = j$ | The hauptmodul for a Fuchsian group Δ of genus zero, page 26 |
| $K(X(\Delta))$ | The function field of the Riemann surface $X(\Delta)$, page 24 |
| $\Lambda_{(x_i, x_j)}$ | The standard map, page 61 |
| $M_n(R)$ | The set of all $n \times n$ matrices with entries in the ring R , page 3 |
| $O_{(x_i, x_{i+1})}^{(d)}$ | Odd pairing matrix, page 62 |
| P_Δ | The set of all cusps of a Fuchsian group Δ , page 15 |
| π_Δ | The projection from $\mathbb{H}^* \rightarrow X(\Delta)$, page 16 |
| $\pi_1(X, x_0)$ | The fundamental group of X with base point x_0 , page 19 |
| $\mathbb{P}^n(k)$ | Projective, n -dimensional space over the field k , page 3 |
| $PSL_n(R)$ | The projective, special linear group, page 3 |
| $PSL_2^*(\mathbb{R})$ | The extended group of Möbius transformations, page 9 |
| \mathbb{Q} | The rational numbers, page 3 |

| | |
|-----------------------|------------------------------------------------------------------------------------------------------------------------------------------------------------------------|
| $q = q_w$ | The expansion parameter $q = q_w = \exp(2\pi i\tau/w)$, page 24 |
| \mathbb{R} | The real numbers, page 3 |
| $R_{a,b}$ | The matrix $R_{a,b}$, page 37 |
| $\mathbb{R}_{\geq 0}$ | Non-negative, real numbers, page 3 |
| R_Γ | The rational covering $R_\Gamma: \mathbb{P}^1(\mathbb{C}) \rightarrow \mathbb{P}^1(\mathbb{C})$, page 27 |
| $\rho_{a,b}$ | An alternative name for the edge $z_b = \csc \frac{\pi}{a} \left(\cos \frac{\pi}{a} + e^{i\frac{\pi}{b}} \right)$ of the hyperbolic triangle, page 37 |
| S_a | The matrix S_a , page 37 |
| $\mathcal{S}(f)(z)$ | The Schwarzian derivative of f with respect to z , page 73 |
| $S(\Delta)$ | The set of all cusp forms, page 23 |
| $S_k(\Delta)$ | The set of cusp forms of weight k of a Fuchsian group, page 23 |
| $SL_n(R)$ | The special linear group - of group of all $n \times n$ -matrices with determinate one, page 3 |
| \mathfrak{S}_n | The symmetric group on n letters, page 4 |
| $T_{a,b}$ | The matrix $T_{a,b}$, page 37 |
| τ_a | The reflection τ_a , page 35 |
| τ_b | The reflection τ_b , page 35 |
| τ_c | The reflection τ_c , page 35 |
| $\text{tr}(A)$ | The trace of the matrix A , page 3 |
| $X(\Delta)$ | Compactified Riemann surface associated to the Fuchsian group Δ , page 16 |
| $Y(\Delta)$ | Uncompactified Riemann surface associated to Δ , page 15 |
| \mathbb{Z} | The integer numbers, page 3 |
| z_a | The edge $z_a = i$ of a hyperbolic triangle, page 35 |
| z_b | The edge $z_b = \cot \frac{\pi}{a} + \cos \frac{\pi}{b} \csc \frac{\pi}{a} + i \left(\csc \frac{\pi}{a} \sin \frac{\pi}{b} \right)$ of a hyperbolic triangle, page 35 |
| z_c | The edge $z_c = i\infty$ of a hyperbolic triangle, page 35 |

Index

- (2, n)-special polygon, 53
- n/d -odd pairing, 60
- f -edge, 52

- Accessory parameter, 76
- Automorphic forms, 22
- Automorphic forms of weight k , 22
- Automorphic, meromorphic forms, 22
- Automorphisms of the upper half plane, 10

- Belyĭ's theorem, 44
- Belyĭ function
 - Definition, 43

- Complete geodesic, 7
- Complete Farey sequence, 56
- Conformal mappings, 75
- Cosine rules of hyperbolic geometry, 8
- Covering
 - Definition, 17
 - operation of the fundamental group, 19
- Cusp, 12, 16
- Cusp forms of weight k , 23
- Cusp width, 24

- Dessin d'enfants
 - Computation of corresponding Belyĭ function, 47
 - Definition, 44
 - Description as permutations, 46
 - Examples, 44
- Dimension formulas for automorphic forms, 26

- Eisenstein series, 25

- Elliptic element of $\mathrm{PSL}_2(\mathbb{R})$, 12
- Elliptic point
 - on \mathbb{H} , 12
 - on $X(\Delta)$, 16
- Even edge, 52
- Even pairing, 60
- Even pairing matrix, 62
- Even vertex, 52
- Extended group of Möbius transformations, 9

- Farey sequence
 - Support of a hole, 57
- Farey sequence, 56
 - Hole in the sequence, 56
 - Length of a hole, 56
- Farey symbol
 - Definition, 61
- Farey symbols
 - Pairings, 59
- Fourier expansion of an automorphic form, 24
- Free pairing, 60
- Free pairing matrix, 63
- Fuchsian group, 11
 - Examples, 11
 - of the first kind, 16
 - of the second kind, 16
- Function field, 24
- Fundamental domain, 13
 - Example: D_4 operates on square, 14
 - Example: Modular group operates on upper half plane, 14
- Fundamental group
 - Definition, 19
 - of a Riemann surface, 19

- operation on the fiber of a covering, 19
- G-pairing, 38
- Genus of a Fuchsian group, 16
- Geodesic, 7
 - Description on the upper half plane, 7
- Hauptmodul, 26
- Hecke group
 - Definition, 29
 - Generators, 38
- Hole in a Farey sequence, 56
- Homotopy, 19
- Hyperbolic element of $\mathrm{PSL}_2(\mathbb{R})$, 12
- Hyperbolic point
 - on \mathbb{H} , 12
- Hyperbolic polygon, 7
- Hyperbolic triangle with given angles, 35
- Hyperbolic trigonometry, 7
- Isometries of the upper half plane, 10
- Klein's j -invariant, 25
- Length of a hole, 56
- Möbius transformation, 9
- Monodromy, 20
- Monodromy representation, 40
 - Membership test, 41
- Odd edge, 52
- Odd pairing, 60
- Odd pairing matrix, 62
- Odd vertex, 52
- Pairings
 - Farey symbol, 59
- Parabolic element of $\mathrm{PSL}_2(\mathbb{R})$, 12
- Parabolic point
 - on \mathbb{H} , 12
- Partial Farey sequence, 56
- Poincaré series, 25
- Projective space, 3
- Properly discontinuously group operations, 11
- Rational covering induced by a subgroup of a Fuchsian group, 27
- Reduction to an elementary cusp, 86
- Riemann surface
 - Fundamental group, 19
- Riemann surface associated to a Fuchsian group, 15
 - Compactification, 16
- Schwarzian derivative
 - Basic properties, 73
 - Definition, 73
- Side pairings, 17
- Sine rule of hyperbolic geometry, 8
- Slash operator, 22
- Special polygon, 53
- Standard map, 61
- Stern-Brocot tree, 58
- Support of a hole, 57
- Symmetric group, 4
- Triangle group
 - Classification, 29
 - Definition, 29
 - Euclidian, 29
 - Extended triangle group, 30
 - Hyperbolic, 29
 - Spherical, 29
- Upper half plane
 - Length, 6
- Upper half plane, 5
 - Closed $-$, 6
 - Definition, 6
 - Metric on $-$, 6
- Word problem, 41